CONTINUOUS GPS: PILOT APPLICATIONS – PHASE II

FINAL REPORT

Project F2001 OR 05

GeoResearch Group

Caltrans

Research & Innovation

CONTINUOUS GPS: PILOT APPLICATIONS – PHASE II

FINAL REPORT
F-2001-OR-05
FHWA/CA/IR-2003/05

August 2003

Loren L. Turner, P.E.
California Department of Transportation
Division of Research & Innovation
The GeoResearch Group
5900 Folsom Blvd. MS-5
Sacramento CA 95819
(916) 227-7174
loren.turner@dot.ca.gov

STATE OF CALIFORNIA DEPARTMENT OF TRANSPORTATION

TECHNICAL REPORT DOCUMENTATION PAGE

TR0003 (REV. 10/98)

1. REPORT NUMBER	2. GOVERNMENT ASSOCIATION NUMBER	3. RECIPIENT'S CATALOG NUMBER
FHWA/CA/IR-2003/05		

4. TITLE AND SUBTITLE	5. REPORT DATE
CONTINUOUS GPS: PILOT APPLICATIONS – PHASE II	August 2003
	6. PERFORMING ORGANIZATION CODE
7. AUTHOR(S)	8. PERFORMING ORGANIZATION REPORT NO.
Loren L. Turner	65-339/65-680422
9. PERFORMING ORGANIZATION NAME AND ADDRESS	10. WORK UNIT NUMBER
California Department of Transportation Division of Research & Innovation The GeoResearch Group 5900 Folsom Blvd. MS-5 Sacramento, CA 95819	11. CONTRACT OR GRANT NUMBER F-2001-OR-05
12. SPONSORING AGENCY AND ADDRESS	13. TYPE OF REPORT AND PERIOD COVERED
California Department of Transportation Sacramento, CA 95819	Final Report
	14. SPONSORING AGENCY CODE

15. SUPPLEMENTAL NOTES

16. ABSTRACT

With recent advancements in Global Positioning System (GPS) technologies, measurements of ground surface displacements under static as well as dynamic conditions have become easier to obtain with greater accuracy and lower costs. In geotechnical practice and research, measurements of soil mass deformations are frequently required. Landslides, lateral spreading from earthquakes, fill settlements, and retaining wall movements represent just some of the geotechnical problems where accurate deformation data is critical. The benefits of GPS technology over more conventional instrumentation technologies appear promising for future applications, particularly in remote monitoring of landslides.

Late in 1999, the California Department of Transportation (Caltrans) initiated a focused research effort to look into innovative GPS technologies and applications. The primary objective of the research was to evaluate the feasibility of applying GPS in the study of geotechnical phenomenon through the development, integration, and test deployment of a GPS-based instrumentation package utilizing emerging high precision Real-Time Kinematic GPS (RTK-GPS) and wireless communications technologies. The instrumentation package would be configured primarily for the remote monitoring of landslide movements. Bridge monitoring applications would also be explored during the study.

17. KEY WORDS	18. DISTRIBUTION STATEMENT
landslide monitoring, real-time kinematic global positioning system, RTK-GPS, bridge monitoring, instrumentation, liquefaction, lateral spread	No restrictions. This document is available to the public through the National Technical Information Service, Springfield, VA 22161

19. SECURITY CLASSIFICATION (of this report)	20. NUMBER OF PAGES	21. PRICE
Unclassified	161	

Reproduction of completed page authorized

DISCLAIMER STATEMENT

The contents of this report reflect the views of the author who is responsible for the facts and the accuracy of the data presented herein. The contents do not necessarily reflect the official views or policies of the STATE OF CALIFORNIA or the FEDERAL HIGHWAY ADMINISTRATION. This report does not constitute a standard, specification, or regulation. This report does not constitute an endorsement by the Department of any product described herein.

Table of Contents

1.0 Introduction……..……..……. 1

2.0 Literature Search

2.1 Background……..……. 4

2.2 GPS Technology……..……. 6

3.0 Validation Testing

3.1 Testing Method……..……. 11

3.2 Single Frequency Receiver Testing ……. 16

3.3 Dual Frequency Receiver Testing……..……..…. 19

4.0 Systems Integration and Prototype Development

4.1 Hardware ……..……. 24

4.2 Software ……..……. 30

4.3 Prototype System ……..……. 32

5.0 Full-Scale Lateral Spread Test in Japan

5.1 Background……..……. 41

5.2 Description of the Test Site……..……. 43

5.3 Deployment of the GPS Field Units ……..……. 51

5.4 Establishment of the Monitoring Center ……..……. 74

5.5 Creating the Lateral Spread ……. 76

6.0 Measurements From The Tests in Japan

6.1 Data Collection and Processing ……..……. 84

6.2 General Discussion of Pre and Post-Blast Survey Results …….. 110

6.3 General Discussion of Time-History Records ……..……. 121

6.4 Observations of Liquefaction from the November Test …….. 125

6.5 Validity of Measurements……. 130

7.0 Conclusions…….132

8.0 Acknowledgements……..……134

9.0 References……...……136

Appendices.……..……...……..…… 139

1.0 Introduction

With recent advancements in Global Positioning System (GPS) technologies, measurements of ground surface displacements under static as well as dynamic conditions have become easier to obtain with greater accuracy and lower costs (Langley 1998). In geotechnical practice and research, measurements of soil mass deformations are frequently required. Landslides, lateral spreading from earthquakes, fill settlements, and retaining wall movements represent just some of the geotechnical problems where accurate deformation data is critical. The benefits of GPS technology over more conventional instrumentation technologies appear promising for future applications, particularly in remote monitoring of landslides.

Late in 1999, the California Department of Transportation (Caltrans) initiated a focused research effort to look into innovative GPS technologies and applications (Turner 2000, 2001). The primary objective of the research was to evaluate the feasibility of applying GPS in the study of geotechnical phenomenon through the development, integration, and test deployment of a GPS-based instrumentation package utilizing emerging high precision Real-Time Kinematic GPS (RTK-GPS) and wireless communications technologies. The instrumentation package would be configured primarily for the remote monitoring of landslide movements. Bridge monitoring applications would also be explored during the study.

Caltrans expends significant resources in dealing with landslide hazards adjacent to the State highway system. With an estimated 1200 miles of landslide prone highway corridors throughout California, approximately 200 landslides and 10 road closures occur per year at rough cost of $10 million for clean up and mitigation. Most notably, in the Winter of 1997 the Mill Creek Landslide closed down State Route 50 and dammed the American River for several hours. The landslide caused significant damage to many homes and roadways in that area as shown in the photos in Figures 1 and 2. State Route 50 was closed for almost a month which severely impacted travel and the South Lake Tahoe region's economy.

Remote monitoring programs have been successfully employed in the past to collect information on landslide movements in response to critical environmental parameters such as rainfall and groundwater levels. Geotechnical engineers use this data to understand landslide failure mechanisms and develop effective mitigation strategies to address issues of traveler safety and convenience. GPS provides an opportunity to collect more relevant and reliable deformation information for the engineer.

This report presents the work performed to date on the development of a remote monitoring system incorporating GPS for deformation measurements. This includes validation testing, systems integration, prototype development, and, finally, a test deployment of the system in a full scale earthquake experiment at a shipping port facility in northern Japan in November and December 2001.

Figure 1 – 1997 Mill Creek Landslide

Figure 2 – Large scarps at the top of the Mill Creek Landslide

2.0 Literature Search

2.1 Background

Acquiring accurate displacement measurements has always been challenging for geotechnical engineers studying and monitoring the movements of landslides. In the past, more conventional techniques have been employed to gather measurements of surface deformations including periodic surveying, tilt meters, and surface extensometers.

Surveying a defined circuit of benchmarks on a weekly or monthly basis over an extended period of time using optical or laser-based electronic surveying instruments can provide an accurate historical record of changes to surface geometry over the period studied. However, the process is time consuming and requires a survey crew to collect and process each data set. Furthermore, the data sets only provide a "snap shot" of the changing topography at the time of the survey.

Wire extensometers, laser-based distance measurement devices, and tilt meters, can provide deformation information at more frequent intervals and lends themselves to automated remote monitoring systems. However, each of these technologies has significant shortcomings that impede its use in remote landslide monitoring applications. For example, surface mounted wire extensometers can provide an indication of movement, such as the progressive movement of a slide along a lateral scarp. However, since the extensometer only measures the

extension or retraction of the wire, it can only provide changes in distance between two points, and not vectoral movements in a three dimensional space. Tilt meters can provide a good indication of movement since movements of the slide mass are likely to deform the ground in such a manner as to cause tilting. As with extensometers, however, quantification of direction and magnitude are difficult. These instruments, particularly surface extensometers, are also susceptible to false indications of movement resulting from ice buildup and interference from animals.

Accelerometers have been commonly used to measure motions where rapid deformation occurs over the course of seconds, such as that in bridges. However, deriving displacements from acceleration requires two mathematical integrations and some assumptions which introduce errors in displacements. This is particularly difficult for long-span bridges where larger motions occur over longer periods of time. RTK-GPS shows promise of providing accurate deformation measurements under these circumstances.

Early research into GPS technologies for deformation monitoring applications demonstrated the viability of GPS for accurate displacement measurements (Celebi et.al. 1999, Hudnut et.al. 1998); however, high equipment costs limited its widespread application. Advances in GPS technologies over the past few years have now made it possible to economically determine displacements of remote installations, in near real-time, with reasonably high accuracies. For example, an autonomous GPS-based remote monitoring system has been shown to provide positioning data from four points at a remote site up to 20 miles away, while

producing reliable centimeter-level solutions in real-time at up to 10 positions per second for approximately $26,000 (see Appendix A for more detailed information). As a result displacement monitoring applications using GPS, such as landslide hazard assessment or even deformation monitoring of bridges and other civil structures, is now a viable and cost-effective alternative to conventional monitoring techniques (Turner and Schuster 1996).

2.2 GPS Technology

The development of the Navigation System with Timing and Ranging (NAVSTAR) Global Positioning System (GPS) was initiated in 1973 under the direction of the United States Air Force Systems Command, Space Division, and the Department of Defense (DoD). The system was originally conceived for military applications for determination of position, velocity, and time anywhere in the world (Hofmann-Wellenhof et.al. 1997).

Fundamentally, GPS is based upon a ranging technology to determine the distance between known satellites positions and unknown positions on the ground, or in the sea, air, and space. The entire system is comprised of three segments: (1) the space segment, (2) the control segment, and (3) the user segment. The space segment is comprised of 24 GPS satellites, in 6 orbital planes, with 4 satellites per orbital plane. This satellite configuration insures consistent coverage for users to receive satellite signals anywhere in the world. The control segment consists of a network of worldwide satellite monitoring stations and a master control station located at Falcon Air Force Base in Colorado Springs, Colorado. The master control station tracks and predicts satellite orbital paths

and synchronizes timing information between satellites. The control segment insures that precise satellite positions are calculated and known at all times to maintain the integrity of the GPS satellite signals. The user segment consists of the GPS devices, such as the receivers and antennas, that surveyors, soldiers, and civilians use to receive satellite signals to determine their position.

Although GPS is a term generally used to describe the satellite-based positioning system, GPS technology actually covers a wide range of hardware components and data processing methods, each with unique limitations and benefits in terms of performance, accuracy, and cost.

In its simplest augmentation, referred to as *Standalone Positioning Service* (SPS), a single GPS receiver and antenna is used to collect and estimate the travel time of signals emitted from a minimum of four GPS satellites. Four satellites are needed in order to solve for four unknowns: x, y, z, and time. Using the signal travel time and knowing the speed of the signal through the atmosphere, a receiver can quickly calculate the distance from its antenna to the satellite. SPS is by far the most common implementation for consumer grade handheld and vehicle mounted GPS devices. Currently, the positioning accuracy with SPS is approximately 22m horizontal and 27.7m vertical as specified in the 1999 Federal Radionavigation Plan (U.S.DOT 1999). GPS accuracies are typically expressed as the value of two standard deviations of radial error from the actual antenna position, referred to as 2drms (two-distance root-mean-squared).

Differential GPS (DGPS) was developed to reduce much of the error associated with the SPS solution. These errors are primarily caused by tropospheric and ionospheric effects which impact the GPS signal travel time. The concept of DGPS is to quantify the error in the calculated distance between a satellite and receiver. Using a receiver, commonly referred to as a base station, placed at a location with known coordinates, these errors can be determined and used as corrections by other nearby receivers to improve accuracies. DGPS accuracies are highly dependent upon the distance between the base station and the other receiver. For distances less than 30km, horizontal accuracies can be about 1m and vertical accuracies about 1.5m. The correction process can be done in real-time, provided that there is a data communications link, or at a later time after the data is collected.

Carrier Phase Differential GPS is similar to DGPS. However, in this implementation the carrier signal itself, in addition to the standard GPS timing information, is used for ranging. Special hardware and software are required to analyze the complex carrier signals for this type of processing. However, the benefits in accuracies are impressive. A *Post-processed Static Carrier Phase* method can provide 1 to 5cm horizontal accuracies with 15 minutes to 1 hour of data collection. Horizontal accuracies of 4 to 10cm can be achieved using the *Rapid Static* technique with 15 minute collection periods. The *Real-Time-Kinematic (RTK)* method can provide centimeter accurate horizontal measurements in real time provided a data communications link is used. Carrier phase differential GPS techniques are commonly being used in the surveying community.

These various GPS technologies were evaluated for their applicability to remote landslide monitoring. Considering the accuracies required and the need for real-time information, a *Networked RTK* system, based upon RTK-GPS, was determined to provide the best balance of performance, accuracy, and cost. A Networked RTK system is based upon differential carrier phase positioning using at least two GPS receivers, one base and multiple rover receivers. In a Networked RTK system, all of the raw code and carrier data from the base and rover receivers are transmitted wirelessly to a single offsite computer which processes and calculates positions. This differs from a conventional RTK-GPS surveying application where data is processed by the GPS hardware in the field with positions provided directly to the user at that time. Networked RTK effectively reduces the complexity and processing requirements needed in the field GPS receivers by using the processing power of a separate personal computer offsite. The resulting system is one with minimal GPS hardware deployed in the field and all of the advanced processing performed on a centralized computer back in the office.

Carrier phase differential GPS methods rely upon GPS satellite microwave carrier signals. GPS satellites actually transmit timing information on two frequencies, one at 1575.42Mhz, called the *L1 frequency,* which carries the SPS code information, and the other at 1227.60Mhz, called the *L2 frequency,* which is used to reduce ionospheric errors. *Single frequency receivers* use only the L1 carrier signals, whereas *dual frequency receivers* use both the L1 and L2 carrier signals. In general, dual frequency receivers can resolve carrier signal ambiguities quicker during start up or after loss of satellite signals. Both single

and dual frequency receivers can provide centimeter level solutions. However, dual frequency receivers are typically an order of magnitude more expensive than single frequency receivers.

3.0 Validation Testing

3.1 Testing Method

In an effort to quantify real-world performance and demonstrate the use of RTK-GPS as a displacement measurement tool, a series of proof tests were performed. The tests were designed to simulate the range of magnitudes, rates, and frequencies of displacements typically encountered in bridge and landslide monitoring applications. The objective of the tests was to show the relative error between displacements measured by both single and dual frequency GPS receivers in comparison to measurements made by independent means.

In order to the meet the test objectives, a test bench was assembled for the study as shown in Figures 3 through 5. The device consisted of a 760mm precision linear slider bearing and shuttle assembly to which a GPS antenna was mounted. A 760mm range linear position transducer was mounted at one end of the slider assembly with the cable end attached to the shuttle. Random linear motions could then be initiated manually, as shown in Figure 6, with the relative displacements from both the GPS and the linear displacement transducer recorded by a data acquisition system. Continuous data acquisition from both devices provided the data sets to make a direct comparison of the displacement measurements under static and random dynamic motions. An additional scale was also fixed to the test bench for a redundant visual measurement system.

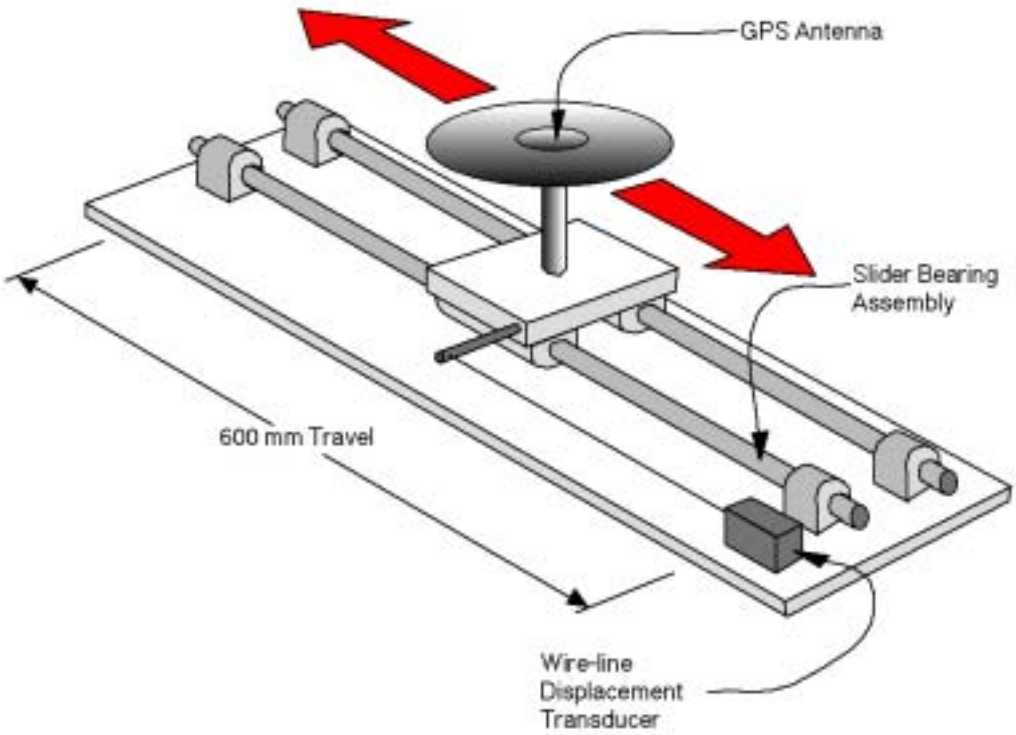

Figure 3 – Test Bench Assembly

Figure 4 – Test Bench Assembly

Figure 5 – 760mm range linear position transducer

Figure 6 – Initiating random linear motions

For each series of tests, a pair of GPS receivers were used, one as the base station with the antenna fixed atop a tripod, and the other as the rover with the antenna mounted on the slider's shuttle as shown in Figure 4. Both GPS receivers were connected to a portable computer through the RS-232 serial interface. GPS processing software, *RTKNav* from Waypoint Consulting, was used to process the data, compute real-time antenna positions, and pass a stream of corrected data to another program written for data management, visualization, and file storage functions.

Voltages from the displacement transducer were digitized and converted to engineering units through a 16-channel analog to digital PC card in the portable computer. With this configuration, data from both the GPS and the displacement transducer could be logged simultaneously.

In order to calculate relative displacements for the GPS rover antenna, it was necessary to first establish the initial position of the antenna on the test bench. With the initial XYZ position established as a reference point, subsequent positions of the rover could be calculated based upon the vector difference between the initial and extended positions. Positioning data were acquired in latitude/longitude/height in the World Geodetic System 1984 (WGS-84) datum and then converted to Earth-Centered-Earth-Fixed (ECEF) coordinates, a three-dimensional Cartesian system in a XYZ format.

The baseline length, or length between the base and rover receivers, was approximately 1m for the tests. Since some of the errors in GPS measurements

are a direct function of baseline length, these tests represented ideal conditions that wouldn't necessarily be present in the field deployments. The error introduced by longer baselines is typically on the order of 1 to 2 parts per million (ppm). For example, a rover antenna located 2000m away from the base antenna would potentially introduce an additional 2 to 4mm of error.

Test results are presented as time-history displacement plots showing time data on the x-axis and displacement data on the y-axis. For the transducer data, the y-axis displacement data represents the difference between the shuttle's initial position and its position at that time instance. At one end of the slider, the transducer was in a fully retracted position with the readout set to zero. At the other extreme slider position, the transducer was in a fully extended position which corresponded to a reading of about 650 mm. For the GPS data, the y-axis displacement data represents the vector difference between the antenna's initial ECEF position and its ECEF position at that time instance. The GPS versus displacement data plots show both data sets plotted as data pairs for any given time instance. Using the same scale on both the x and y-axes, a line plotted at 45° extending from the origin would represent a perfect correlation between the two measurements.

For the validations tests, both single and dual frequency GPS receivers were tested. For the single frequency receiver, the *Allstar* by the Canadian Marconi Company (CMC), was evaluated. For the dual frequency receiver, the *Legacy* by Topcon Position Systems (TPS), was evaluated.

Both the CMC and TPS receivers incorporated state-of-the-art GPS technologies while representing two of the lowest cost systems on the market at the time of testing. General specifications for these receivers are shown in Table 1.

Receiver	CMC Allstar	TPS Legacy
Tracking Channels	12	20
Signals Tracked	L1, C/A Code, Carrier Phase	L1/L2, C/A and P Code and Carrier
Raw Data Output Rate	10 Hz	20 Hz
Power Requirements	1.4 Watts (5 VDC)	3.0 Watts (6 to 28 VDC)
Antenna Type	Active Geodetic, L1, with Choke Ring (Aero Antenna)	Active Geodetic, L1/L2, with Ground Plane (TPS *Legant*)
Approximate Costs:		
Receiver	$800	$6,000
Antenna	$800	$1,200
TOTAL	$1,600	$7,200

Table 1 – GPS receiver and antenna specifications

3.2 Single Frequency Receiver Testing

Test results using the single frequency CMC Allstar are presented in Figures 7 through 10. Figure 7 shows the complete time history record. A range of random motions were tested to encompass the types of motions to be measured in the field deployments. From 0 to 200 seconds, the antenna was moved to various positions on the slider and held for 10 to 20 seconds, demonstrating static conditions as shown in Figure 8. From 440 to 480 seconds, the antenna was moved slowly from one end of the slider to the other, a kinematic measurement typical of landslide deformations, as shown in Figure 9. From approximately 500

to 550 seconds, a series of roughly 1 to 3 Hz motions were initiated, as shown in Figure 10, a typical response in many California bridges.

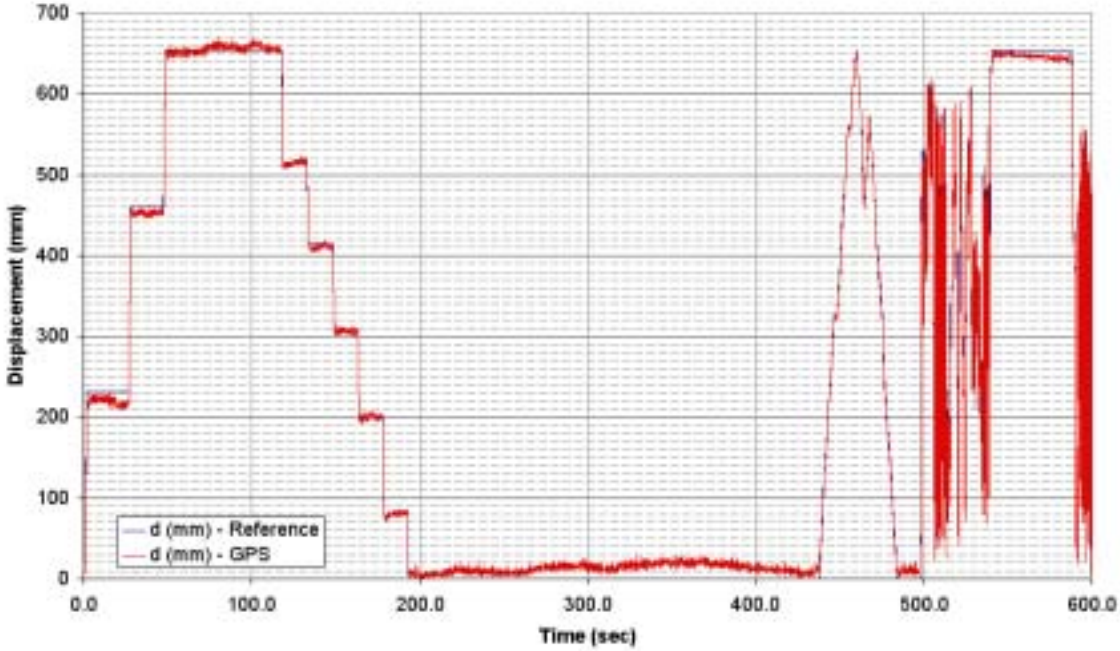

Figure 7 – Complete Time-History Record for CMC AllStar

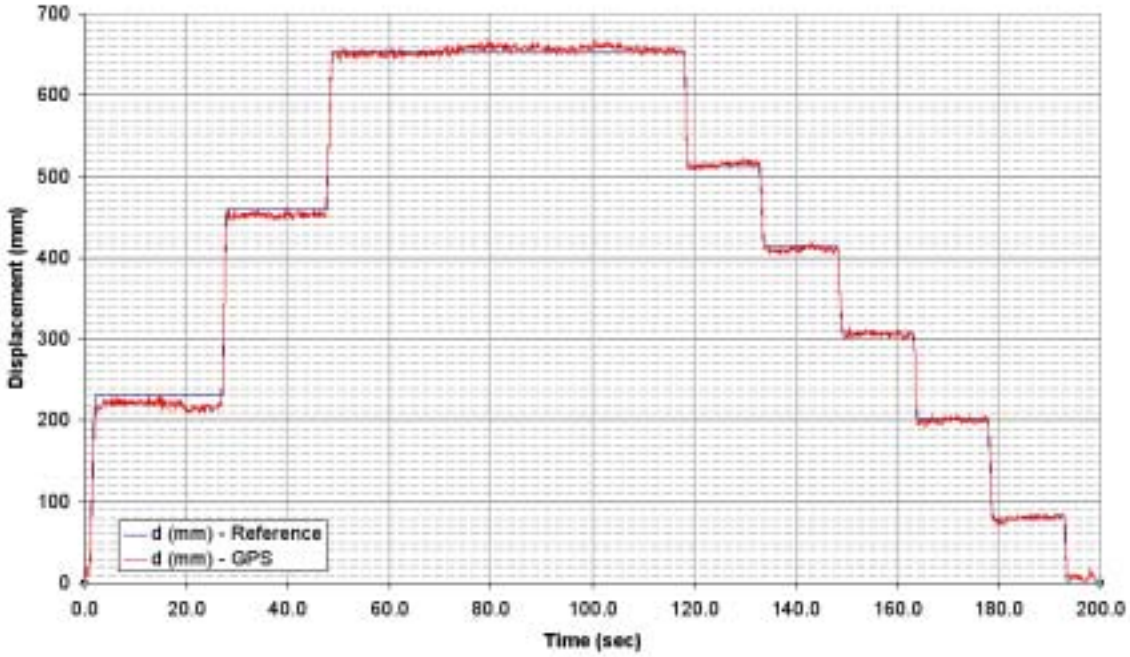

Figure 8 – Static condition measurements

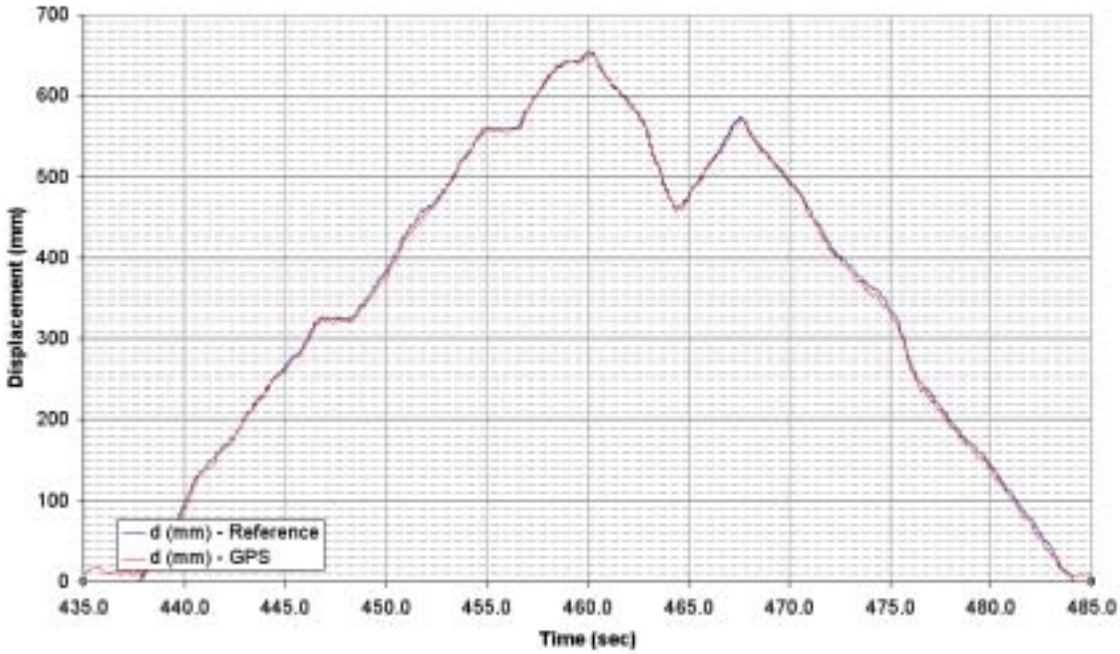

Figure 9 – Kinematic measurement typical of landslide deformations

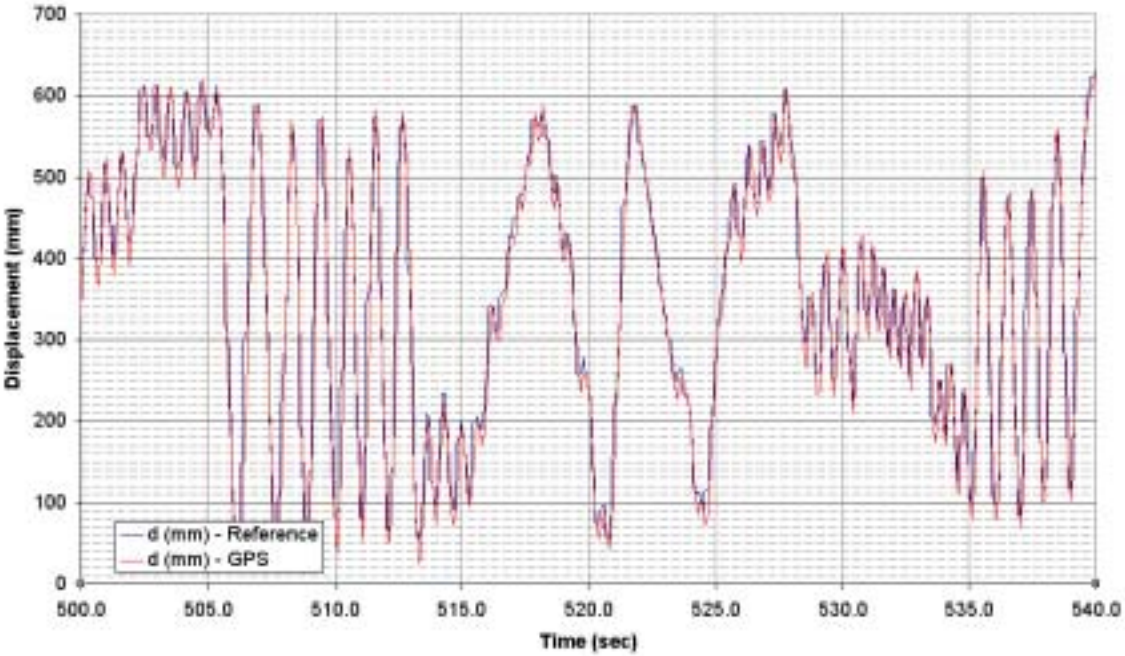

Figure 10 – 1 to 3Hz motions, typical of bridge response

In general, the time history data showed relatively good agreement between the vector displacements from the GPS as compared to the displacements measured from the displacement transducer. Errors between the GPS and transducer measurements were typically less than 15mm during static conditions; however, errors as much as 80mm were observed during the higher rate motions between 500 to 600 seconds. Figure 11 shows a time-history plot of the relative error between GPS and transducer measurements over the period of testing. The RMS errors over the entire time period was calculated to be 14mm. Between 500 to 600 seconds, the RMS error was calculated to be 24mm. Overall these measurements were consistent with expected single-frequency GPS accuracies using RTK processing techniques.

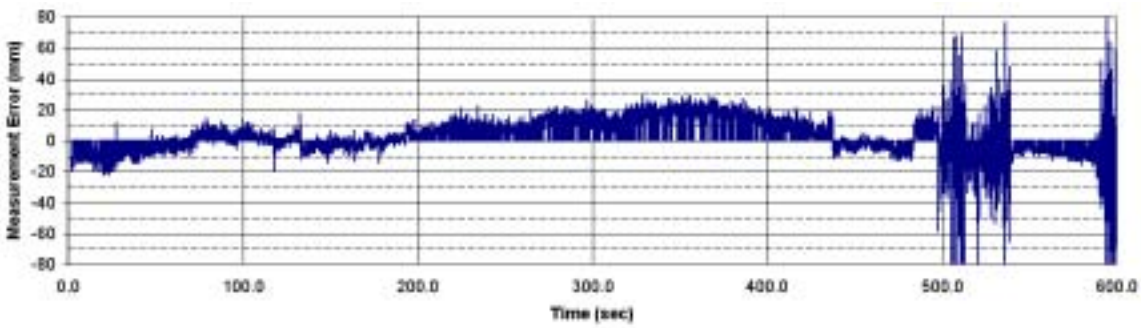

Figure 11 – Time-history of measurement errors for CMC Allstar

3.3 Dual Frequency Receiver Testing

The complete time history record for the TPS Legacy receiver is shown in Figure 12. As with the CMC Allstar tests, a range of random motions were initiated to encompass the types of motions to be measured in typical field deployments.

From 0 to 200 seconds, the antenna was moved to various positions on the slider and held for 10 to 50 seconds, demonstrating static measurements. From 410 to 430 seconds, the antenna was moved slowly from one end of the slider to the other. From approximately 570 to 650 seconds, a series of roughly 1 to 3 Hz motions were initiated. Data from these three types of motions are shown in Figures 13 through 15.

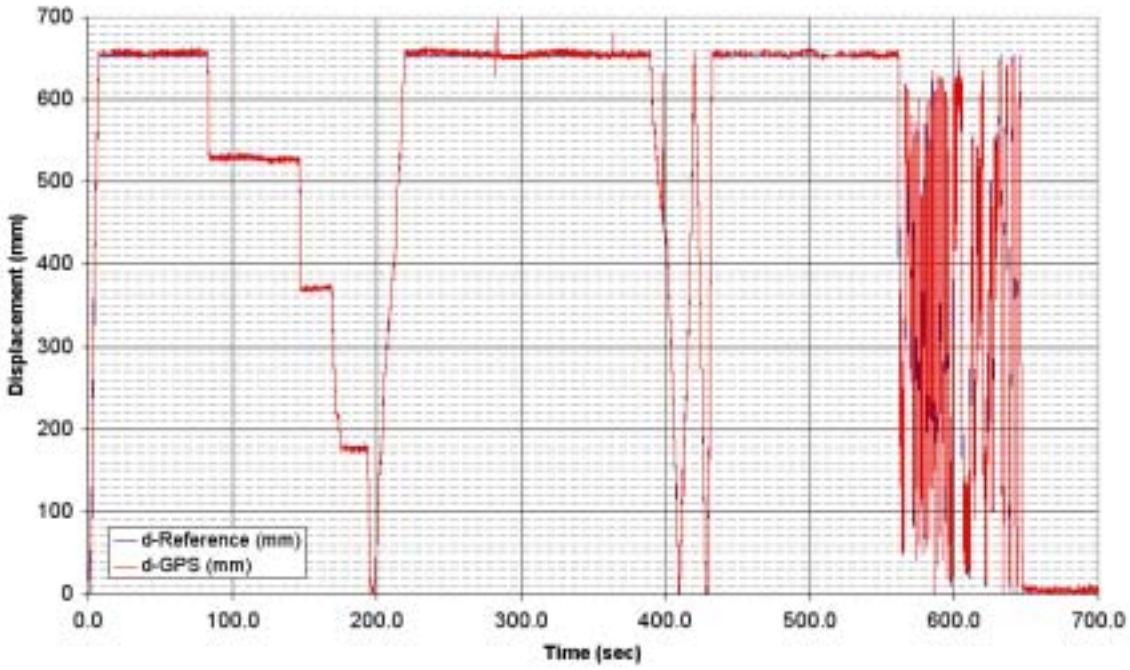

Figure 12 – Complete Time-History Record for TPS Legacy

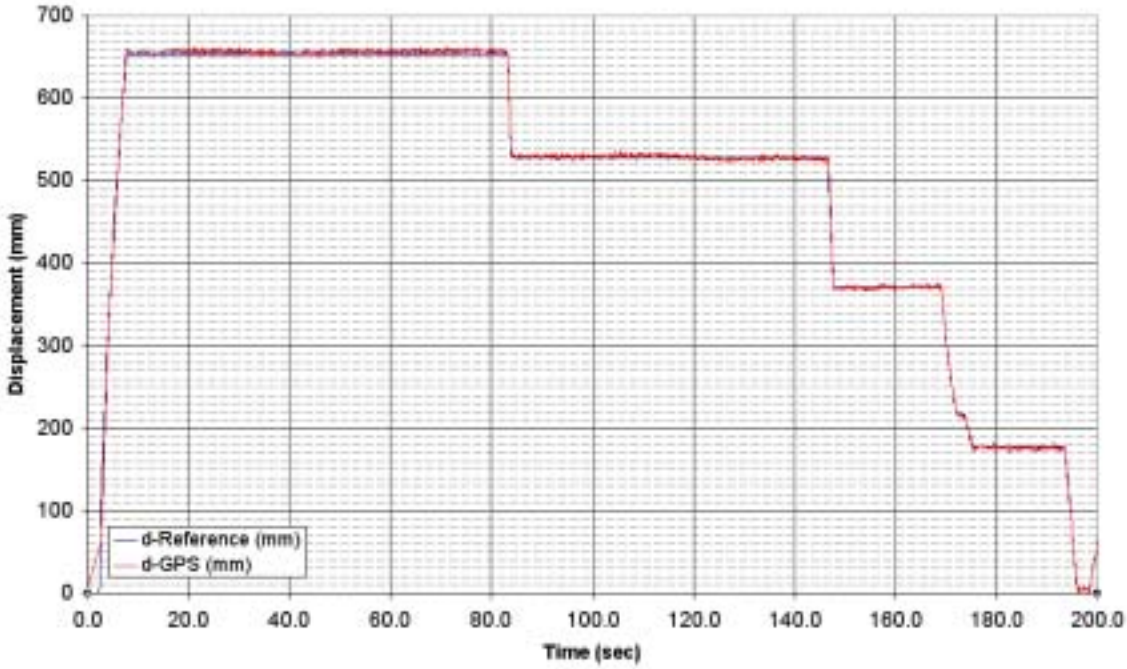

Figure 13 – Static condition measurements

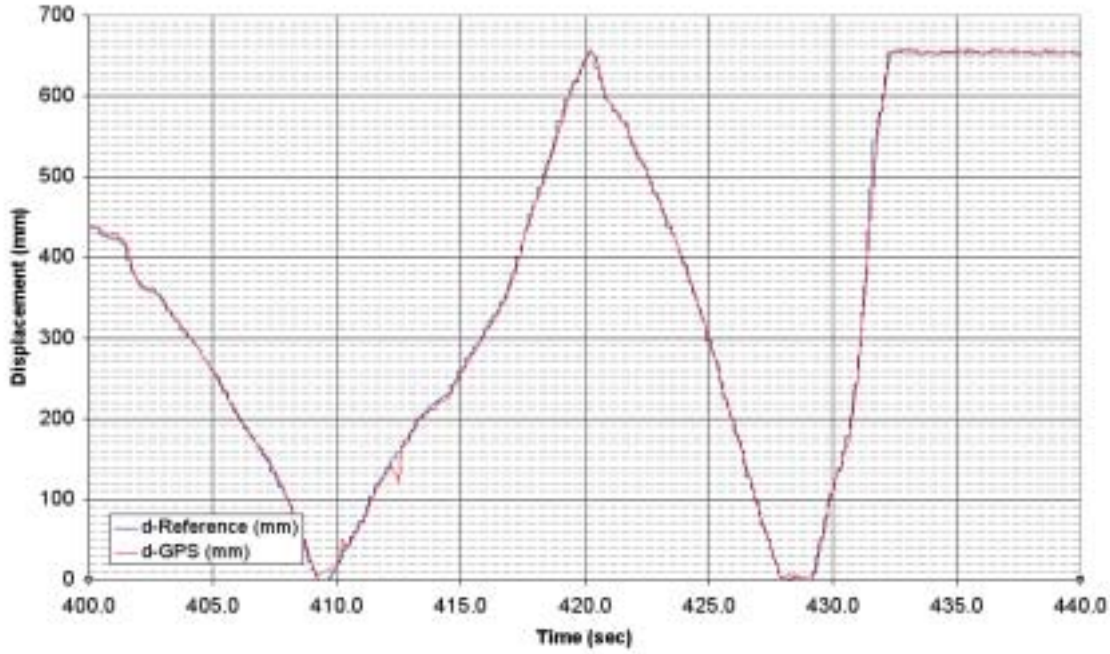

Figure 14 – Kinematic measurement typical of landslide deformations

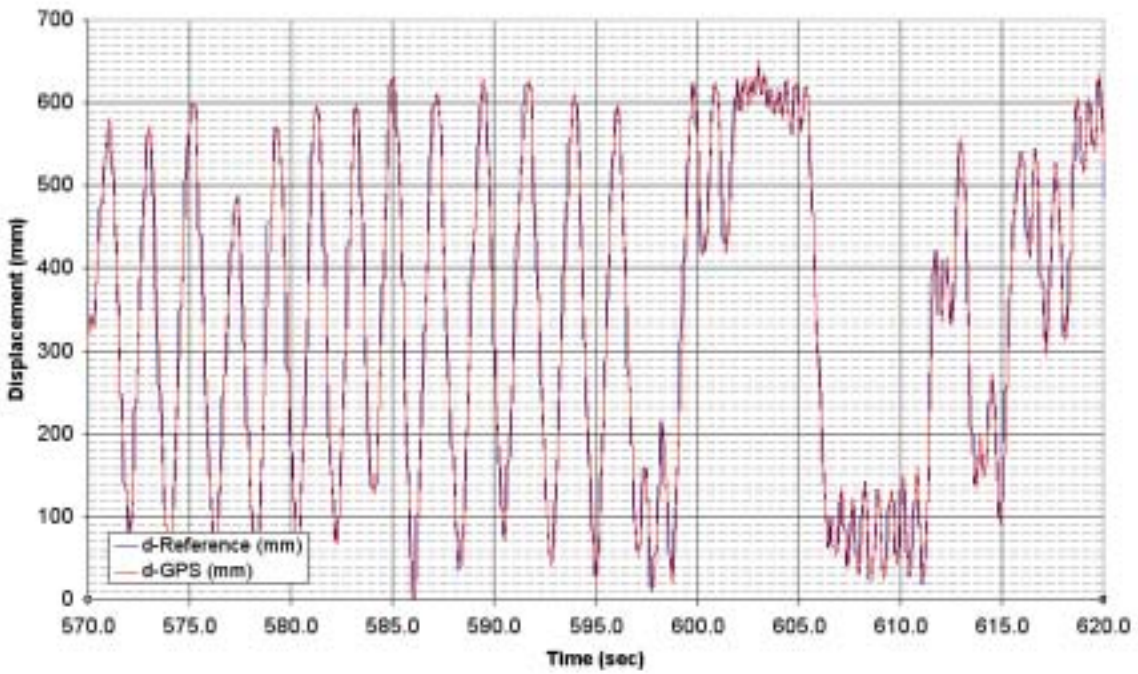

Figure 15 – 1 to 3Hz motions, typical of bridge response

As with the CMC Allstar receivers, the time history data showed relatively good agreement between the vector displacements from the GPS as compared to the displacements measured from the displacement transducer. In general, errors between the GPS and transducer measurements were typically less than 10mm during static conditions; however, errors as much as 50mm were observed during the higher rate motions between 570 to 650 seconds. Figure 16 shows a time-history plot of the relative error between GPS and transducer measurements over the period of testing. The RMS errors over the entire time period was calculated to be 7mm. Between 570 to 650 seconds, the RMS error was calculated to be 13mm. These measurements were consistent with expected dual-frequency GPS accuracies using RTK processing techniques.

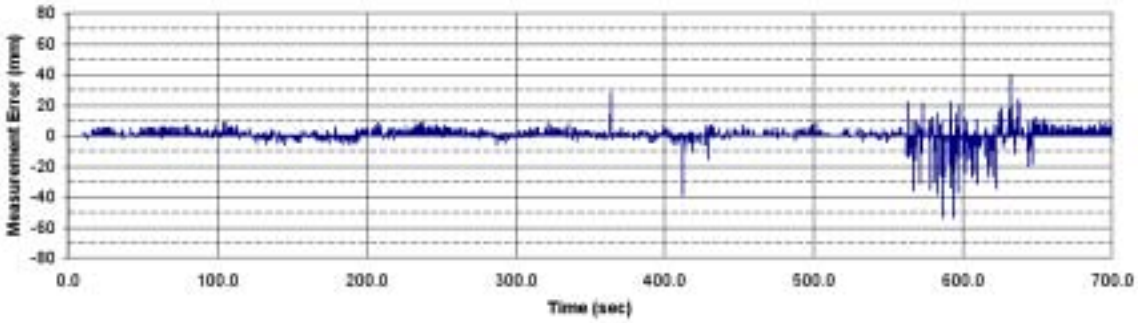

Figure 16 – Time-history of measurement errors for TPS Legacy

In summary, both the single-frequency and dual-frequency receivers provided impressive measurements under static and dynamic test conditions. The dual-frequency receivers performed significantly better under all conditions with an overall RMS error of 7mm, compared with the single-frequency receivers generating an overall RMS error of 14mm. Dual-frequency receiver measurements also proved to be more consistent and less prone to drift. The drift in the data apparent in the single-frequency measurements can be attributed to ionospheric effects that are more effectively negated by receivers processing both the L1 and L2 carrier signals. It is important to note, however, that the single-frequency receivers provided good results considering the cost of the hardware is an order of magnitude less than the dual-frequency receivers.

4.0 Systems Integration and Prototype Development

RTK-GPS using single and dual frequency receivers has been shown to provide reliable centimeter level measurements at rates of up to 20 samples per second. Although the technology was validated, the implementation of a Networked RTK system for remote deformation monitoring had additional design and deployment challenges such as data communications, data processing and management, environmental packaging, and autonomous power systems.

4.1 Hardware

A remotely distributed Networked RTK system is comprised of GPS receivers and antennas, communications equipment, power systems, and a computer processing station.

The general architecture of a Networked RTK system with one reference unit, referred to as the *base station*, and two field units, referred to as *rover units*, is shown in Figure 17. The GPS receivers, antennas, communications equipment, and power systems shown on the right half of Figure 17 are located in the field either on the landslide or affixed to the bridge. Raw GPS data is collected through the GPS antennas, interpreted by the GPS receivers, and transmitted back to a central location. Data transmission can be accomplished through cables. However, for most monitoring situations, longer distances and real-time data streaming necessitate the use of some type of fast, reliable, and long range wireless communications device, such as spread spectrum 900Mhz wireless data

transceivers. Back at an offsite location the data is collected and processed by a PC using RTK-GPS software to determine final positioning information.

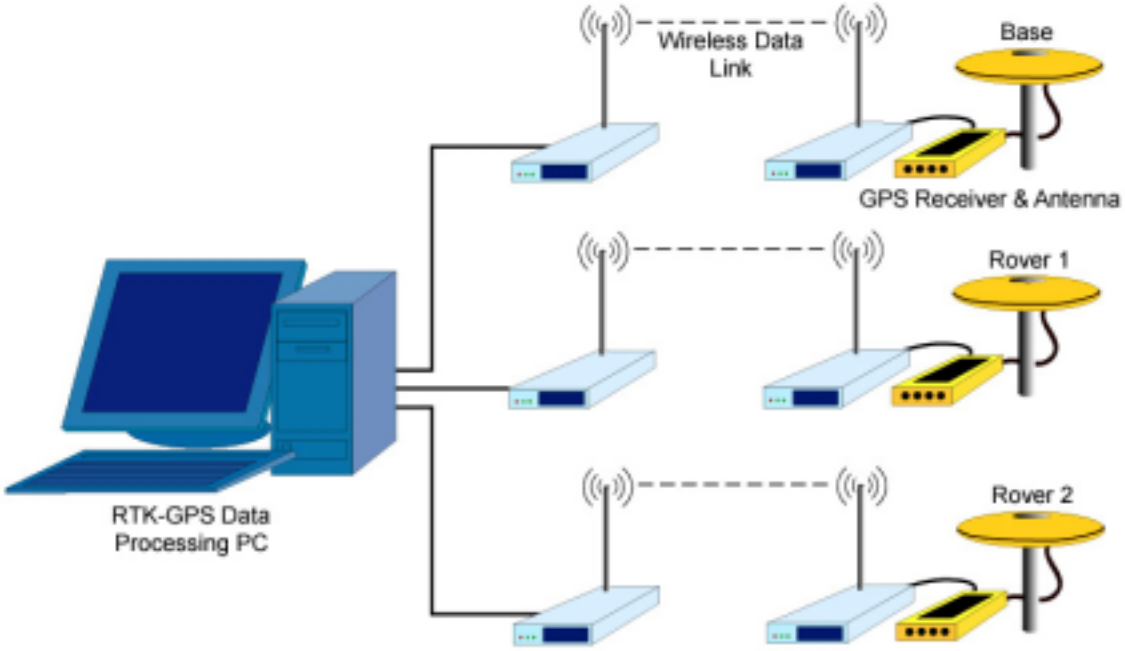

Figure 17 – Networked RTK-GPS architecture

With these components in place, the system provides a real-time data stream of positioning data at 10 to 20 Hz with centimeter horizontal accuracy.

Specific field hardware varies depending upon the particular application. Three configurations were explored over the course of the project to meet the needs of: (1) landslide monitoring, (2) bridge monitoring, and (3) smaller research applications. Landslide and bridge monitoring applications require the most robust systems since they may be deployed for months to years at a time in remote locations. A smaller research application conducted in Japan will be discussed in a later section.

The primary components of the field units are the GPS receiver and antenna, radio modem and antenna, power system, and packaging. In a landslide deformation monitoring system, the field units can be integrated into a single pole mounted system as shown in Figure 18. In this configuration, solar power and battery backup are used to supply power to electronics components. In a bridge monitoring system, where AC power is usually readily available from overhead lighting, the system could be configured as shown in Figure 19.

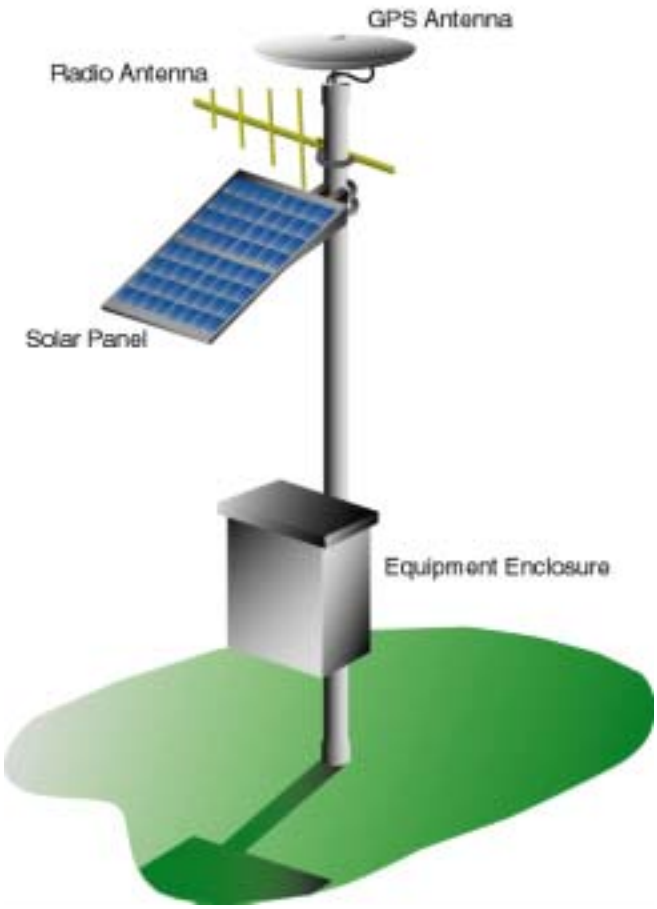

Figure 18 – Field unit for landslide monitoring application

Figure 19 – Field unit for bridge monitoring application

The solar power system for the landslide monitoring application was designed to provide a continuous 12VDC supply to the system. Selection of solar panels and batteries were based upon the power requirements of the CMC Allstar GPS receiver (12VDC, 1.4W) and the FreeWave spread spectrum transceiver (12VDC, 2.0W). A total daily energy of 83Watt-hours/day for the system was calculated as follows:

(1.4W)(24 hrs/day)	= 49W-hrs/day	GPS Receiver
(2.0W)(24 hrs/day)	= 34W-hrs/day	Transceiver

The total daily energy was increased by 35% to 111Watt-hours/day to account for inefficiencies in the system. Conservatively assuming 4 hours of full sunlight during the day, a single solar panel rated at 40W provides sufficient power. A battery is necessary for energy storage during periods when sunlight is not available. Although periods of a few weeks of no sunlight is conceivable in areas where snowfall is likely, a design period of five days was used to accommodate most landslide installations while still providing an economical system. For 111Watt-hours/day at 12V, the battery was sized as follows:

$$\left(\frac{111W \cdot hrs}{day}\right)\left(\frac{1}{12V}\right)(5days)\left(\frac{1}{0.50discharge}\right) = 93A \cdot hrs$$

As such, a 12V deep-cycle battery rated at 100Amp-hours was integrated into the system.

Backup power systems for bridge monitoring installations were based upon similar calculations as those for landslide applications. However, in lieu of a solar panel, an AC trickle charger tapped into the lighting conduit on the bridge is used to continuously keep a 100Amp-hour deep-cycle battery at full charge in the event of a power failure.

The selection of a wireless communications technology was driven by the need for fast, reliable, and low-powered devices. In many cases monitoring sites are located in remote areas with limited access to conventional communications such as telephone lines, computer networks or even cellular data systems such as the

Cellular Digital Packet Data (CDPD) network. Furthermore, the most interesting data from a deformation monitoring system is likely to result from a natural disaster such as an earthquakes or a landslide, where conventional communications systems are more likely to be impacted with increased traffic or physical damage.

A communications system based upon 900Mhz license-free spread spectrum technologies was selected to meet the needs of an independent system. Many commercially available products are available incorporating this technology; however, the *DGR-115R* from FreeWave Technologies, Inc., was selected due to positive past experiences with these devices in other remote monitoring applications. These transceivers are low powered, using 1W during transmit, and 0.1W during standby mode. They interface directly with most GPS receivers using a relatively high speed (115kbaud) RS-232 serial interface. They can transmit data over 20 miles line-of sight using the license-free 908-928Mhz frequency band. Finally, these transceivers are relatively easy to configure and implement. Optimizing the configuration of these transceivers for the GPS application involved a process of trial and error over a series of test deployments. Recommended transmission parameters and settings for the FreeWave DGR-115R transceivers are documented in Appendix E.

Synchronization of the data streams from the multiple rover units is controlled through the use of the GPS timing signal. An accurate and synchronized timing signal is the basis for all GPS ranging calculations. Recall from the earlier explanation of GPS in Section 2.2 that four satellites are required to resolve an

x,y,z position in space in addition to a time, t. Each GPS satellite has an onboard atomic clock that is constantly monitored and updated by the control segment. Although the synchronization of timing signals is well established between the satellites, receivers in the user segment typically do not incorporate clocks of such performance. This shortcoming is handled by the use of a fourth GPS satellite signal which provides the data necessary to resolve ambiguities in the multiple timing signals. The result is a universal timing signal available to all GPS receivers in the user segment, accurate to 100ns.

4.2 Software

Processing and dissemination of positioning data is handled on multiple levels in the system architecture as shown in Figure 20. The GPS receiver has an integrated processor to interpret the incoming data from the satellites and package it for efficient transmission to a *RTK-GPS Data Processing PC* as was shown in Figure 17. The PC processes the incoming real-time data stream from the multiple GPS receivers to produce corrected RTK positions for each GPS unit. For small monitoring applications this system provides the end-user with positioning data at an offsite location. For broader applications where widespread data access is required, a server networked to the *RTK-GPS Data Processing PC* is used to capture the processed data stream for data management and dissemination. This server would run a software application developed to filter the data, notify key personnel by email and pager if the data (displacements, velocities, or accelerations) exceeds any predetermined thresholds, generate time-history plots of recorded parameters, generate plan

and elevation views of positioning data over specified time intervals, and publish near real-time plots to an internet web site for clients as shown on the right side of Figure 20.

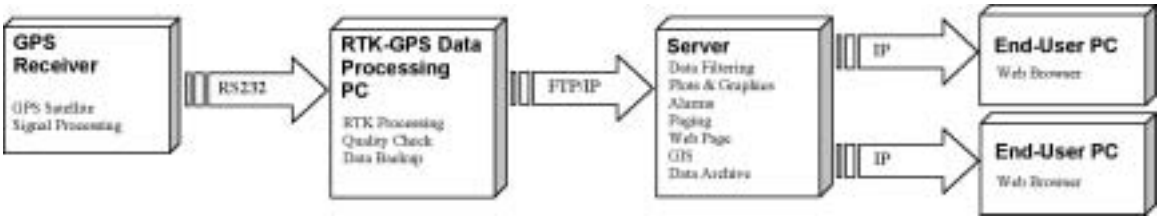

Figure 20 – Data processing architecture

The *RTK-GPS Data Processing PC* provides two main functions in the system architecture: (1) it is the first layer that provides real-time corrected positioning data, and (2) it serves as the primary data backup system in the event of communications or power losses in the downstream components of the system. The *RTK-GPS Data Processing PC* is typically located in close proximity to the GPS units in the field, limited by the range of the wireless communications link, and functions as the data acquisition and logging system. To this end, the *RTK-GPS Data Processing PC* runs two applications, the RTK-GPS processing software, *RTKNav* from Waypoint Consulting, and a data management and FTP server application developed with National Instrument's *LabView*.

RTKNav processes the raw GPS data from multiple GPS receivers, their respective data arriving through multiple serial ports on the field computer. *RTKNav* sends corrected positioning data as a delimited ASCII string through a separate dedicated serial port. The format of the output string, developed by

Waypoint Consulting specifically for this project, includes basic GPS information such as station ID, time, date, latitude, longitude, and elevation. Additional parameters are also included to assist in data quality evaluation. This includes the number of satellites used in the calculations, the position dilution of precision (PDOP), L1 RMS, CA RMS, and an overall quality indicator.

The *LabView* application runs as a parallel application on the data processing PC. The serial data output from *RTKNav* is routed back into another serial port on the field laptop, effectively creating a data stream of corrected positions into the LabView application. The primary function of the application is to evaluate the incoming data to determine the quality of the measurements. High quality measurements are recorded and used in reporting positions. A small fraction of the poor quality measurements are recorded to assist in systems troubleshooting. However, this data is not used in subsequent analyses. A secondary function of the application is to create small archive files of the positioning data. Files containing 3 to 6 minutes of data are created with file names indicative of the date and time of the data. These files are automatically compressed and placed in a specific directory for transfer to a server. Finally, the application turns the data processing PC into a File Transfer Protocol (FTP) Server. The compressed data files are made accessible over an intranet or internet to a server and other registered FTP clients.

4.3 Prototype System

A prototype monitoring system was integrated and deployed at the Caltrans Transportation Laboratory (TransLab) facilities, located at 5900 Folsom Blvd in

Sacramento, California, beginning in September 2000, with a fully operational system in place by early December 2000. The purpose of the prototype system was to subject a fully operational system to real environmental conditions to troubleshoot and correct system deficiencies, identify design improvements, and establish a real-time data stream to facilitate data management applications development. A map of the system deployment is shown in Figure 21. The system consisted of one base and three rover units. The base and one rover unit, R1, were installed on the rooftop of the Structure Materials Annex, a two story concrete structure. The other two rover units were installed on the perimeters of parking lots on the Translab facilities. Data was transmitted using spread spectrum wireless transceivers to a trailer office which housed the data processing PC. A diagram of the rover units with parts list is provided in Appendix C.

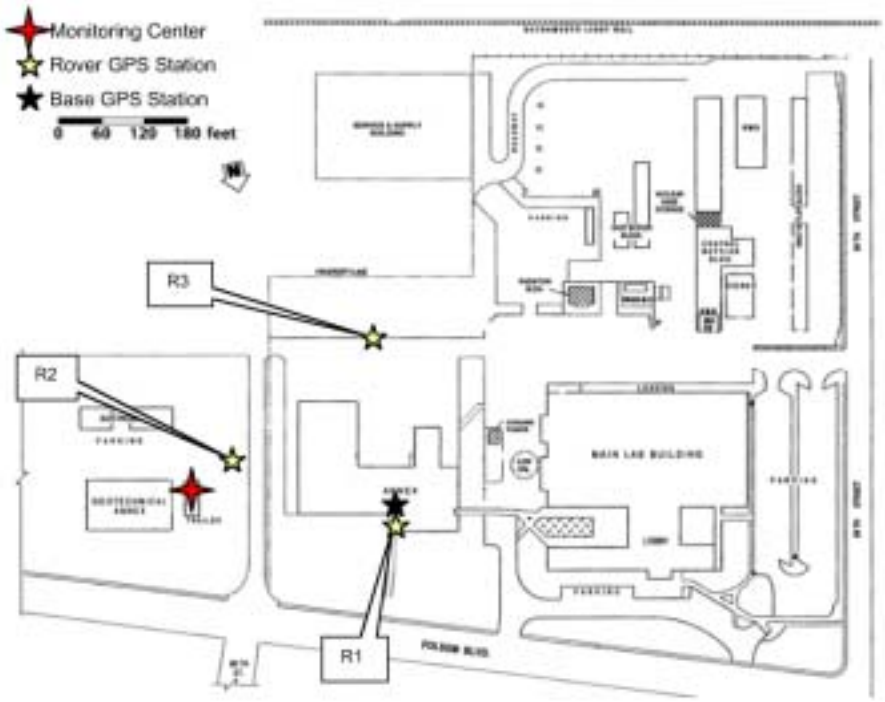

Figure 21 – Prototype system deployment at TransLab

The prototype system was deployed to simulate, as close as possible, the environmental conditions and hardware requirement demands for a landslide monitoring system. Solar and battery power systems were designed and used at the remote locations where no electrical facilities were readily available. Since this is the case with most landslide monitoring sites, an autonomous power supply is the only feasible alternative. Special weatherproof and vented NEMA-3 enclosures were procured to house the electronic and battery power components that were to be located outdoors and exposed to the weather. Mounting hardware, including posts, brackets, and bolts, were sized and selected to provide a durable installation and a relatively stable platform for precision GPS measurements.

In September 2000 the GPS receivers and communications equipment for the base and rover unit, R1, were installed in a single enclosure mounted to a concrete rail on the second floor rooftop of the Structure Materials Annex as shown in Figure 22. Power was supplied by a 120VAC outlet adjacent to the enclosure. The GPS and spread spectrum radio antennas were mounted on steel brackets anchored to a concrete railing.

Figure 22 – Base and Rover R1 unit on top of Structure Materials Building

This particular site was used extensively during earlier validation testing of GPS receivers and antennas. Its optimal rooftop location for satellite tracking, availability of power, and accessibility to system hardware made it an ideal location. Although this setup was not entirely representative of a typical field installation, it served as a good platform for testing and for the location of the base unit.

In November 2000 station R2 was installed in a parking lot near the Electrical Annex building. The installation consisted of the GPS receiver, spread spectrum data transceiver, deep cycle battery, and power regulator components mounted

in an environmental enclosure as shown in Figure 23. The enclosure was mounted to a galvanized steel fence pole which also served as a support for a solar panel , GPS antenna, and yagi radio antenna as shown in Figure 24.

In December 2000 station R3 was installed in the parking lot to the south of the Structure Materials Annex building. As with station R2, the installation consisted of the GPS receiver, spread spectrum radio receiver, gel-cell battery, and regulator hardware mounted in an environmental enclosure. The enclosure was mounted to a galvanized steel fence pole which also served as a support for a solar panel , GPS antenna, and yagi radio antenna as shown in Figure 25.

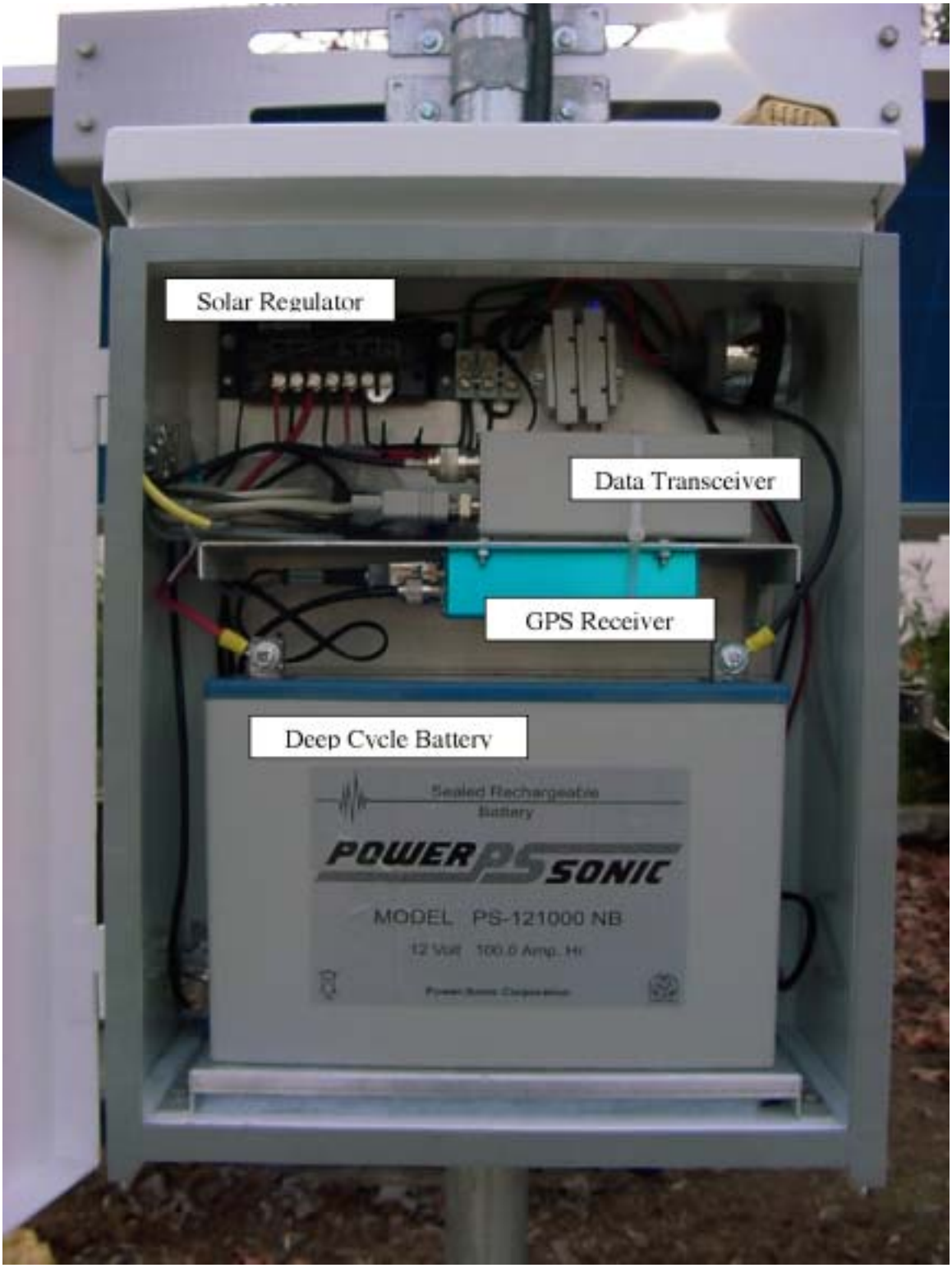

Figure 23 – Equipment enclosure

Figure 24 – Rover R2

Figure 25 – Rover R3

A monitoring center was established in a trailer office which consisted of data transceivers connected to a portable computer. The spread spectrum radios provided the data communication link to the GPS units at the remote stations. Directional yagi antennas were mounted on a mast fixed to the trailer to improve radio signal strength and reduce data loss.

The system was fully operational for over eight months. Rover R3 was removed in the summer of 2001 due to construction activities in the parking lot area. Rovers R1 and R2 continue to operate as of this date and are delivering positioning data in real-time to the office trailer.

The deployment of the prototype system provided an opportunity to evaluate overall system performance and to refine hardware details. In general, the system performed as expected, consistently delivering data throughout the evaluation time. Periods of data loss were typically traceable back to power system or communication failures, or in the case of rover R2, poor initial placement of the unit. R2 was installed in close proximity to a large tree which reduced the efficiency of the solar panel during the winter months. Foliage in the tree also blocked some of the satellite signals and degraded the positioning data during parts of the day. In subsequent field deployments, it will be important to locate the GPS antennas at locations where clear view of the sky is available 360°, and clear of large obstructions (e.g. trees, buildings, walls, etc.) above a conical plane 15° from horizontal. Improvements to system hardware were identified such as the use of tamper resistant connectors, optimized battery capacities, solar panel size and placement, improved wireless transceiver antenna performance, and more efficient packaging.

5.0 Full-Scale Lateral Spread Tests in Japan

5.1 Background

A unique opportunity arose to deploy the Networked RTK system in a controlled test environment for two full-scale earthquake tests conducted in Japan in late 2001. The intention of study was to collect data on the response of civil structures such as bridge foundations, sea walls, and utility pipelines during severe loading induced by earthquakes (Ashford 2001). When shaken, loose saturated sandy soils can undergo a dramatic loss of strength known as *liquefaction*. The occurrence of liquefaction can lead to large ground deformations, or *lateral spread*, that may impart forces on these structures that, to date, are not well understood or quantifiable. Forces due to lateral spread are illustrated in Figure 26. Two full-scale seismic tests were conducted by using controlled blasting techniques to induce liquefaction and lateral spread.

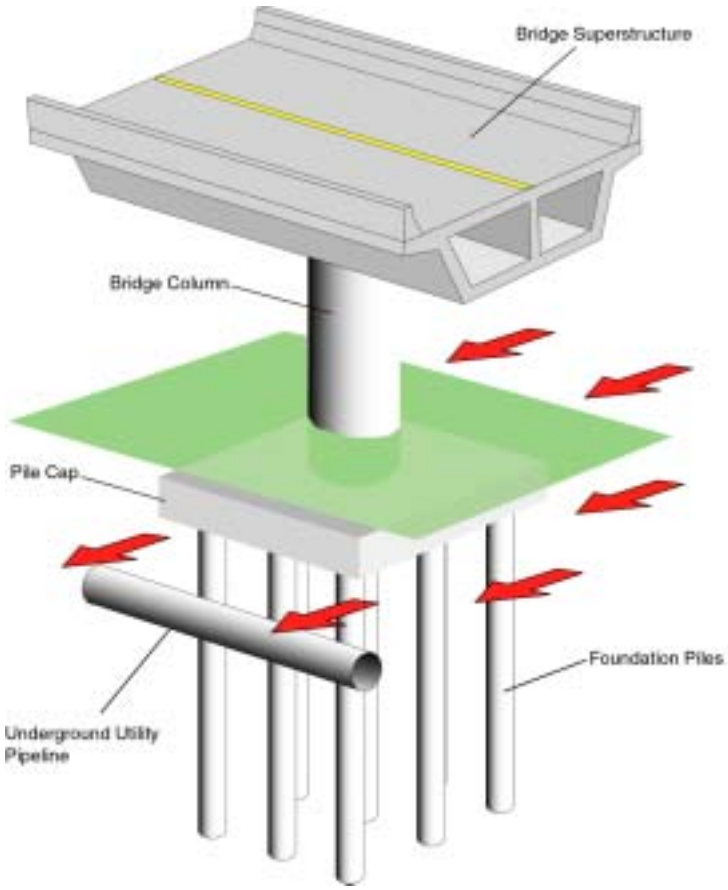

Figure 26 – Lateral spread imparts forces on bridge foundations and lifelines.

A team of researchers from Caltrans were invited to assist with two full-scale seismic tests conducted at the Port of Tokachi on the island of Hokkaido, Japan. The team was led by Loren Turner and included Cliff Roblee and Tom Shantz from the Division of New Technology and Research.

The results presented here were part of an internationally-partnered project involving several universities, research institutes, industrial participants, and governmental agencies from Japan and the United States. The U.S. sponsors supporting the investigation of lateral spread effects on lifeline components are from the Lifelines Program of the Pacific Earthquake Engineering Research

(PEER) Center that includes the California Department of Transportation, the California Energy Commission, and the Pacific Gas & Electric Company. The Japanese sponsors include the Japan Port and Airport Research Institute (PARI), the Japan Civil Engineering Research Institute, Waseda University, University of Tokyo, Kyoto University, Sato Kogyo, Kanden Kogyo, Tokyo Electric Power Company, Japan Gas Association, Japan Association for Marine Structures, Japan Association for Steel Piles, and the Japan Reclamation and Dredging Association.

Accurate measurements of ground deformations during the generated seismic events were a critical component of the research and are extremely difficult to obtain by conventional instrumentation techniques. The use of the GPS network in the Japan tests provided the opportunity to strengthen the experimental control on liquefaction while further demonstrating the Networked RTK systems' capabilities for future remote monitoring applications envisioned for Caltrans.

5.2 Description of the Test Site

The two tests were conducted at the Port of Tokachi, a commercial shipping facility primarily used to transport concrete products and raw materials. As part of a relatively recent effort to expand the port operations and its capacity, additional work areas were created through the conventional use of sea walls and fills. This practice involved the installation of perimeter quay walls which were subsequently filled by hydraulically placing soils. The soil type, the construction method, and groundwater conditions all contributed to a site highly susceptible to liquefaction and lateral spread.

For the first test in November 2001, the test site was comprised of an area approximately 25m wide by 100m long. One end of the site was bordered by a large waterway with the soil retained by a quay wall as shown in Figure 27. Moving away from the water, the ground surface sloped gently upwards such that the other end of the site was approximately 2.00m higher. The ground surface elevation near the sea wall was +3.00m, and the ground surface elevation at the top of the slope was +5.00m. The waterway elevation fluctuated throughout the day, as did the groundwater elevation, between 0.00m and +2.00m as a result of the proximity to the Pacific Ocean. The entire test area was surrounded by sheet piling installed to tip elevation -9.00m in the vicinity of the quay wall, and elevation –5.00m everywhere else. Figure 28 shows the site layout.

Figure 27 – November 2001 test site.

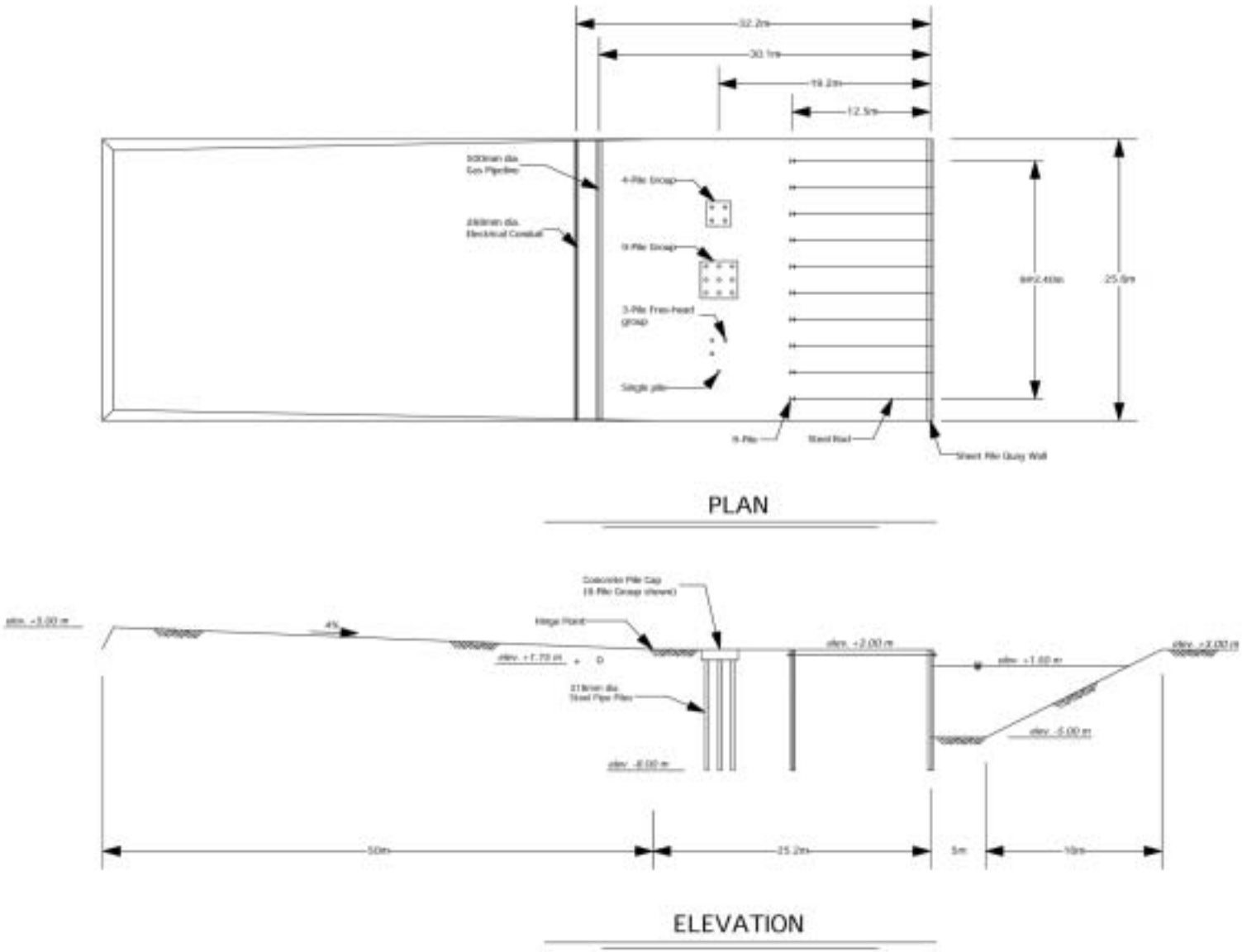

Figure 28 – Test Site Layout, November 2001 Test

For the second test in December 2001, the test site was significantly modified in an attempt to induce additional ground deformations. The quay walls and perimeter sheet piling installed as part of the first test were removed, since they tended to impede displacements. Additionally, the test site was regraded to create a steeper slope as shown in Figures 29 and 30.

Figure 29 – December 2001 test site.

Several full-scale test specimens were placed within the test zone for evaluation under lateral spread. These included four sets of pipe pile foundations and three underground utility pipelines. Figures 28 and 30 show the locations of the test specimens.

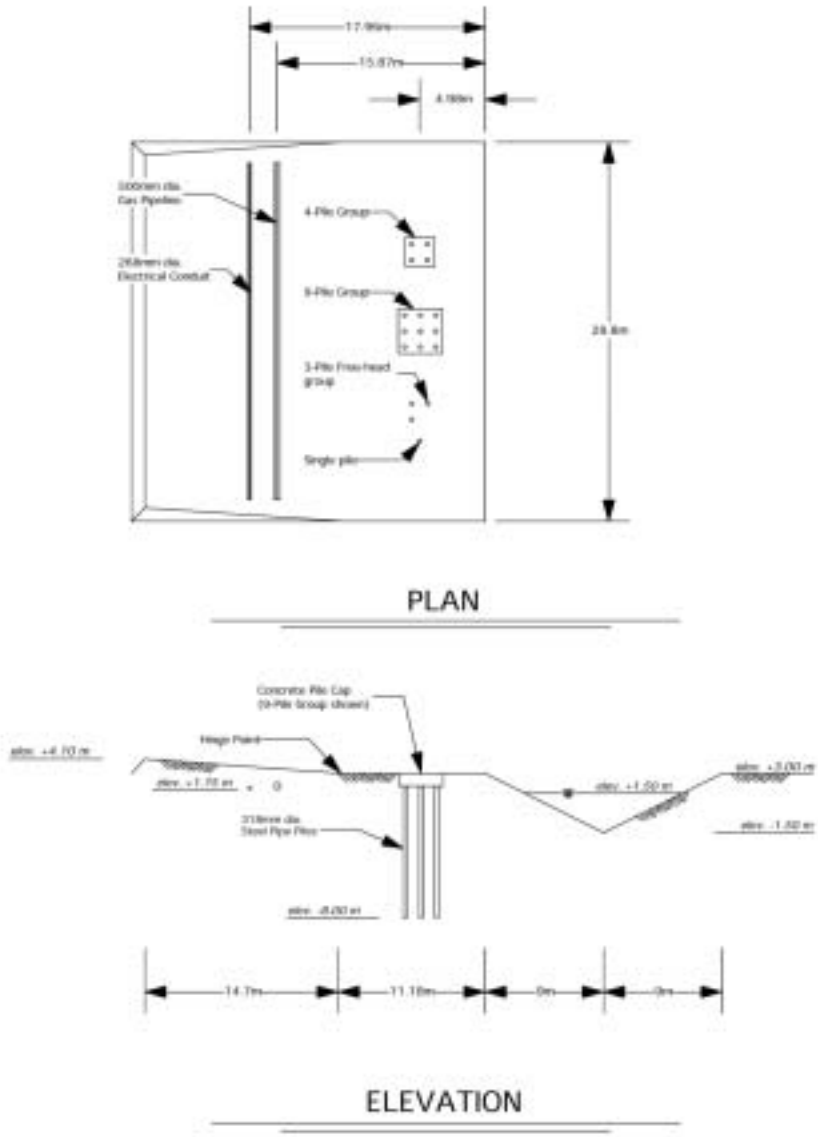

Figure 30 – Test Site Layout, December 2001 Test

Subsurface conditions at the site were characterized by hydraulically placed sandy fill underlain by very dense native gravels as shown in Figure 31. Very loose sand extended from a ground surface elevation of +3.00m down to elevation –0.80m. Uncorrected Standard Penetration Test (SPT) blow counts ranged from 1 to 5 blows per foot in this layer. From elevation –0.40m to elevation –4.30m was sandy silt to soft clay. Uncorrected SPT blow counts ranged from 0 to 2 blows per foot in this layer. Below elevation –4.30m the soil was found to be medium dense sand to very dense gravel with uncorrected SPT blow counts greater than 50 blows per foot.

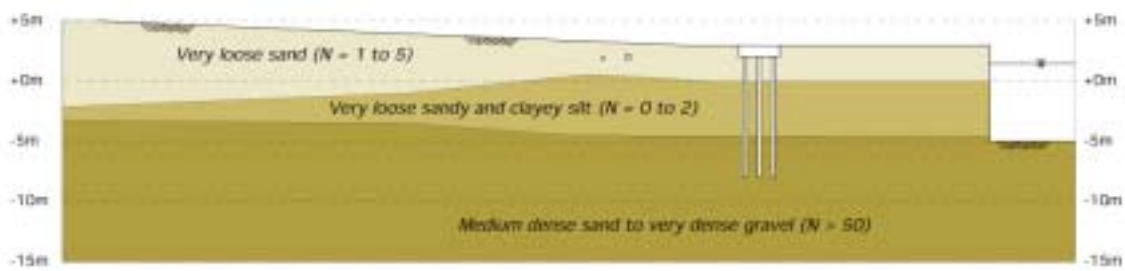

Figure 31 – Subsurface site conditions

The pipe piles for all of the deep foundations were 318mm diameter with wall thickness of 10.5mm, a nominal length of 10m, and constructed of 400MPa yield strength steel. Piles were installed using impact driving methods. In two of the deep foundations, the pile tops were fixed from rotation by reinforced concrete pile caps that were 1m thick. This included a nine pile group arranged in a 3x3 matrix, and a four pile group arranged in a 2x2 matrix, both employing 3.5 pile diameters center-to-center spacing for the piles. Most of the piles in these two

groups were driven full length to an approximate elevation of –8.00m. These piles were driven well into the denser soils to generate fixity at the pile tips. A three pile group was installed at 3.5 pile diameters center-to-center spacing without a pile cap allowing free rotation at the pile head. On average, these piles were driven to an approximate elevation of –5.60m leaving 1.40m of the pile above ground. Since these piles were not driven far into the denser soil layer, fixity of the pile tips was not certain. Finally, a single pile was installed, also allowing for free rotation at the pile head. This pile was driven to elevation –8.17m leaving 0.33m of the pile above ground. As with the four pile and nine pile groups, this pile was driven well into the denser soils to generate fixity at the pile tip.

Although three underground utility pipelines were installed and instrumented in the test site, only two of them were instrumented with GPS sensors. The two pipelines, a gas pipeline and an electrical conduit, were oriented transversely across the site and were anchored at either end to the sheet pile wall bordering the site limits. The connections to the sheet pile wall were designed to allow for some rotation at the ends of the pipes. The gas pipeline consisted of a 500mm diameter steel pipe with a wall thickness of 6mm and yield strength of 400MPa. The electrical conduit consisted of a 268mm diameter pipe with a wall thickness of 6mm and yield strength of 400MPa. Both pipelines were approximately 25m in length. The two pipelines were installed within 2m of each other in a single excavated trench 3.10m wide and 1.45m deep. The bottoms of both pipelines were set at elevation +1.75m. The trench was backfilled in multiple compacted layers.

5.3 Deployment of the GPS Field Units

A total of twelve GPS units were deployed for the tests. Two of the units served as reference base stations at an offsite monitoring center. The ten remaining units were deployed throughout the site to measure movements of the ground surface, pile foundations, and pipelines. Each of the ten field units were comprised of a GPS receiver and antenna, wireless data transceiver and antenna, and battery backup power system. The equipment was packaged in small weatherproof enclosures to which the GPS and wireless transceiver antennas were attached as shown in Figure 32. The components of a typical field unit consisting of the equipment enclosure, wireless transceiver antenna, and GPS antenna are shown in Figure 33. A detailed listing of parts is included in Appendix D.

Figure 32 – Equipment enclosure housing the GPS receiver, wireless equipment, and backup power system

Figure 33 – Typical field unit with equipment enclosure (left), wireless transceiver antenna (center), and GPS antenna (right).

The locations of the GPS field units are summarized in Tables 3 and 4, and Figures 34 and 35, for the November and December tests, respectively. The layouts for both tests were identical with the exception of the location of Unit 2E. The GPS units used for the tests were the dual frequency Topcon Legacy receivers.

GPS Unit Desig.	Location of GPS Antenna
1A	Mounted to concrete pile cap for 9-pile group
1B	Mounted directly to top of slope inclinometer casing, ~1.6m in front of 9-pile group
1C	Mounted to raft and secured to slope inclinometer casing, ~6.9m in front of 9-pile group
1D	Mounted to the top of the single pile
1E	Mounted to slope inclinometer casing, ~1.0m in front of the single pile
2A	Mounted to concrete pile cap for 4-pile group
2B	Mounted to raft and secured to slope inclinometer casing, ~10.4m in front of 4-pile group
2C	Mounted to the top of the leading pile in the 3-pile free-headed pile group.
2D	Mounted to a vertical post affixed to the gas pipeline
2E	Mounted to a vertical post affixed to the electrical conduit

Table 3 – Location of GPS field units for November 2001 test

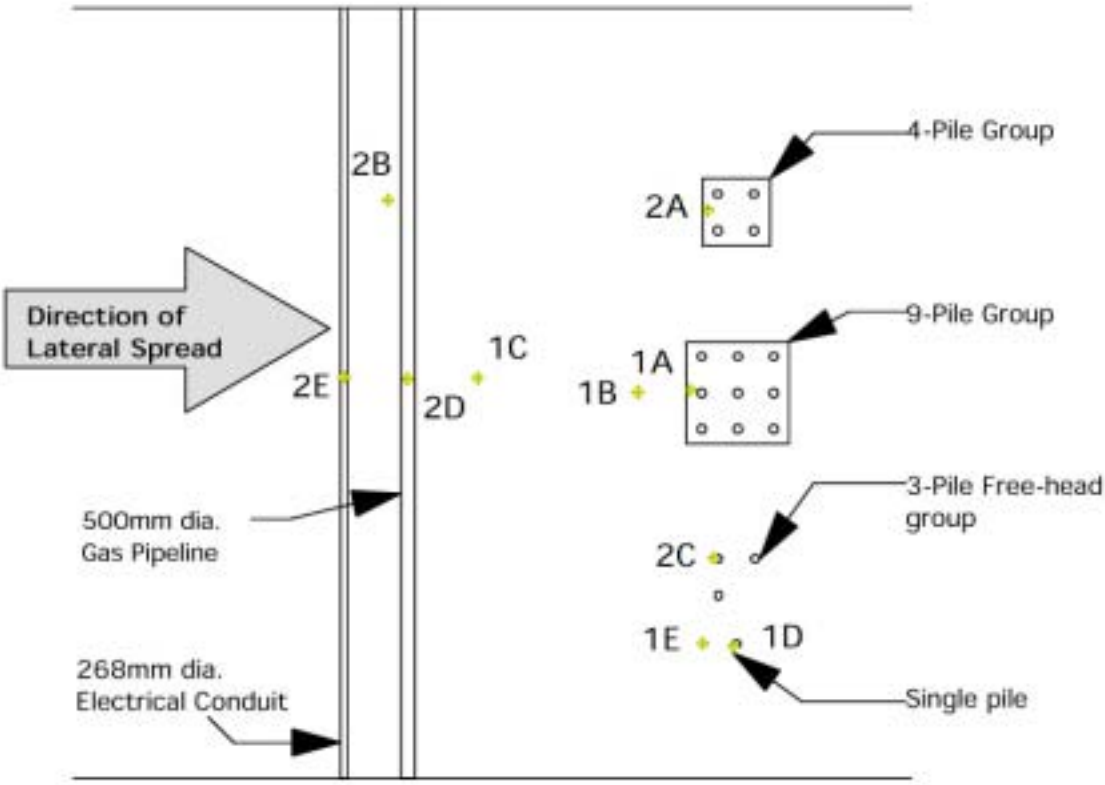

Figure 34 – Layout of GPS field units for November 2001 test

GPS Unit Desig.	Location of GPS Antenna
1A	Mounted to concrete pile cap for 9-pile group
1B	Mounted directly to top of slope inclinometer casing, ~1.5m in front of 9-pile group
1C	Mounted directly to top of slope inclinometer casing, ~7.2m in front of 9-pile group
1D	Mounted to the top of the single pile
1E	Mounted directly to top of slope inclinometer casing, ~1.0m in front of the single pile
2A	Mounted to concrete pile cap for 4-pile group
2B	Mounted directly to top of slope inclinometer casing, ~10.8m in front of 4-pile group
2C	Mounted to the top of the leading pile in the 3-pile free-headed pile group.
2D	Mounted to a vertical post affixed to the gas pipeline
2E	Mounted directly to top of slope inclinometer casing, between 4-pile and 9-pile groups

Table 4 – Location of GPS field units for December 2001 test

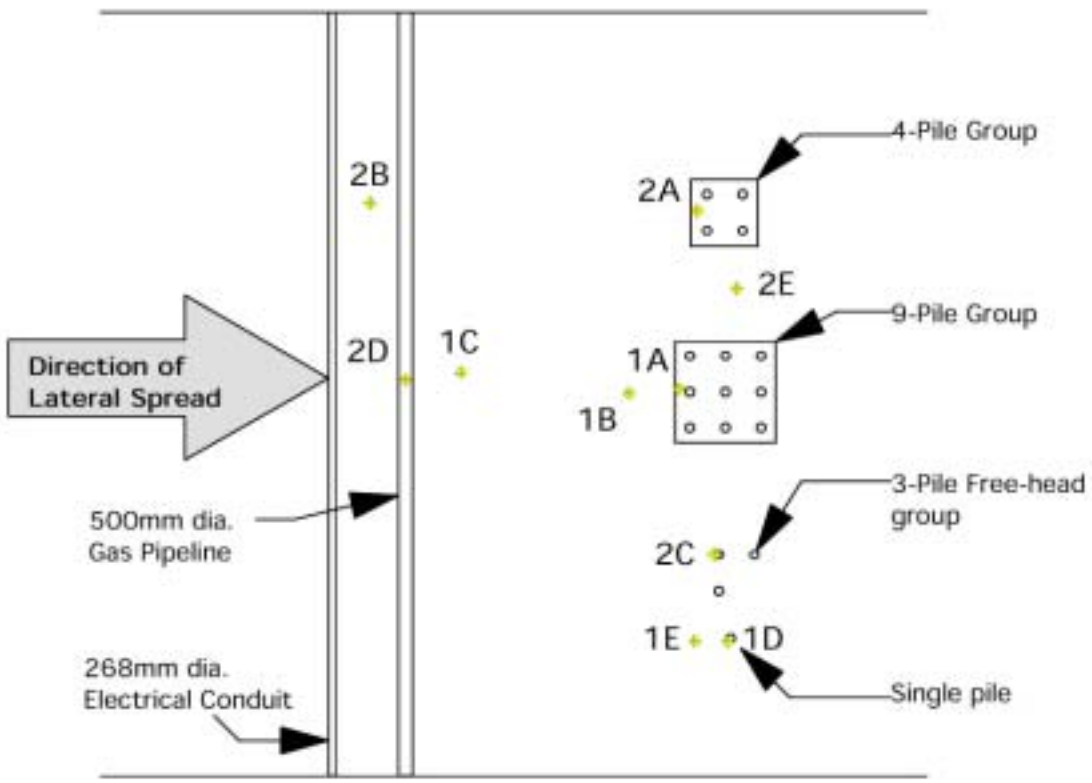

Figure 35 – Layout of GPS field units for December 2001 test

The center of the GPS antenna for Unit 1A was located near the front edge on the concrete pile cap for the 9-pile group. The mid-height of the antenna was positioned 43.5cm above the top concrete surface using steel brackets and threaded rod. The antenna was mounted at this location for both the November and December tests. Figure 36 provides details on the installation of the GPS antenna at this location.

The center of the GPS antenna for Unit 1B was located on top of a slope inclinometer casing. The antenna was mounted on to a threaded rod which was attached to the inclinometer casing. For the November test the mid-height of the antenna was positioned 51.2cm above the ground surface (approximated by the elevation of the surface of the pile cap) and 17.5cm above the top of the inclinometer casing. For the December test the mid-height of the antenna was repositioned 66.6cm above the ground surface. Figure 36 shows the dimensions of the position for both the November and December tests for Unit 1B.

The GPS receiver, wireless communications, and power components for Units 1A and 1B were housed in a weatherproof enclosures which were then secured to the pile cap for the 9-pile group. Photos of the installation of Units 1A and 1B for the November test are shown in Figures 37 and 38. A photo of Unit 1A for the December test is shown in Figure 39.

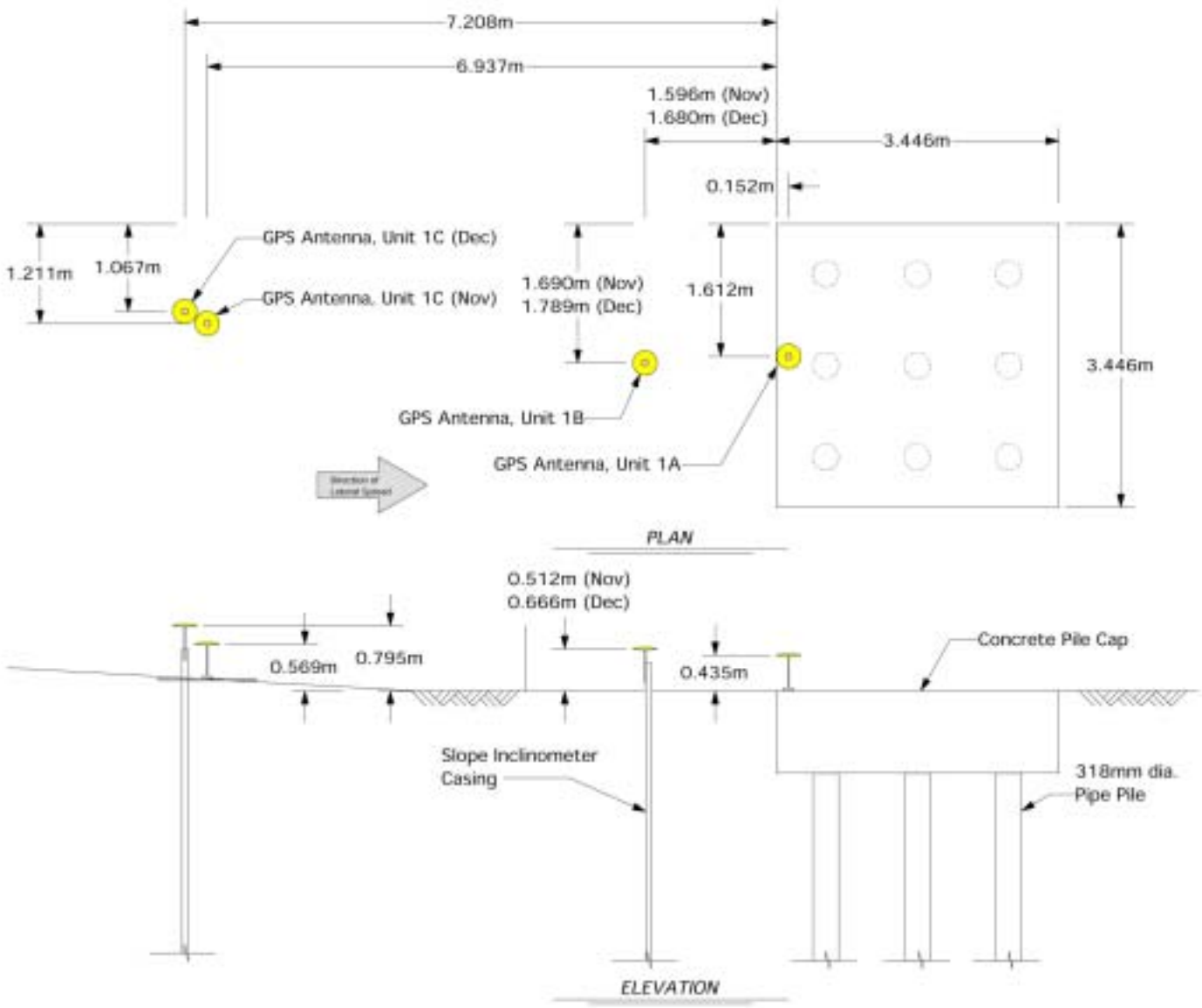

Figure 36 – Position of Units 1A, 1B, and 1C

Figure 37 – Units 1A and 1B, November Test

Figure 38 – Units 1A and 1B, November Test

Figure 39 – Unit 1A, December Test

Unit 1C was affixed to a raft that was tethered to a nearby slope inclinometer casing for the November test. The purpose of this particular installation method was to measure an average displacement of the ground at the location of the inclinometer casing while removing any secondary displacements resulting from tilting and rotation of the casing. To this end a square 1.2m by 1.2m raft was constructed from 10mm thick plywood. The mid-height of the antenna was positioned 42.5cm above the raft surface using steel brackets and threaded rod as shown in Figure 40. The raft was attached to the slope inclinometer casing using steel tie wire and was anchored to the ground using wooden stakes driven approximately 45cm into the soil. A separate raft was constructed to support the

enclosure for the GPS receiver, wireless communications, and power components.

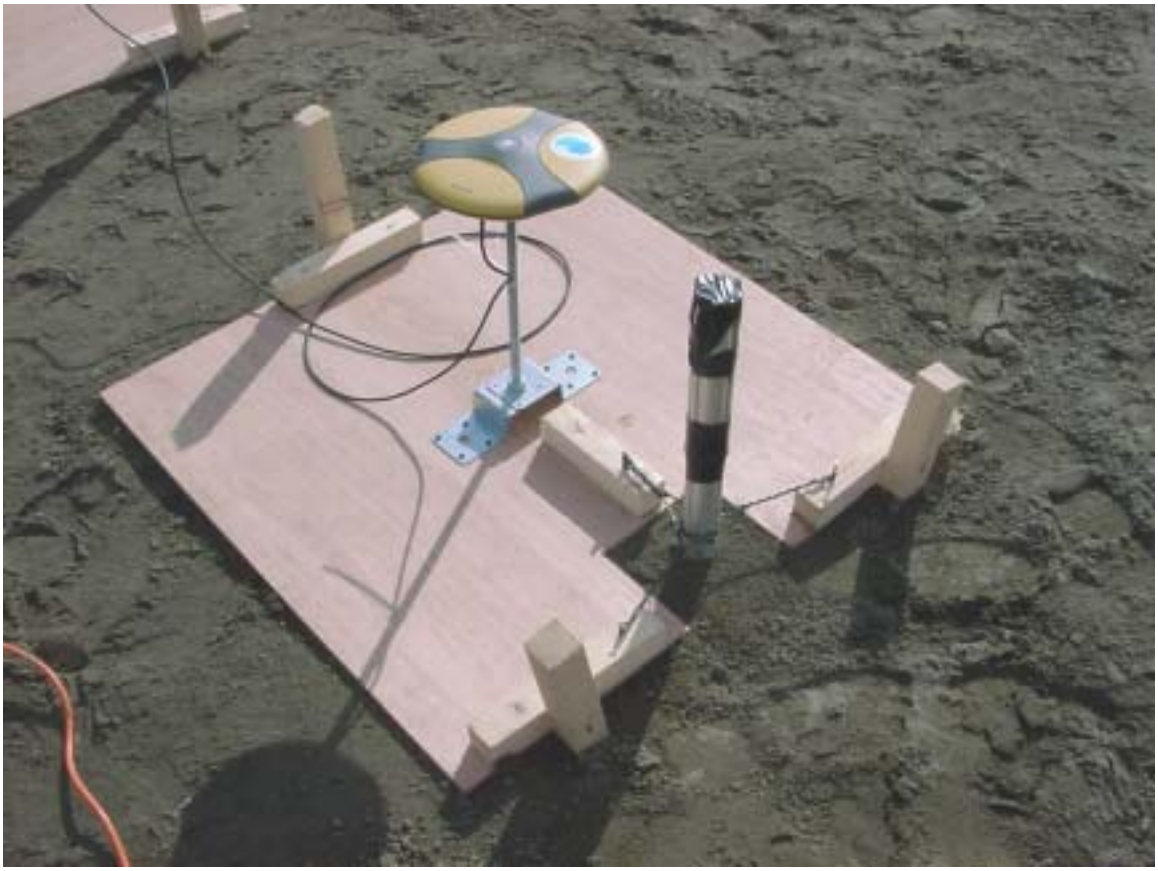

Figure 40 – Unit 1C, November test

For the December test, the raft was not used, and the GPS antenna was located on top of the slope inclinometer casing as shown in Figure 41. The antenna was mounted on to a threaded rod which was attached to the inclinometer casing. The mid-height of the antenna was positioned 79.5cm above the elevation of the surface of the pile cap. Details of both the November and December installation of Unit 1C are shown in Figure 33.

Figure 41 – Unit 1C, December test

Units 1D, 1E, and 2C were positioned to monitor the displacements of the free-head pile specimens and the surrounding ground surface as shown in Figure 42. Unit 1D was mounted to the single pile specimen. The mid-height of the GPS antenna was positioned 35.3cm above the top of the pile and approximately 77.5cm above the ground surface. Unit 1E was mounted to the top of a slope inclinometer casing and was positioned 17.5cm above the top of the pile and approximately 66.5cm above the ground surface. This unit was set approximately 1m in front of the single pile to provide a measurement of near field ground displacements for the pile during the lateral spread.

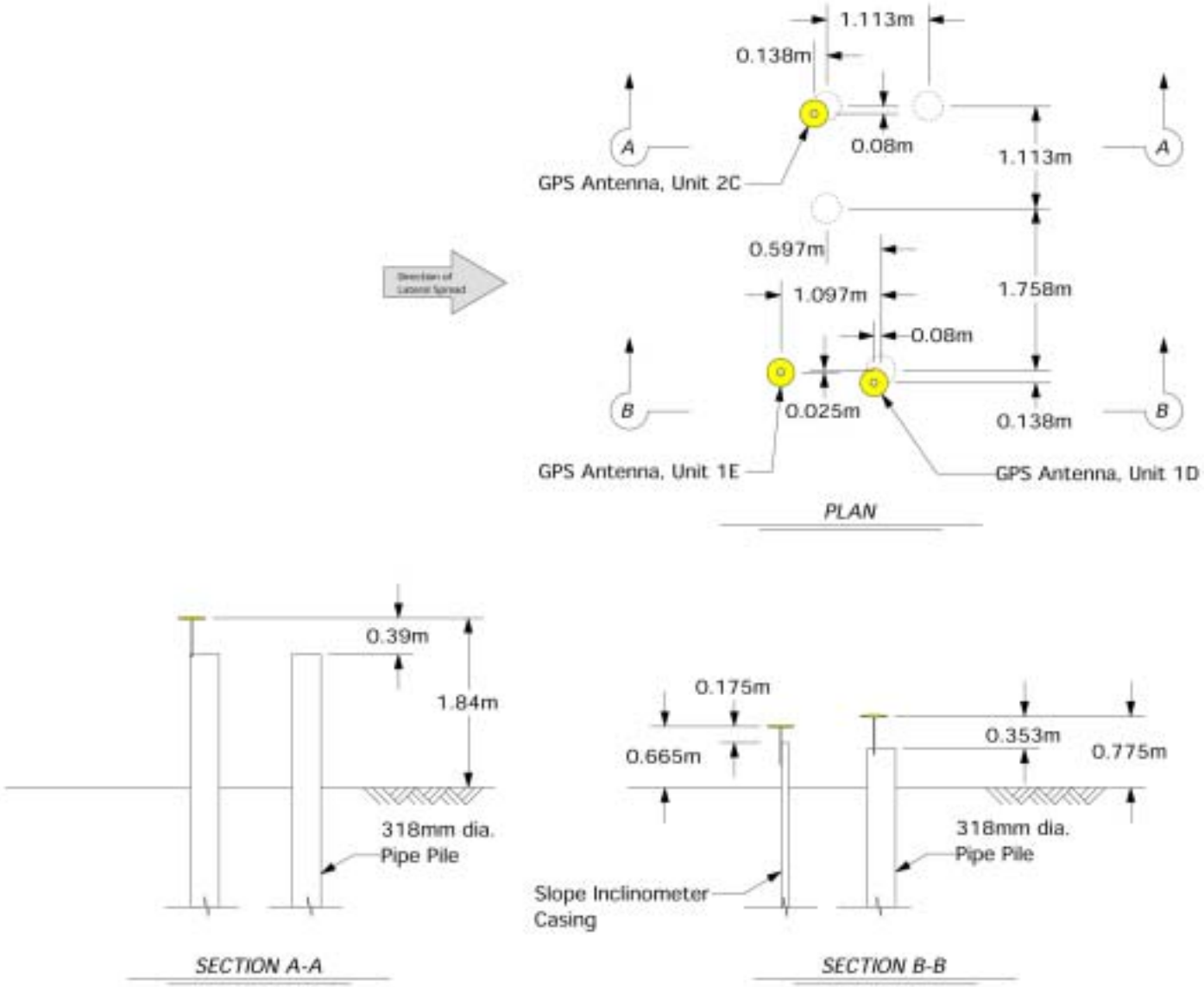

Figure 42 - Position of Units 1D, 1E, and 2C

Unit 2C was mounted to top of the leading pile in the 3-pile free head group. The mid-height of the GPS antenna was mounted 39.0cm above the pile top and approximately 184.0cm above the ground surface. For all of these units, threaded rod and steel brackets were used to secure the antennas to the piles or casings.

The GPS receiver, wireless communications, and power components for Units 1D, 1E, and 2C were housed in a weatherproof enclosures which were attached by wire to the piles. Photos of the installation of Units 1D, 1E, and 2C are shown in Figures 43 and 44.

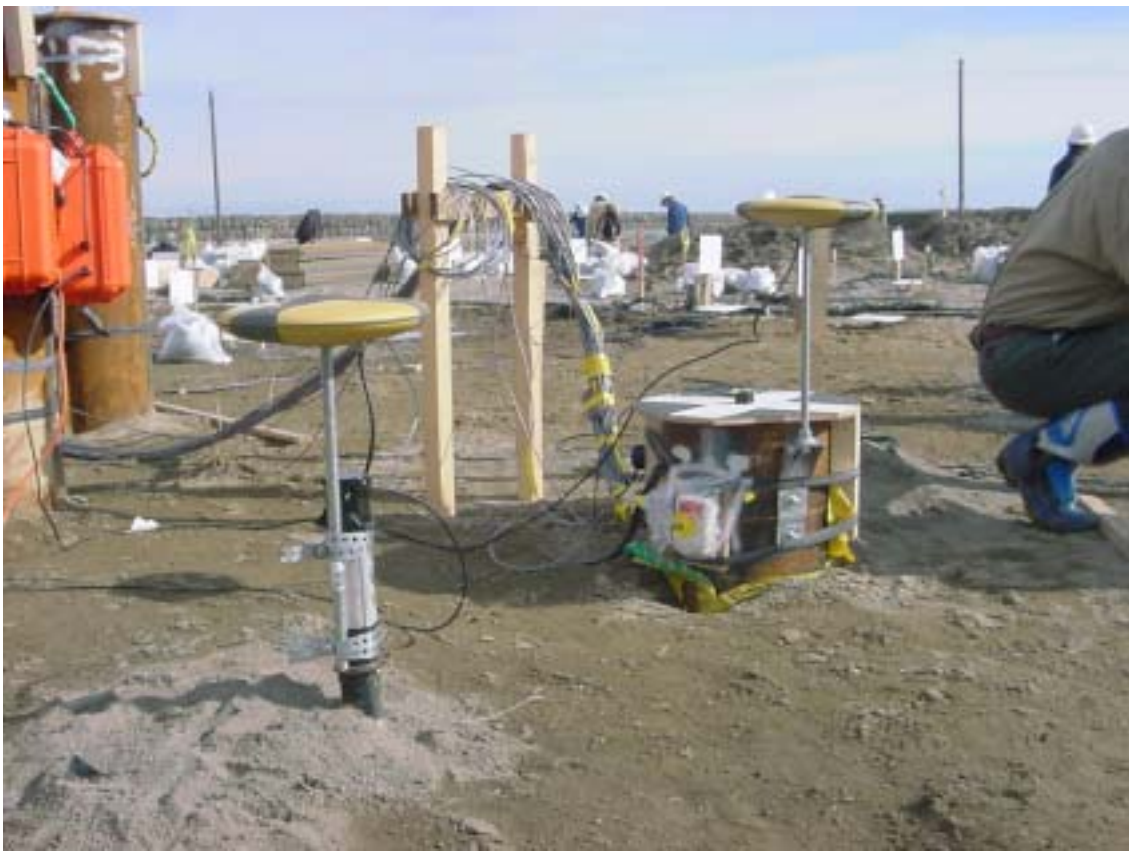

Figure 43 – Units 1D and 1E, November test

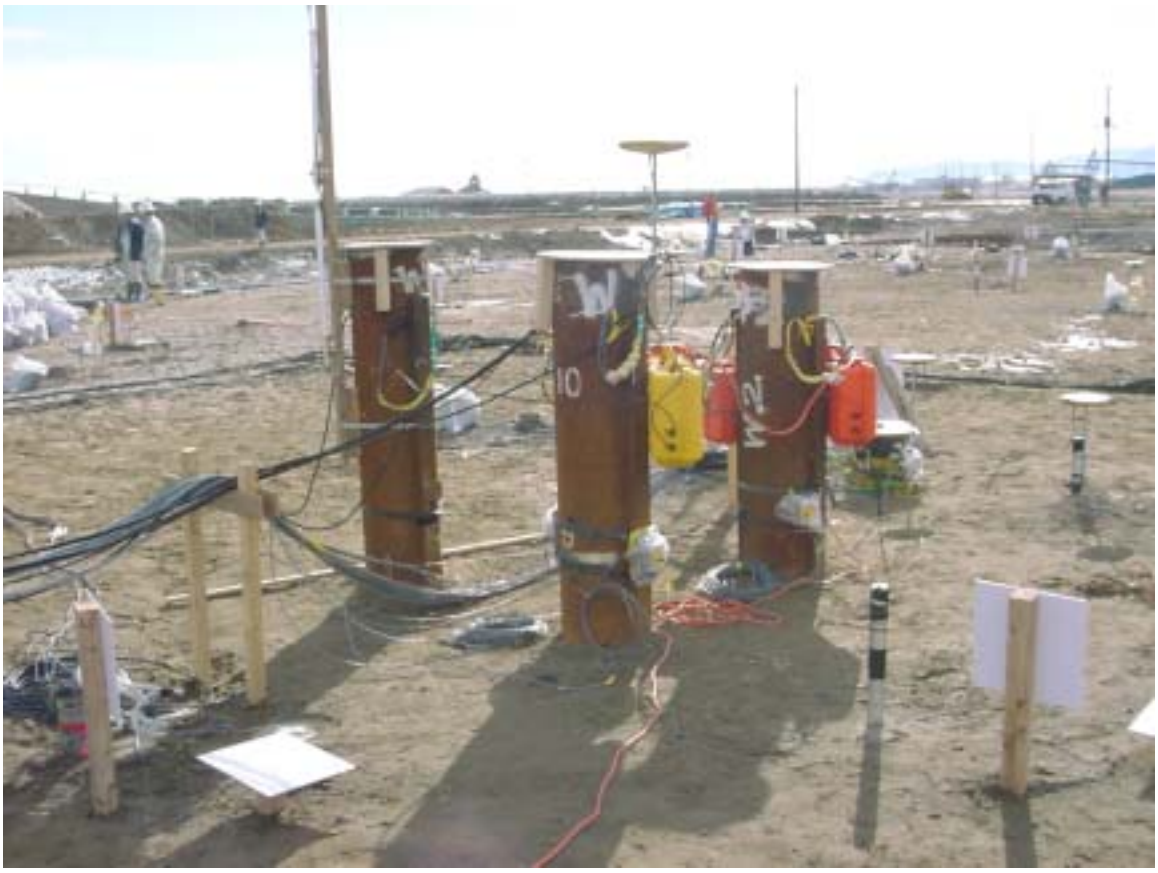

Figure 44 – Units 1D, 1E, and 2C, November test

The center of the GPS antenna for Unit 2A was located near the front edge on the concrete pile cap for the 4-pile group. The mid-height of the antenna was positioned 43.5cm above the top concrete surface using steel brackets and threaded rod. The antenna was mounted at this location for both the November and December tests. Figure 45 provides details on the installation of the GPS antenna at this location.

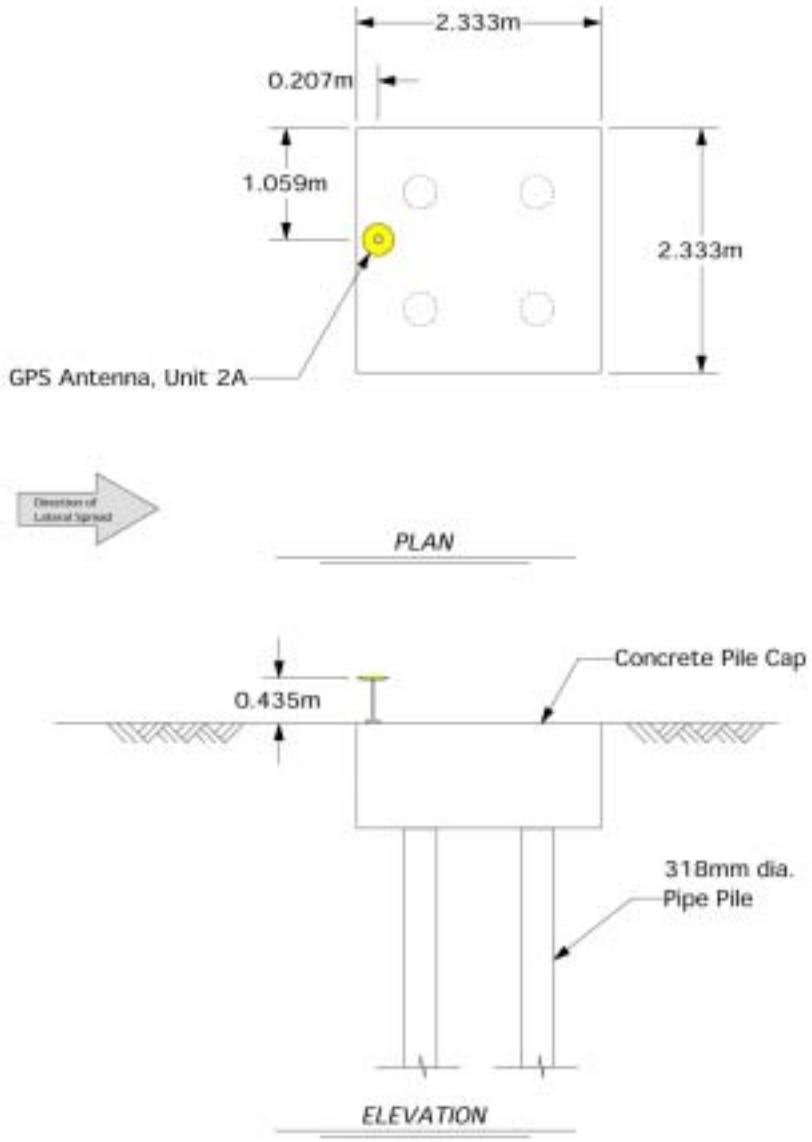

Figure 45 - Position of Unit 2A

Similar to the installation on the 9-pile cap, the GPS antenna for the 4-pile group cap was mounted to the top concrete surface using steel brackets and threaded rod, and the equipment enclosure was secured to the pile cap. A photo of the installation is shown in Figure 46.

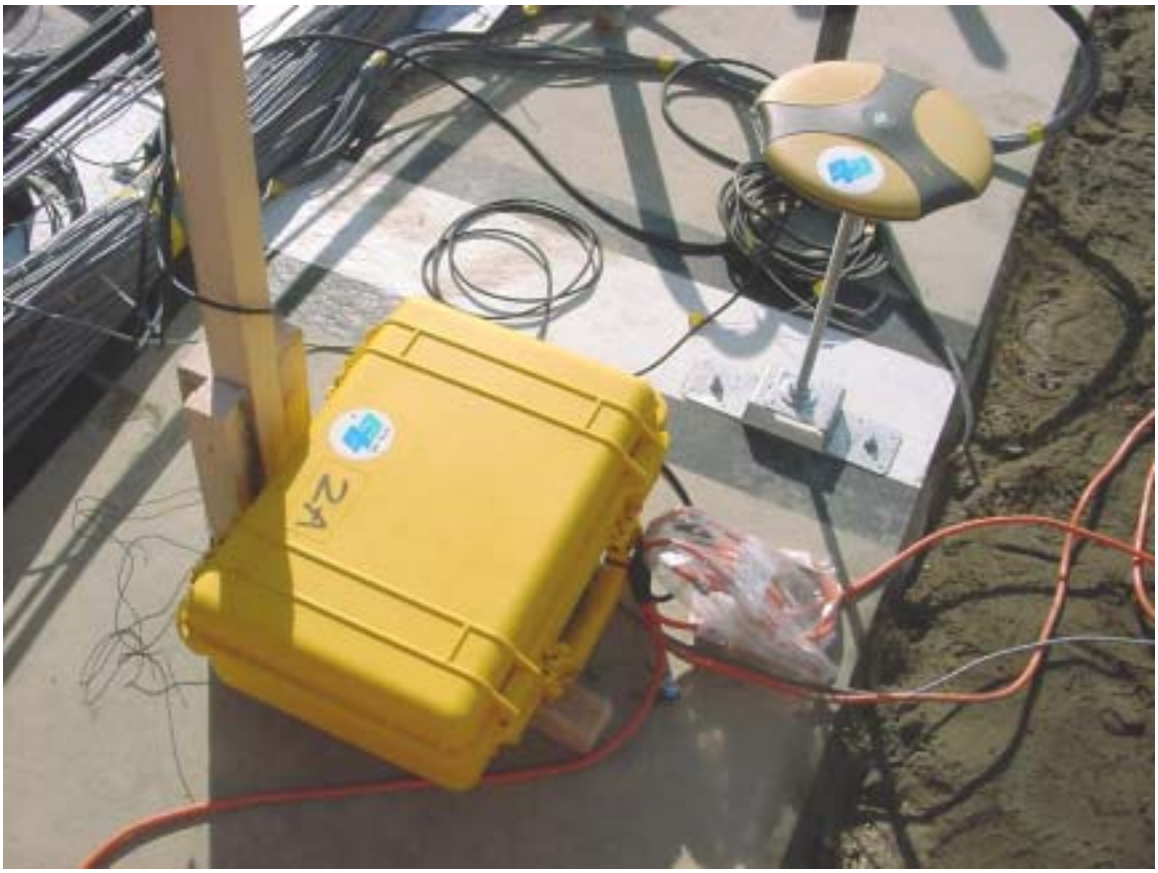

Figure 46 – Unit 2A

Unit 2B was positioned approximately 10.4m in front of and in line with the 4-pile group as shown in Figure 47. Similar to the installation of Unit 1C, Unit 2B was affixed to a raft that was tethered to a nearby slope inclinometer casing for the November test. The mid-height of the antenna was positioned 43.9cm above the raft surface.

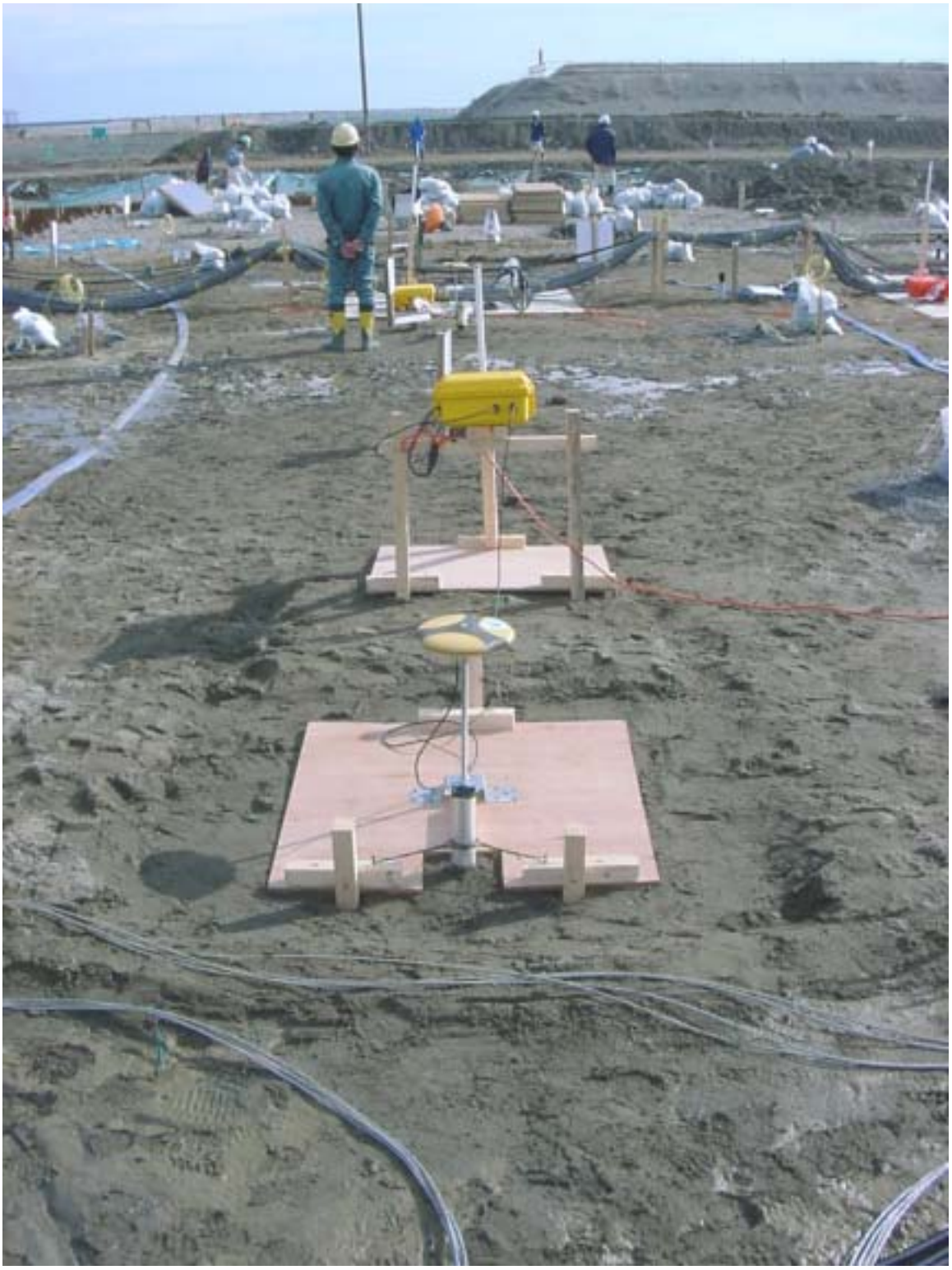

Figure 47 – Unit 2B, November Test

For the December test, the raft was not used, and the GPS antenna was mounted directly to the top of the slope inclinometer casing as shown in Figure 48. The mid-height of the antenna was positioned 79.5cm above the elevation of the surface of the pile cap.

Figure 48 – Unit 2B, December Test

For the November test Units 2D and 2E were installed to measure displacements of the two underground pipeline specimens. Since both utility pipelines were buried below ground, 50mm diameter 1.5m long vertical steel standpipes were welded to the utility pipelines to provide an above ground GPS antenna mount.

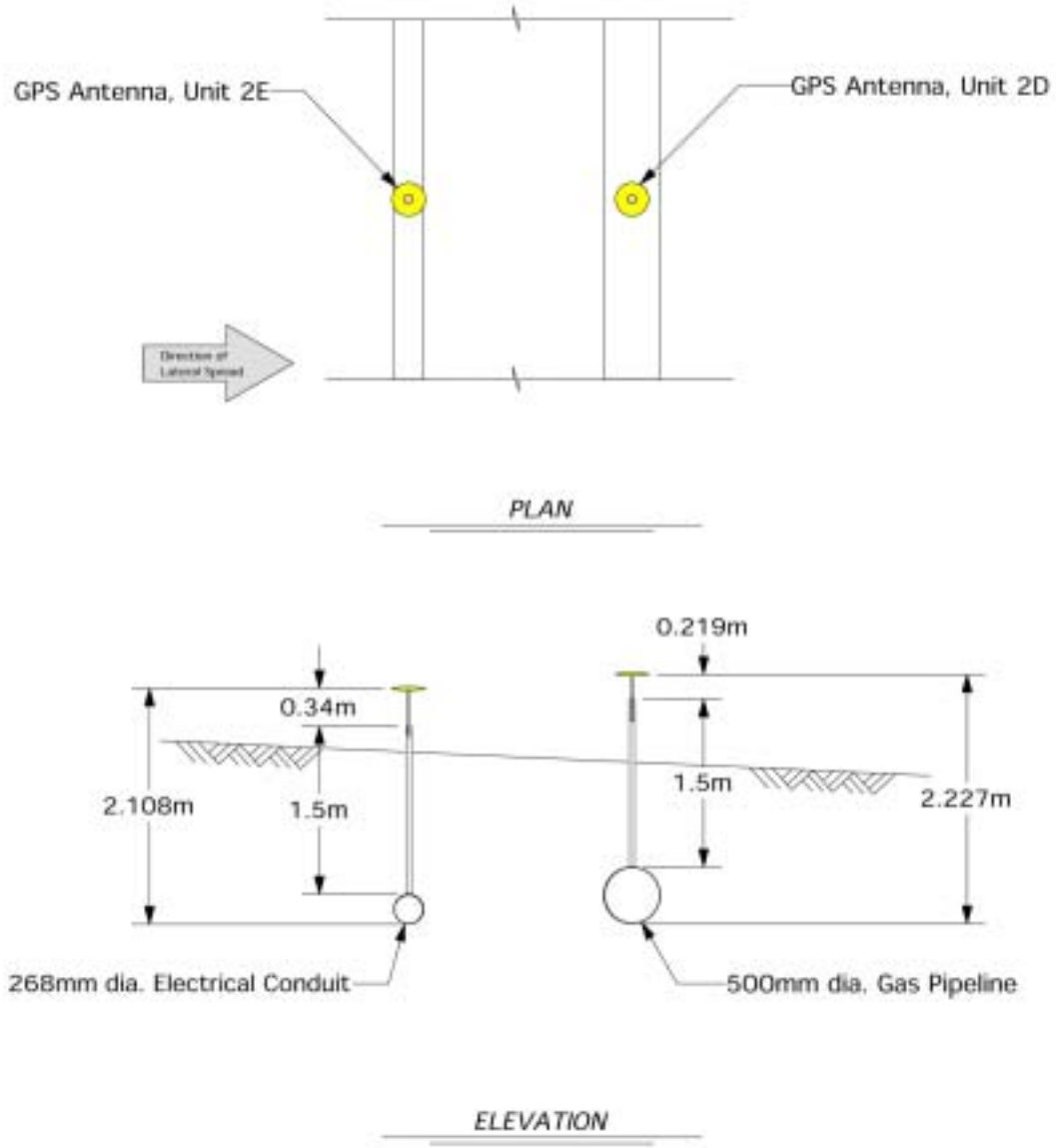

Figure 49 – Units 2D and 2E, November Test

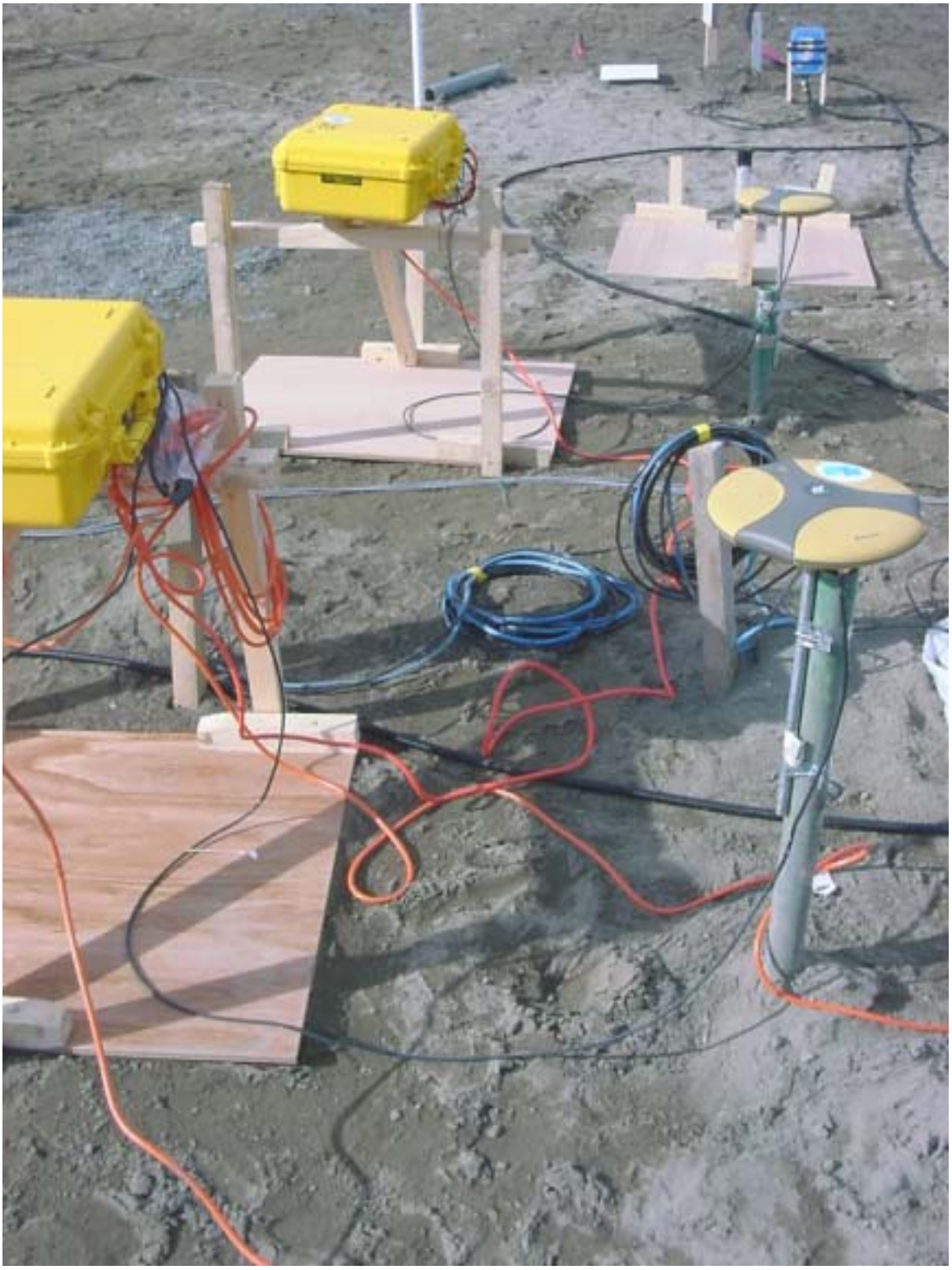

Figure 50 – Units 2D and 2E, November Test

The mid-height of the GPS antennas were 21.9cm and 34.0cm above the tops of the vertical standpipes for Units 2D and 2E, respectively. This configuration allowed above ground measurements for subsurface pipe displacements. Figure 49 provides details on the installation of Units 2D and 2E for the November test. Figure 50 shows a photo from the November test.

For the December test, Unit 2E was removed from the electrical conduit and repositioned on a slope inclinometer casing between the 4-pile group cap and the 9-pile group cap. The mid-height of the GPS antenna was positioned approximately 47.7cm above the ground surface as approximated by the elevation of the surface of the adjacent pile caps. The equipment enclosure was secured to the pile cap for the 4-pile group. Figure 51 shows the position of Unit 2E relative to the adjacent pile groups.

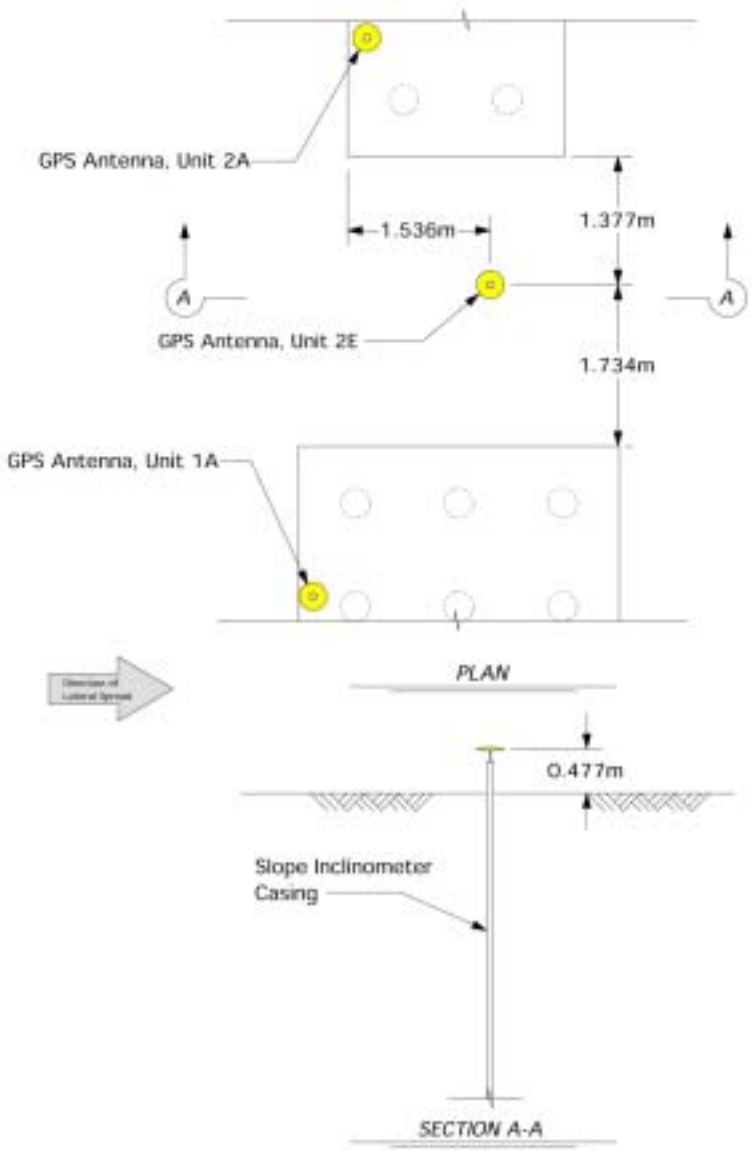

Figure 51 – Unit 2E, December Test

5.4 Monitoring Center

A monitoring center was established approximately 100m away from the blast zone in a temporary trailer office. The monitoring center provided a safe offsite environment for Caltrans staff to observe the test during blasting while monitoring the processing status of the GPS field units. A photo of the monitoring center is shown in Figure 52.

Two base stations were utilized to process the data from the ten field units. Each base station unit was comprised of a GPS receiver and antenna, five wireless data transceivers, and a laptop computer with the RTK-GPS processing software. These components were packaged in a large weatherproof enclosure as shown in Figure 53. A detailed list of equipment is included in Appendix D. A single base station unit could have been used to capture the data for all ten field units, however, the throughput limitations of the wireless data transceivers coupled with the substantial data logging demands of the laptop computer necessitated splitting the processing and data logging tasks between two computers.

The GPS antennas for the two base stations were mounted to the tops of steel poles affixed to the roof of the trailer. This location was chosen to limit potential multipath and line-of-sight errors resulting from nearby steel scaffolding. Additional guy wires and bracing were used to stabilize the poles from wind and other vibration sources. The antennas for the wireless transceivers were also mounted to the pole and provided good line-of-sight with the field units.

Figure 52 – Monitoring center trailer

Figure 53 – Monitoring center unit

5.5 Creating the Lateral Spread

The ground deformations associated with lateral spread were created by using explosives to induce liquefaction throughout the test site. In preparation for both the November and December tests, a Japanese blasting contractor installed multiple explosives in vertically drilled holes spaced at 6.0m on centers in a regular grid pattern throughout the test site as shown in Figure 54. Two explosive charges were placed in each of the blast holes, shallow charges at elevation –0.500m and deeper charges at elevation –4.500m.

Figure 54 – Placing explosives

The blasting sequence was planned such that the explosives at the back corner of the site, farthest from the waterway, would be detonated initially. Blasting proceeded sequentially to adjacent holes in the same row and then moved to the next row proceeding towards the front of the site as shown in Figure 55.

Secondary additional explosives were placed around the perimeter of the test site adjacent to the surrounding sheet pile wall for the November test. These explosives were detonated following the initial blast sequence within the test area. The purpose of these explosives was to loosen the soil adjacent to the sheet pile to allow unimpeded flow of soil within the test area. Sets of tertiary explosives were placed adjacent to the steel tie back rods for the quay wall. These explosives were designed specifically to break the tie back rods, thus allowing more displacement throughout the site. Since the quay wall was expected to effectively retain the liquefied soil following the primary and secondary blasts, the tertiary blasting was necessary to fail the wall to allow the soil to displace beyond the limits of the test area.

For the December test, the sheet pile walls were removed and, as such, additional blasting around the perimeter was not necessary. However, an additional row of explosives were placed on the steeper 2:1 slope between the pile groups and the waterway. These explosives were intended to loosen the toe of the sloped test site to encourage displacements similar to a theoretical infinite slope failure. These explosives were detonated approximately 15 seconds prior to initiating the full blasting sequence.

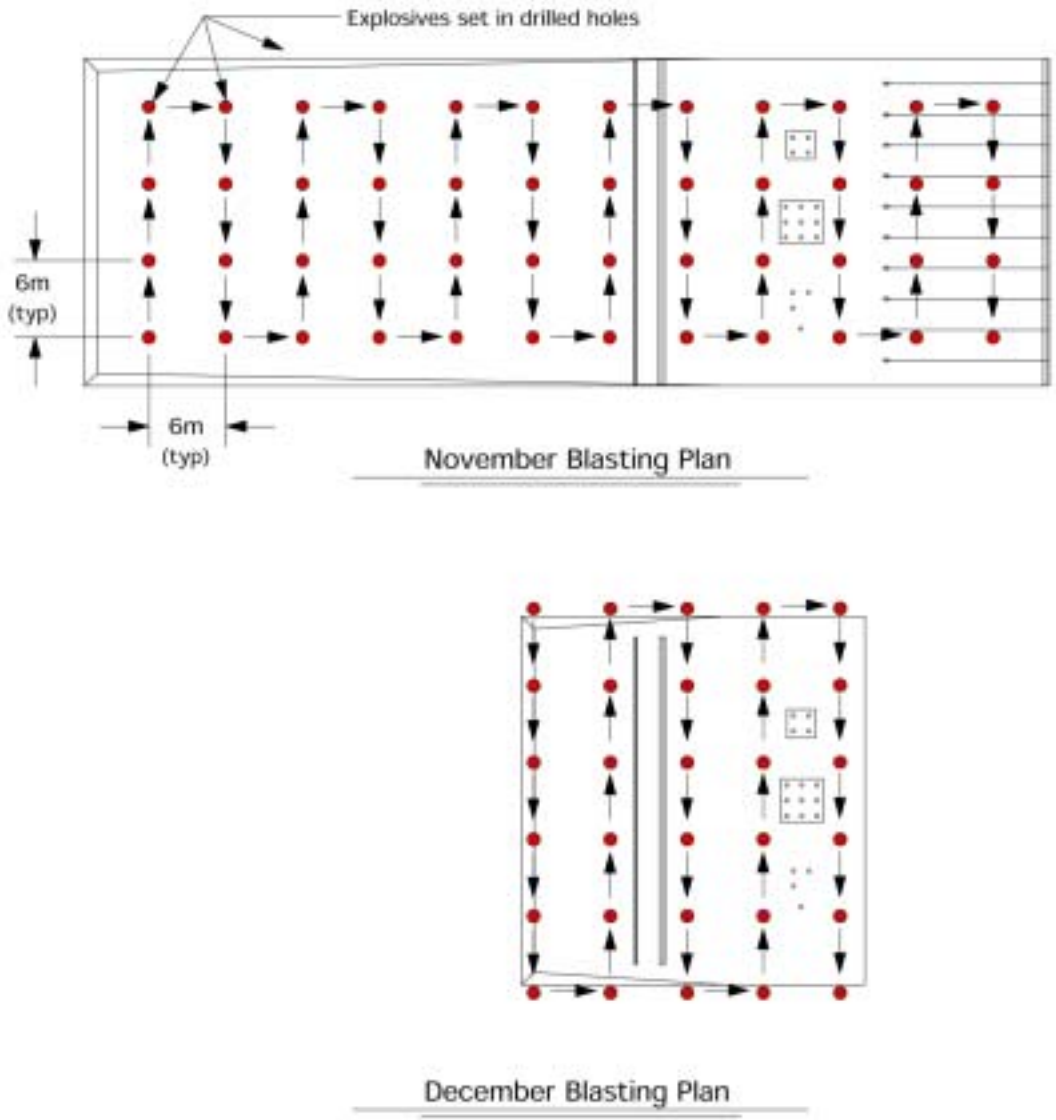

Figure 55 – Blasting plans

Blasting took place on November 13, 2001. The weather was ideal that day with clear skies and temperatures ranging from 0ºC to 10ºC throughout the day. Additional measures were taken the night before the test to improve the probability of successfully liquefying the site and generating lateral spread. This included wetting the site using a series of soaker hoses placed on the ground across the site. Over 400 visitors were present to observe the test, including test sponsors as well as representatives from industry and academic institutions from Japan and the United States.

The primary blast sequence commenced at approximately 2:26:24.30 PM local time (192384.30 GPS time), and proceeded over a period of approximately 36 seconds. Figures 56 and 57 show photos of the site during primary blasting. The secondary explosives were detonated after roughly 6 seconds following the completion of the primary blast sequence. The tertiary explosives near the quay wall were detonated approximately 44 seconds later. Figure 58 shows a photo of the blasting near the quay wall.

Figure 56 – Blasting underway, November Test

Figure 57 – Blasting underway, November Test

Figure 58 – Blasting near the quay wall, November Test

The second test took place on December 14, 2001. The execution of the second test was made challenging due to heavy snowfall, temperatures between –10ºC and 0ºC, and record setting 100kph winds on the day of the test. Ground freeze became an issue since frozen soil is not liquefiable nor conducive to lateral spread. Based upon driving steel stakes throughout sections of the site, the ground freeze was estimated to be approximately 20 to 30cm. As such, on the morning of the test, construction crews used jackhammers to break up the frozen ground surface in an area 3 to 5m buffering the pile groups as shown in Figure 59.

Figure 59 – Jackhammer operation to break up frozen soil surface

The primary blast sequence commenced at approximately 2:16:41.00 PM local time (451001.00 GPS time), and proceeded over a period of approximately 15 seconds. Approximately 19 seconds prior to the primary blast sequence, the explosives near the toe of the slope and the waterway were detonated. Figure 60 shows a photo during the blasting.

Figure 60 – Blasting underway, December Test

6.0 Measurements From the Tests in Japan

6.1 Data Collection and Processing

Raw GPS data was transmitted from the GPS field units back to the monitoring center where it could be processed in real time and logged by the two laptop computers. Multiple sets of data, both raw and processed, were collected for each test including positioning data before the blast, during the blast, immediately following the blast, and the following day. Other data sets were collected such as a survey of the test site to determine the relative positions of the base and field GPS antennas in the local grid system. All data was processed on the laptop computers in real time using the software application *RTKNav 3.0* (Waypoint 2000).

Two types of data files were created by the processing software, RTKNav, for each GPS field unit during the logging process: a raw data file, designated by the suffix *LOG*, and a processed data file, designated by the suffix *OUT*. The LOG file contains fundamental GPS satellite information, such as the position, doppler, and phase measurements from each satellite. The LOG file is useful in the event that the measurements need to be reprocessed. The OUT file contains the processed positioning information including precise GPS time, horizontal coordinates, height, and additional parameters used to assess the measurement quality.

For all data sets, positioning information was collected at a rate of 10Hz. Although 20Hz positioning data was possible from the GPS equipment, the higher data rates and increased throughput requirements could not be supported by the 900MHz spread spectrum wireless transceivers. At 10Hz, LOG files were created at a rate of approximately 3.5kB/sec for each GPS receiver. For 10 receivers over a typical 20 minute logging session, over 40MB were logged. A single OUT file over the same time period for 10 receivers at 10Hz totaled approximately 15MB.

Static GPS antenna positions prior to and following the blasting were determined from data sets collected over periods of approximately 15 minutes or longer. Shorter data sets of 2 to 5 minutes were used to determine positions immediately following blasting. GPS antennas were stationary during these measurements and 10Hz data was collected under ideal surveying conditions. Raw measurements were selectively filtered to include only the highest quality measurements. These were measurements where the GPS satellite constellation and orientation were ideal, the signal strength high, and carrier phase ambiguities readily determined. These parameters were combined into a single parameter, *quality factor*, and reported by the processing software for each measurement. On average 91% of all of the collected measurements met the criteria for the highest quality factor.

Static positions were determined by calculating the statistical average of the data set using the selected measurements. The accuracy of the measurements were consistent with expected accuracies for RTK-GPS processing techniques with a

mean horizontal standard deviation of 3mm and a mean vertical standard deviation of 7mm. The mean standard deviations were determined from the distribution of standard deviations calculated for each field unit from each data set and are provided in Tables 4 through 7.

Field Unit	Standard Deviation of Position Measurements		
	Easting (m)	Northing (m)	Height (m)
1A	0.003	0.003	0.009
1B	0.003	0.003	0.007
1C	0.003	0.004	0.007
1D	0.003	0.004	0.007
1E	0.003	0.003	0.009
2A	0.003	0.003	0.007
2B	0.002	0.003	0.005
2C	0.003	0.003	0.007
2D	0.003	0.003	0.006
2E	0.004	0.004	0.006

Table 4 – November 13, 2001, Pre-Blast Data Set Statistics

Field Unit	Standard Deviation of Position Measurements		
	Easting (m)	Northing (m)	Height (m)
1A	0.002	0.003	0.006
1B	0.002	0.003	0.004
1C	0.003	0.004	0.007
1D	0.003	0.004	0.008
1E	0.004	0.004	0.009
2A	0.004	0.004	0.009
2B	0.000	0.001	0.004
2C	0.000	0.001	0.004
2D	0.003	0.004	0.009
2E	0.004	0.005	0.013

Table 5 – November 13, 2001, Post-Blast Data Set Statistics

Field Unit	Standard Deviation of Position Measurements		
	Easting (m)	Northing (m)	Height (m)
1A	0.001	0.003	0.005
1B	0.002	0.002	0.005
1C	0.002	0.002	0.005
1D	0.002	0.003	0.005
1E	0.003	0.002	0.006
2A	0.002	0.002	0.004
2B	0.003	0.002	0.003
2C	0.003	0.002	0.003
2D	0.002	0.002	0.002
2E	0.002	0.002	0.003

Table 6 – December 14, 2001, Pre-Blast Data Set Statistics

Field Unit	Standard Deviation of Position Measurements		
	Easting (m)	Northing (m)	Height (m)
1A	0.002	0.004	0.010
1B	0.002	0.003	0.010
1C	0.002	0.003	0.011
1D	0.003	0.003	0.013
1E	0.003	0.006	0.009
2A	0.003	0.004	0.008
2B	0.002	0.003	0.008
2C	0.002	0.003	0.009
2D	0.002	0.003	0.008
2E	0.002	0.004	0.010

Table 7 – December 14, 2001, Post-Blast Data Set Statistics

Tables 8 through 11 summarize the results of the pre-blast and post-blast static surveys. Data in the table includes the horizontal northing and easting coordinate as well as height, reported in units of meters in a local grid system established by the test organizers. Changes in the position of the GPS antennas are tabulated in terms of total vector displacement as well as individual horizontal and vertical components. Positioning data is provided for measurements just before the blast, within minutes following the blast, and the day after the blast.

	PreBlast	(192300 GPS Time)		Post Blast	(192455 GPS Time)		Total Vector	Horizontal	Vertical
Location	X (east)	Y (north)	Z (elev)	X (east)	Y (north)	Z (elev)	Displacement (m)	Displacement (m)	Displacement (m)
1A (9-pile group)	162.266	-166.999	0.199						
1B (9-pile near)	160.677	-166.265	0.276						
1C (9-pile free)	156.153	-163.386	0.333	156.445	-163.563	0.332	0.342	0.342	-0.001
1D (1-pile)	159.610	-175.214	0.440	159.936	-175.377	0.446	0.365	0.365	0.006
1E (1-pile SI)	158.758	-174.646	0.330						
2A (4-pile group)	165.535	-161.938	0.201	165.708	-162.069	0.215	0.217	0.217	0.014
2B (free field)	156.265	-156.773	0.398						
2C (3-pile group)	160.374	-172.311	1.505	160.857	-172.579	1.515	0.552	0.552	0.011
2D (gas pipe)	154.089	-162.367	0.742	154.378	-162.607	0.731	0.376	0.376	-0.011
2E (electric pipe)	152.264	-161.349	0.617	152.548	-161.601	0.574	0.382	0.380	-0.043

Table 8 – Pre-blast and Post-Blast Positions, November Test, approximately 3 minutes following blasting

	PreBlast	(192300 GPS Time)		Post Blast	(271840 GPS Time)		Total Vector	Horizontal	Vertical
Location	X (east)	Y (north)	Z (elev)	X (east)	Y (north)	Z (elev)	Displacement (m)	Displacement (m)	Displacement (m)
1A (9-pile group)	162.266	-166.999	0.199	162.403	-167.117	0.213	0.182	0.181	0.013
1B (9-pile near)	160.677	-166.265	0.276	160.916	-166.417	0.308	0.285	0.283	0.032
1C (9-pile free)	156.153	-163.386	0.333	156.439	-163.554	0.243	0.344	0.332	-0.090
1D (1-pile)	159.610	-175.214	0.440	159.923	-175.370	0.448	0.350	0.350	0.008
1E (1-pile SI)	158.758	-174.646	0.330	159.057	-174.804	0.356	0.340	0.339	0.026
2A (4-pile group)	165.535	-161.938	0.201	165.705	-162.065	0.206	0.212	0.212	0.005
2B (free field)	156.265	-156.773	0.398	156.529	-157.009	0.307	0.365	0.354	-0.091
2C (3-pile group)	160.374	-172.311	1.505	160.854	-172.573	1.517	0.548	0.547	0.012
2D (gas pipe)	154.089	-162.367	0.742	154.375	-162.603	0.631	0.387	0.371	-0.111
2E (electric pipe)	152.264	-161.349	0.617	152.550	-161.605	0.489	0.405	0.384	-0.128

Table 9 – Pre-blast and Post-Blast Positions, November Test, approximately 22 hours following blasting

	PreBlast	(450960 GPS Time)		Post Blast	(451040 GPS Time)		Total Vector	Horizontal	Vertical
Location	X (east)	Y (north)	Z (elev)	X (east)	Y (north)	Z (elev)	Displacement (m)	Displacement (m)	Displacement (m)
1A (9-pile group)	162.408	-167.121	0.205	162.536	-167.212	0.214	0.157	0.157	0.009
1B (9-pile near)	160.845	-166.486	0.436	160.971	-166.570	0.502	0.165	0.151	0.066
1C (9-pile free)	156.121	-163.256	0.565	156.272	-163.388	0.580	0.201	0.200	0.015
1D (1-pile)	159.962	-175.389	0.436	160.229	-175.523	0.438	0.299	0.299	0.002
1E (1-pile SI)	158.994	-174.872	0.298	159.219	-174.928	0.308	0.232	0.232	0.010
2A (4-pile group)	165.700	-162.061	0.213	165.857	-162.156	0.222	0.184	0.184	0.009
2B (free field)	156.049	-156.776	0.366	156.122	-156.858	0.394	0.113	0.110	0.028
2C (3-pile group)	160.901	-172.590	1.506	161.322	-172.806	1.487	0.474	0.474	-0.020
2D (gas pipe)	154.375	-162.619	0.440	154.517	-162.715	0.333	0.202	0.171	-0.107
2E (between caps)	165.662	-165.026	0.242	166.049	-165.246	0.227	0.446	0.445	-0.015

Table 10 – Pre-blast and Post-Blast Positions, December Test, approximately 1.3 minutes following blasting

	PreBlast	(450960 GPS Time)		Post Blast	(525076 GPS Time)		Total Vector	Horizontal	Vertical
Location	X (east)	Y (north)	Z (elev)	X (east)	Y (north)	Z (elev)	Displacement (m)	Displacement (m)	Displacement (m)
1A (9-pile group)	162.408	-167.121	0.205	162.530	-167.210	0.204	0.151	0.151	-0.001
1B (9-pile near)	160.845	-166.486	0.436	160.970	-166.569	0.483	0.157	0.150	0.047
1C (9-pile free)	156.121	-163.256	0.565	156.277	-163.375	0.556	0.196	0.196	-0.009
1D (1-pile)	159.962	-175.389	0.436	160.230	-175.515	0.421	0.297	0.297	-0.014
1E (1-pile SI)	158.994	-174.872	0.298	159.218	-174.926	0.286	0.231	0.230	-0.012
2A (4-pile group)	165.700	-162.061	0.213	165.842	-162.158	0.220	0.173	0.173	0.007
2B (free field)	156.049	-156.776	0.366	156.121	-156.864	0.410	0.122	0.114	0.044
2C (3-pile group)	160.901	-172.590	1.506	161.325	-172.804	1.482	0.476	0.475	-0.024
2D (gas pipe)	154.375	-162.619	0.440	154.515	-162.716	0.296	0.223	0.170	-0.145
2E (between caps)	165.662	-165.026	0.242	166.066	-165.244	0.220	0.460	0.460	-0.021

Table 11 – Pre-blast and Post-Blast Positions, December Test, approximately 20 hours following blasting

Measurements were collected as blasting progressed to track the dynamic motions of the GPS antennas resulting from the immediate blast and subsequent lateral spread. As with the static survey, the dynamic data was also collected at 10Hz and processed in real-time. Figures 61 through 76 provide the time history of displacements for lateral, transverse, and vertical components as well as a plot of the complete displacement path in the horizontal plane. For the time history plots, *GPS time* is indicated on the primary axis. GPS time is measured as the cumulative seconds in a single GPS week relative to the global time standard, Coordinated Universal Time (UTC). The time history records shown in Figures 61 through 66 for the November test represent GPS times 192370.0 to 192450.0, or 2:26:10.0 PM to 2:27:30.0 PM local time in Japan. The time history records shown in Figures 67 through 76 for the December test represent GPS times 450960.0 to 451040.0, or 2:16:00.0 PM to 2:17:20.0 PM local time in Japan.

Some data loss occurred during the critical blasting period. The periods of time during the blasting were not captured at all in four of the ten records (Units 1A, 1B, 1E, and 2B) for the November test. In two of the six remaining records, there were short periods of data loss of about 5 seconds. During the December test most of the data was captured. There are two primary factors that are suspected to have contributed to the data loss, particularly during the November test: (1) intermittent GPS antenna interference, and (2) wireless communications parameter settings.

For the November test loose soil at the surface was thrown in the air by the blasting and may have generated interference for both the GPS antennas and the

wireless transceiver antennas. By contrast, for the December test there was significantly less debris thrown in the air since the ground was frozen. Although there was significant snowfall at the time of the December test, GPS satellite signals at 1227.60 MHz and 1575.42 MHz and wireless transceiver signals in the 902 to 928 Mhz band are relatively unaffected by the snowfall or rain.

Following the November test the communication settings of the wireless transceivers were changed as a precautionary measure to reduce the likelihood of data loss during the second test in December. The FreeWave spread spectrum wireless transceivers are configurable through their internal firmware to control a number of communications parameters including data transmission rate, error checking, packet size, and signal strength. As was described in an earlier section, ten master transceivers were located in close proximity at the monitoring center trailer at the test site. With a large number of transceivers close together, the potential of interference between them was likely. For example, if one transceiver is attempting to send a signal as another is attempting to receive a signal, the receiving transceiver may be overpowered by the adjacent transceiver. As such, the master transceivers were synchronized such that all ten would simultaneously transmit and receive at the same time, thereby reducing the likelihood of interference. As an additional measure, the transmission power of the master transceivers was reduced by 90%. Specific settings for the transceivers are included in Appendix E.

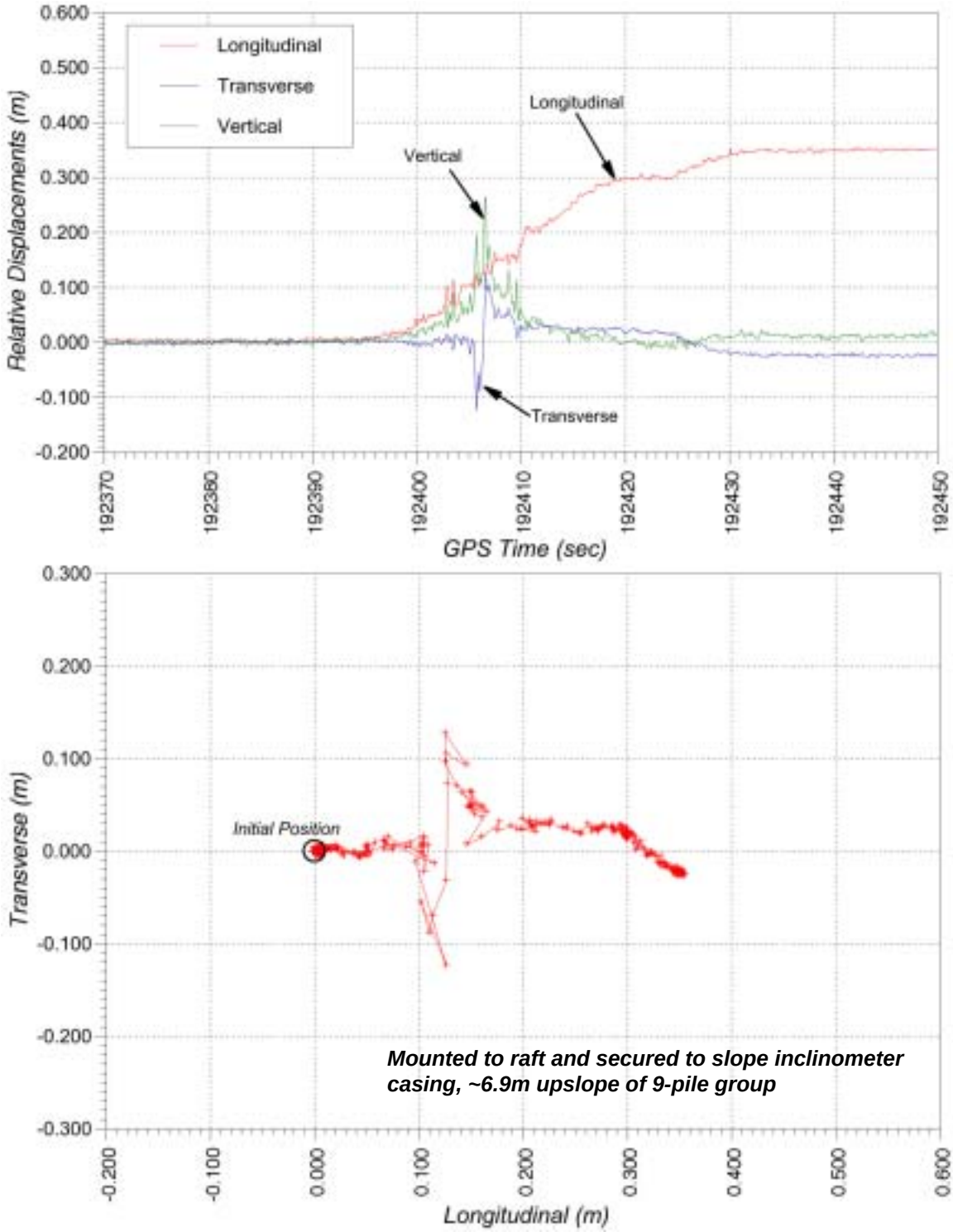

Figure 61 – Time-history record and plot for Unit 1C, November Test

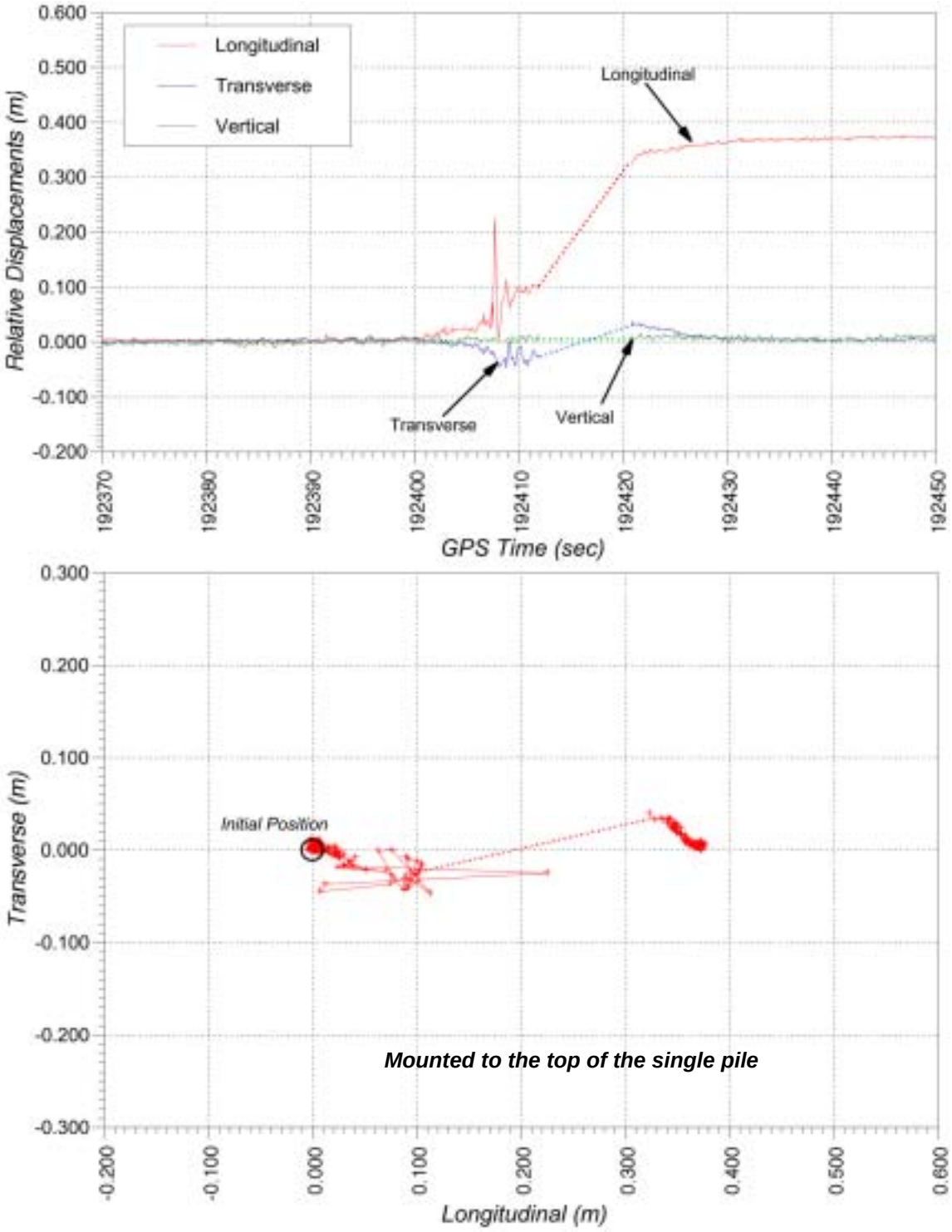

Figure 62 – Time-history record and plot for Unit 1D, November Test

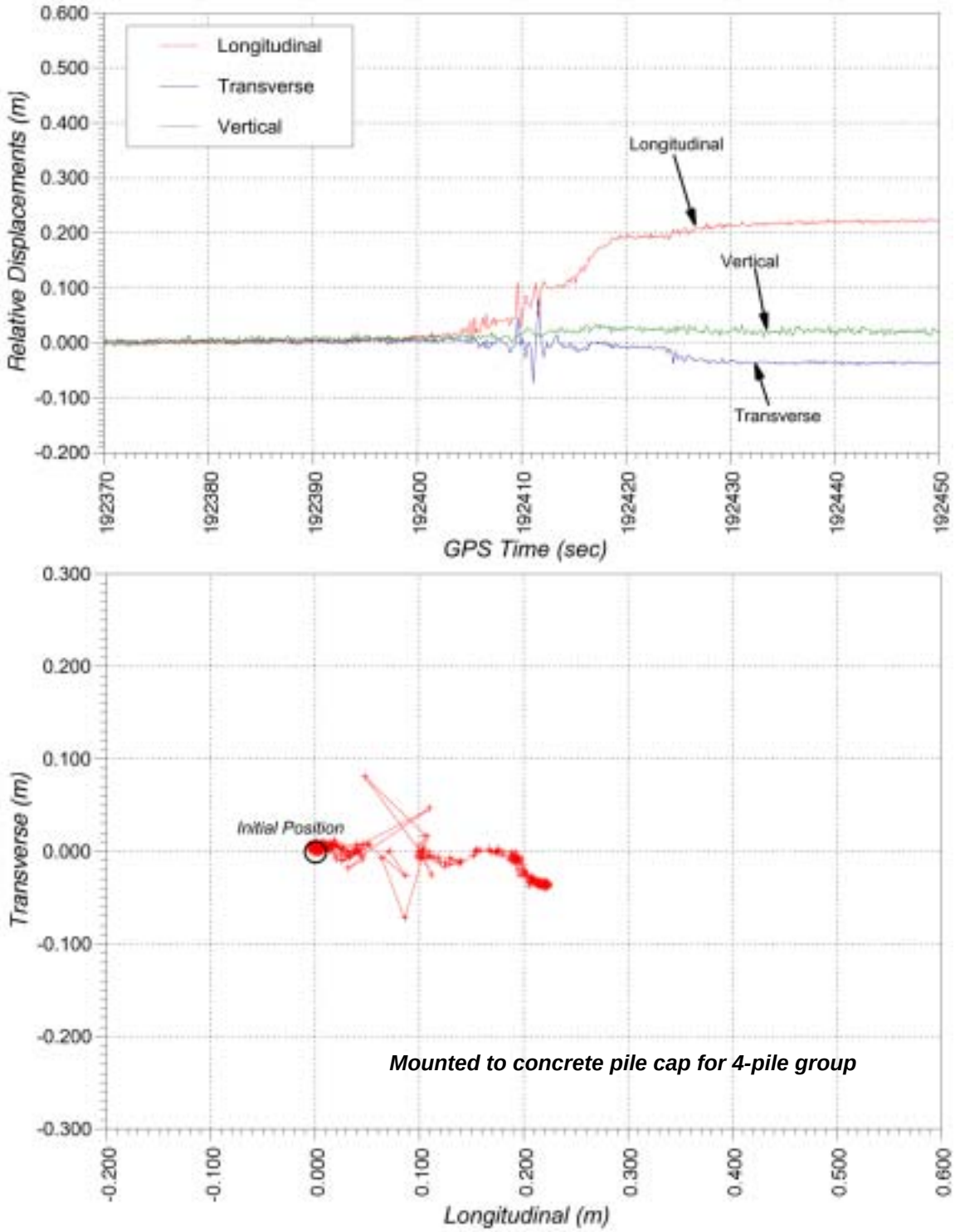

Figure 63 – Time-history record and plot for Unit 2A, November Test

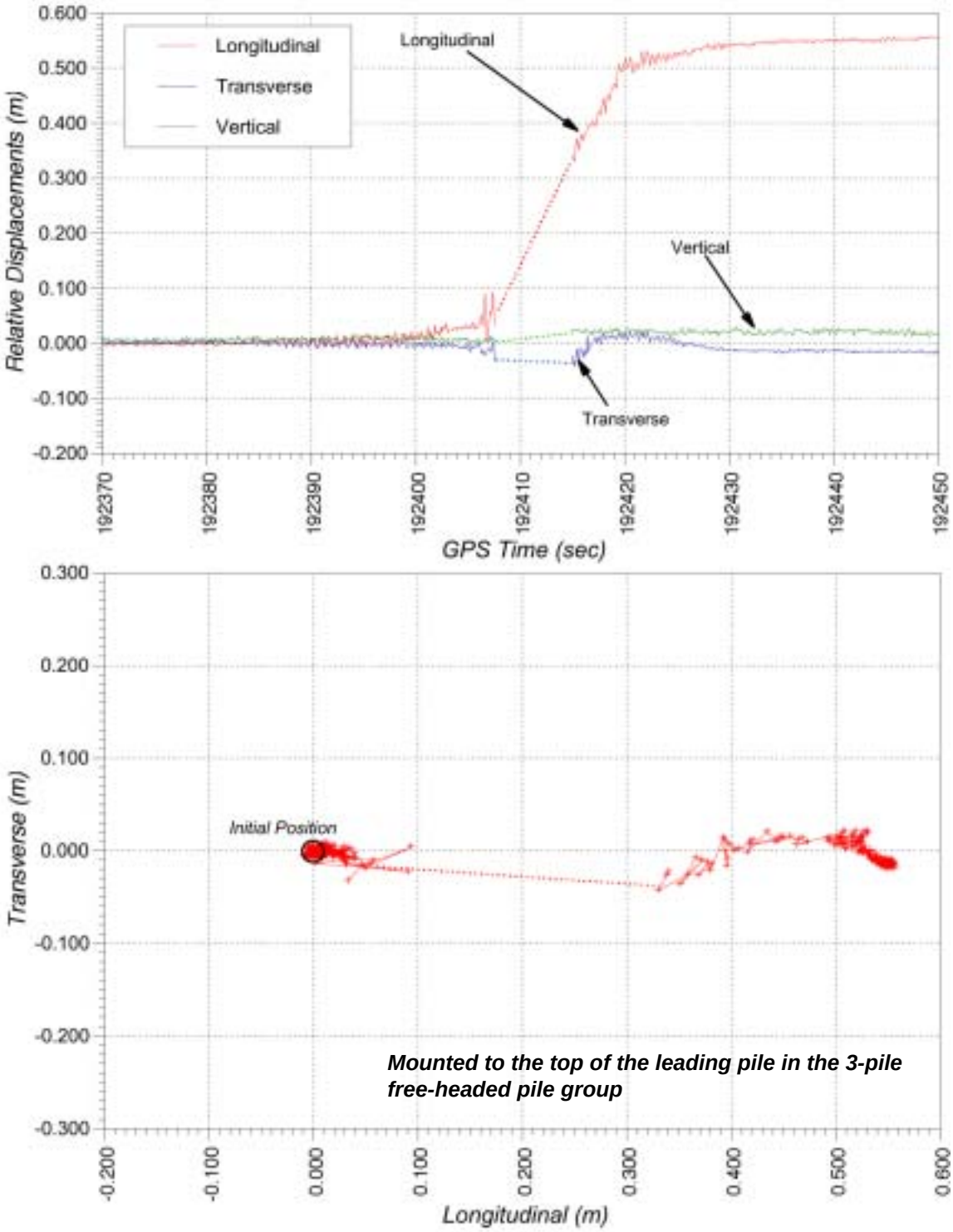

Figure 64 – Time-history record and plot for Unit 2C, November Test

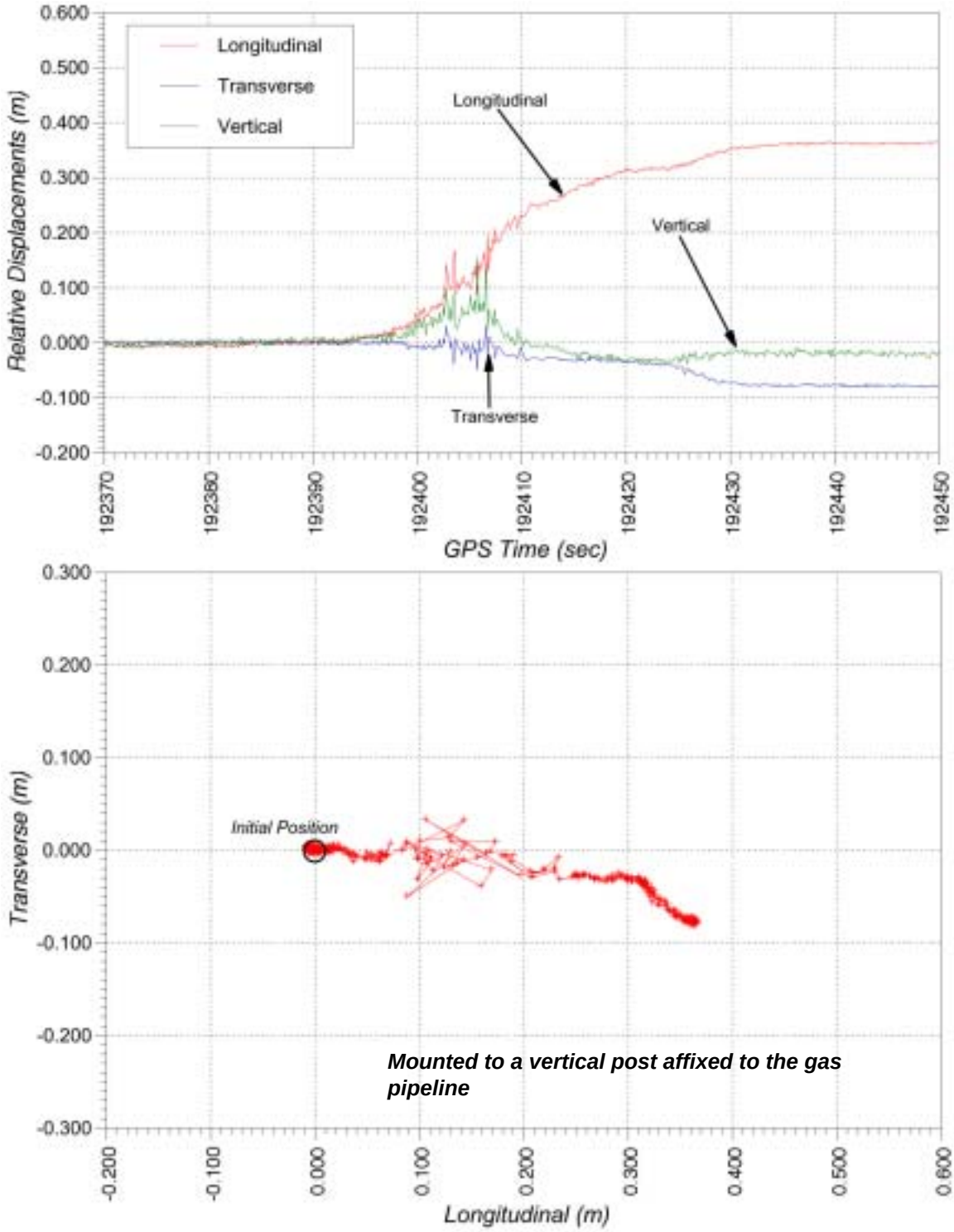

Figure 65 – Time-history record and plot for Unit 2D, November Test

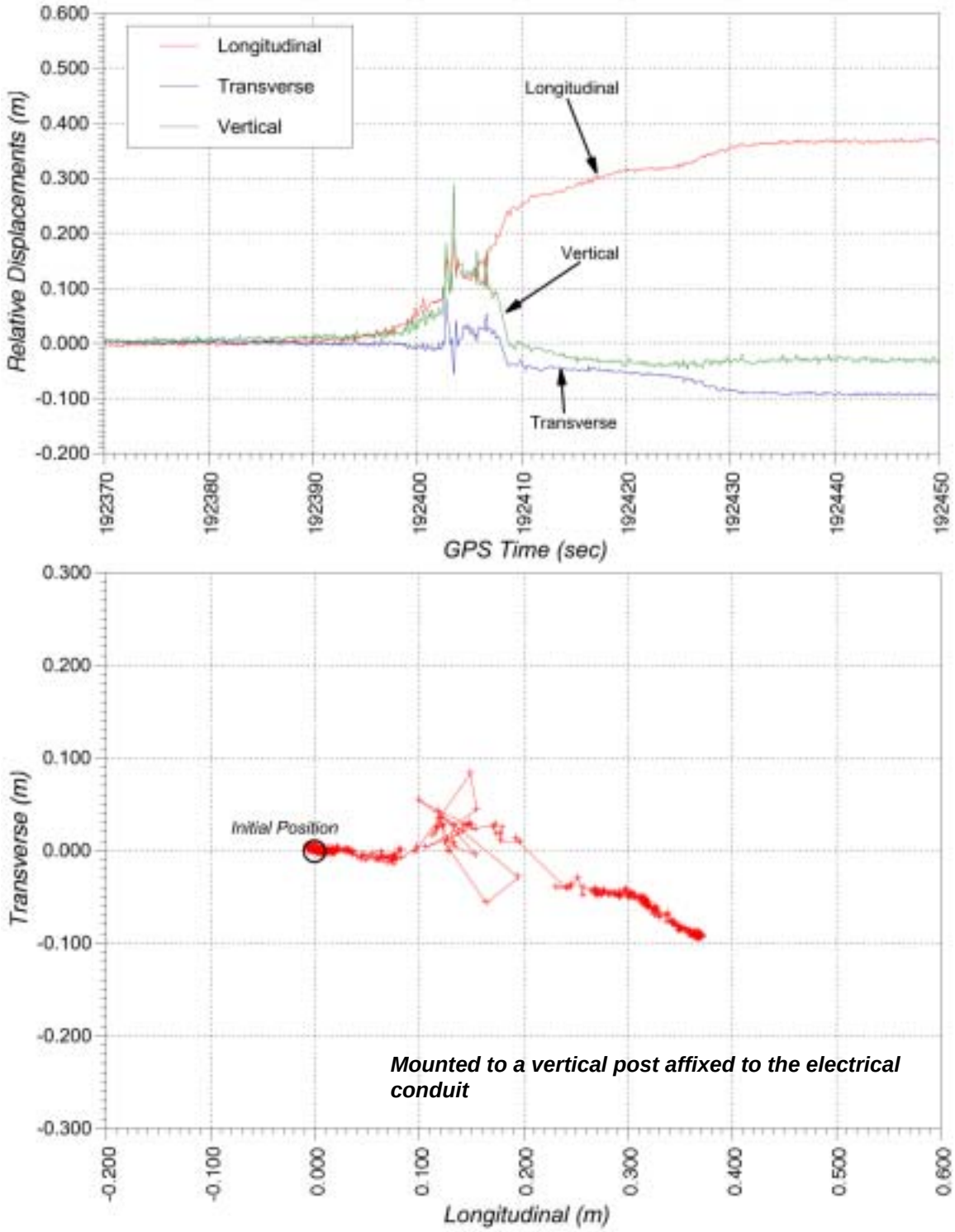

Figure 66 – Time-history record and plot for Unit 2E, November Test

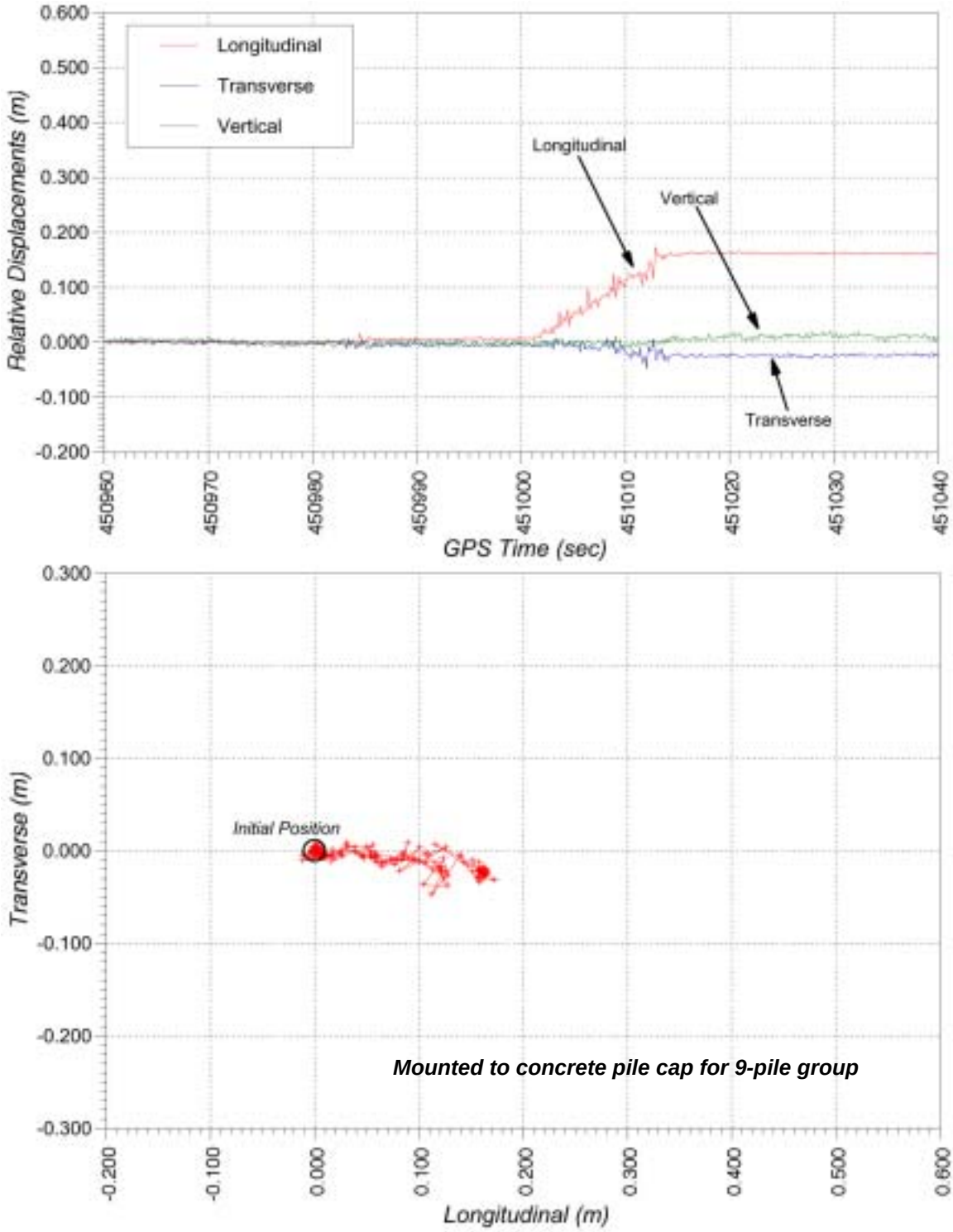

Figure 67 – Time-history record and plot for Unit 1A, December Test

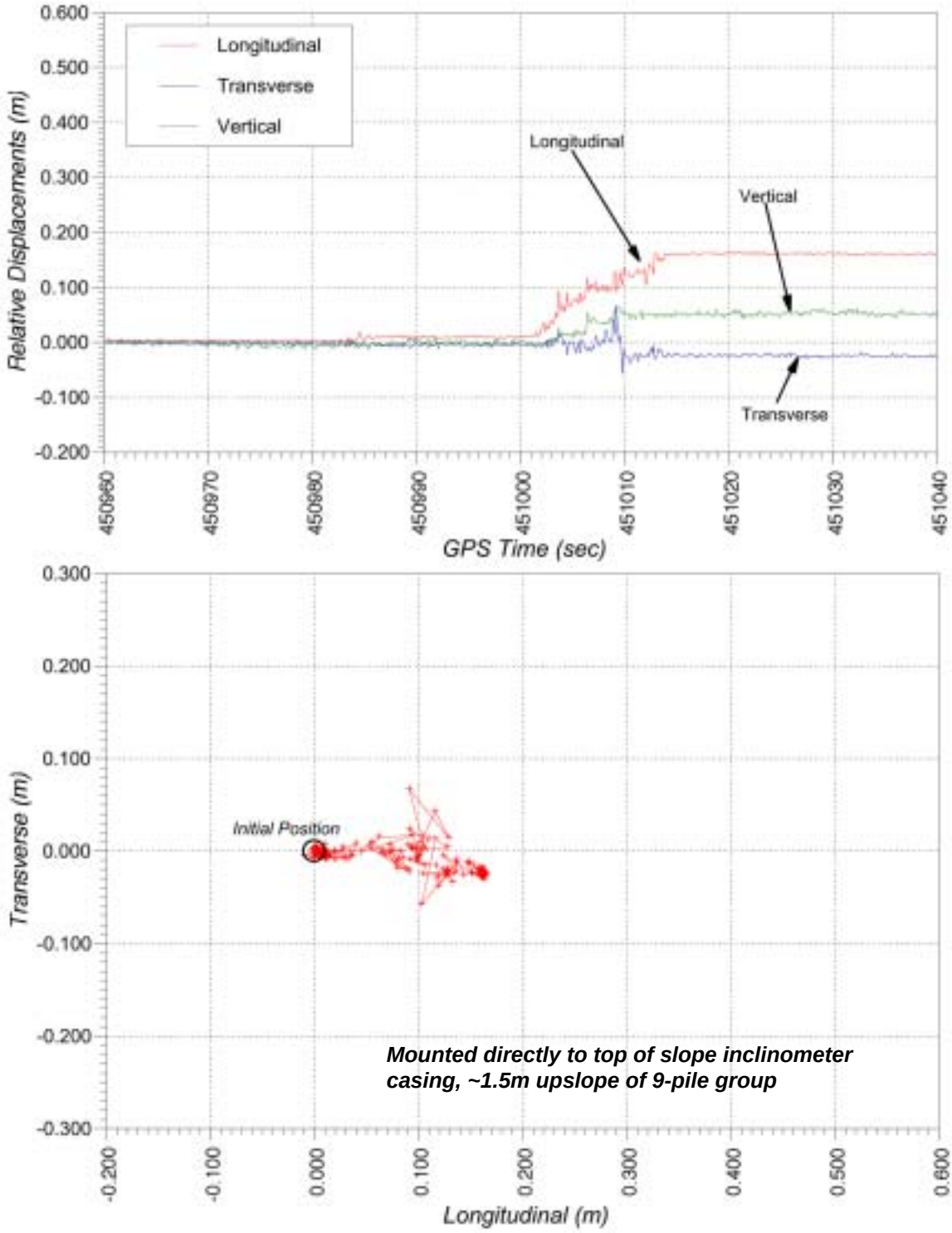

Figure 68 – Time-history record and plot for Unit 1B, December Test

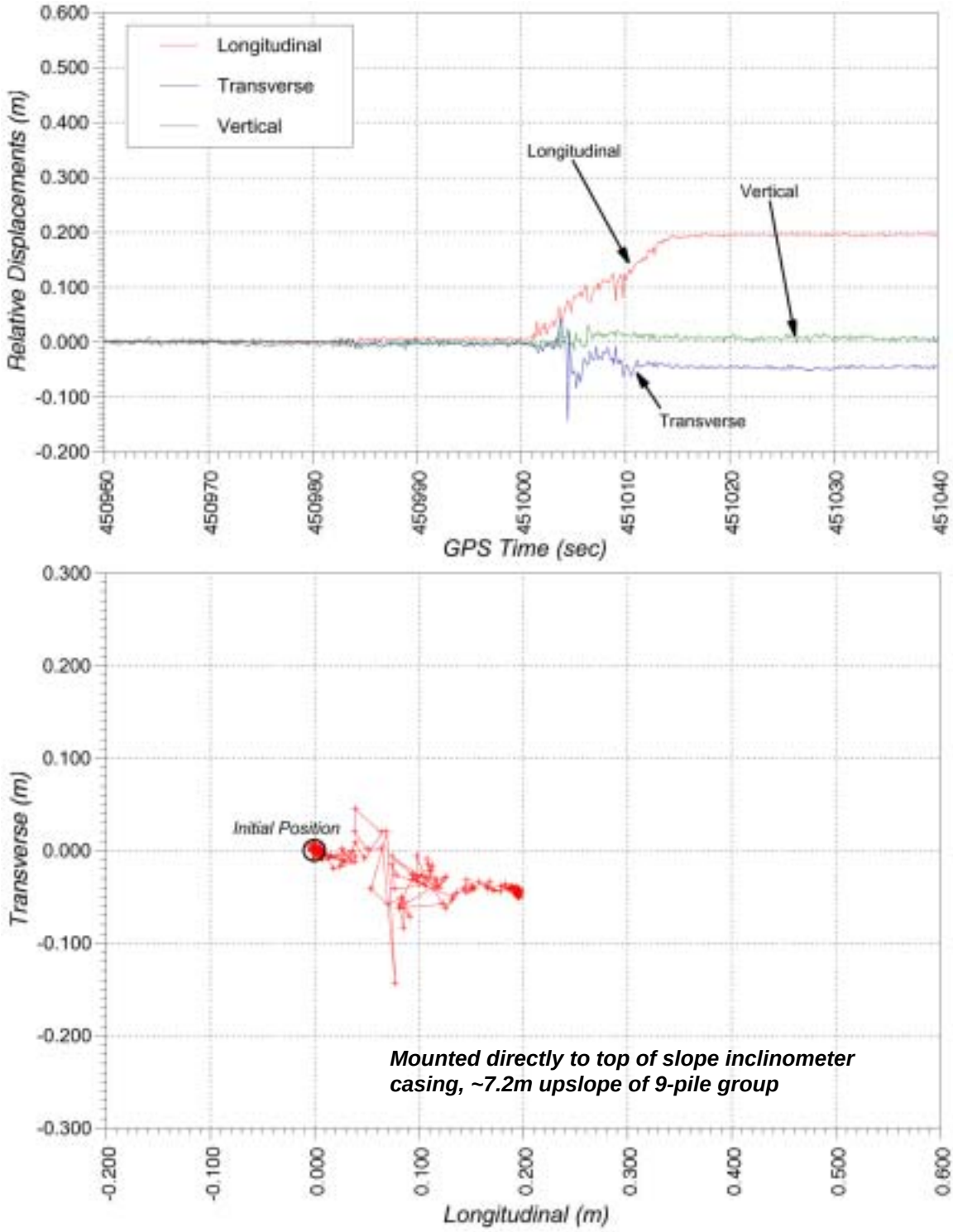

Figure 69 – Time-history record and plot for Unit 1C, December Test

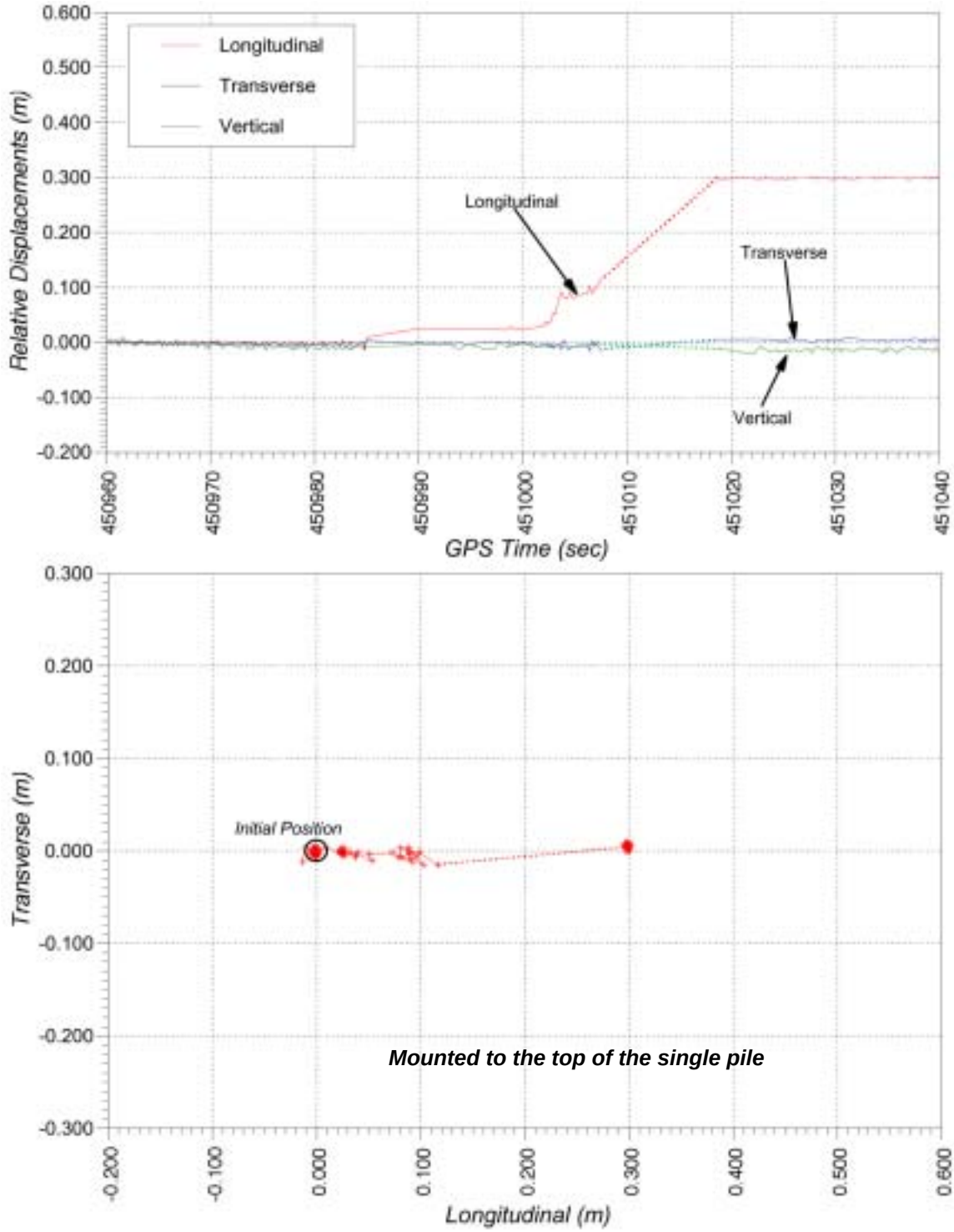

Figure 70 – Time-history record and plot for Unit 1D, December Test

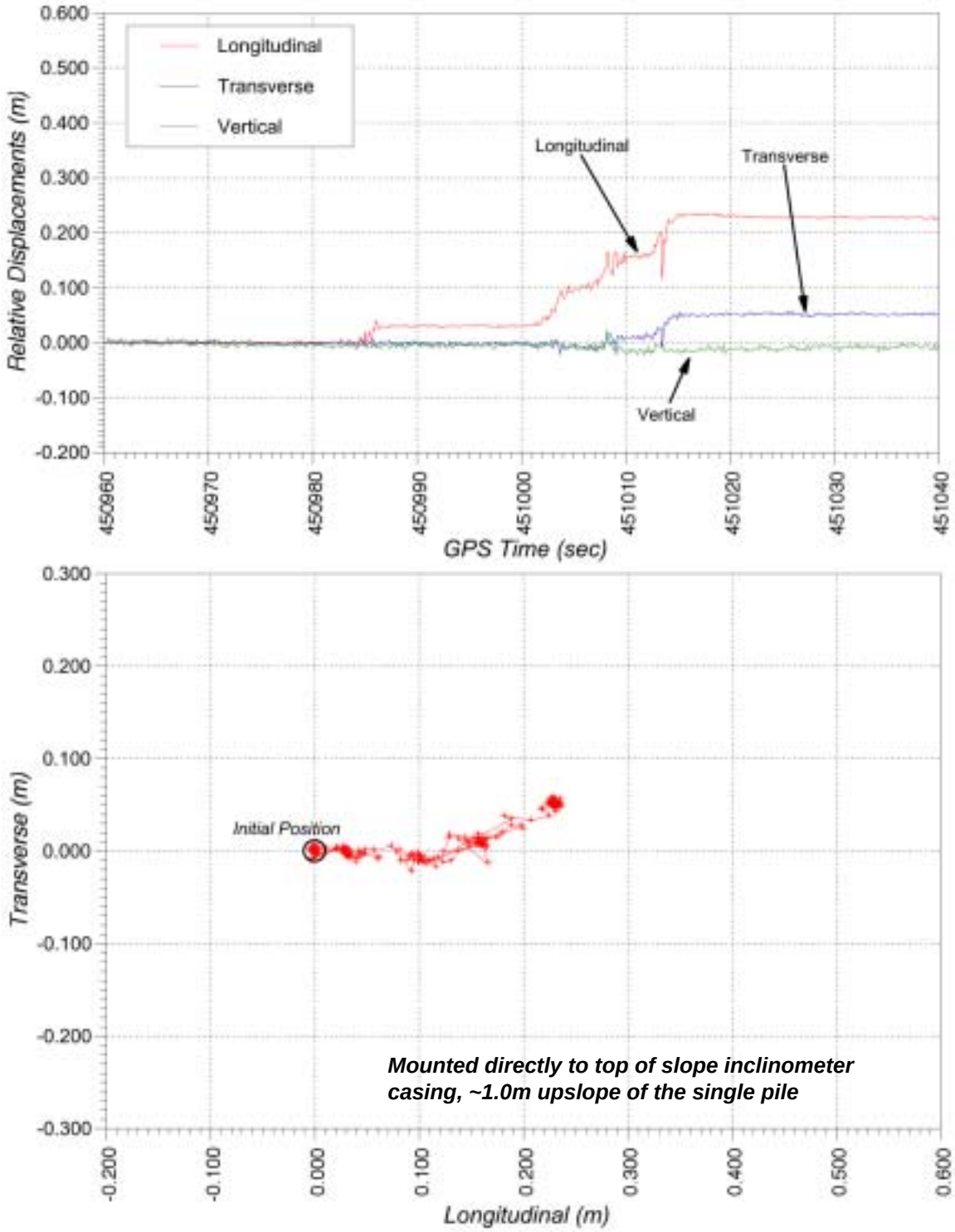

Figure 71 – Time-history record and plot for Unit 1E, December Test

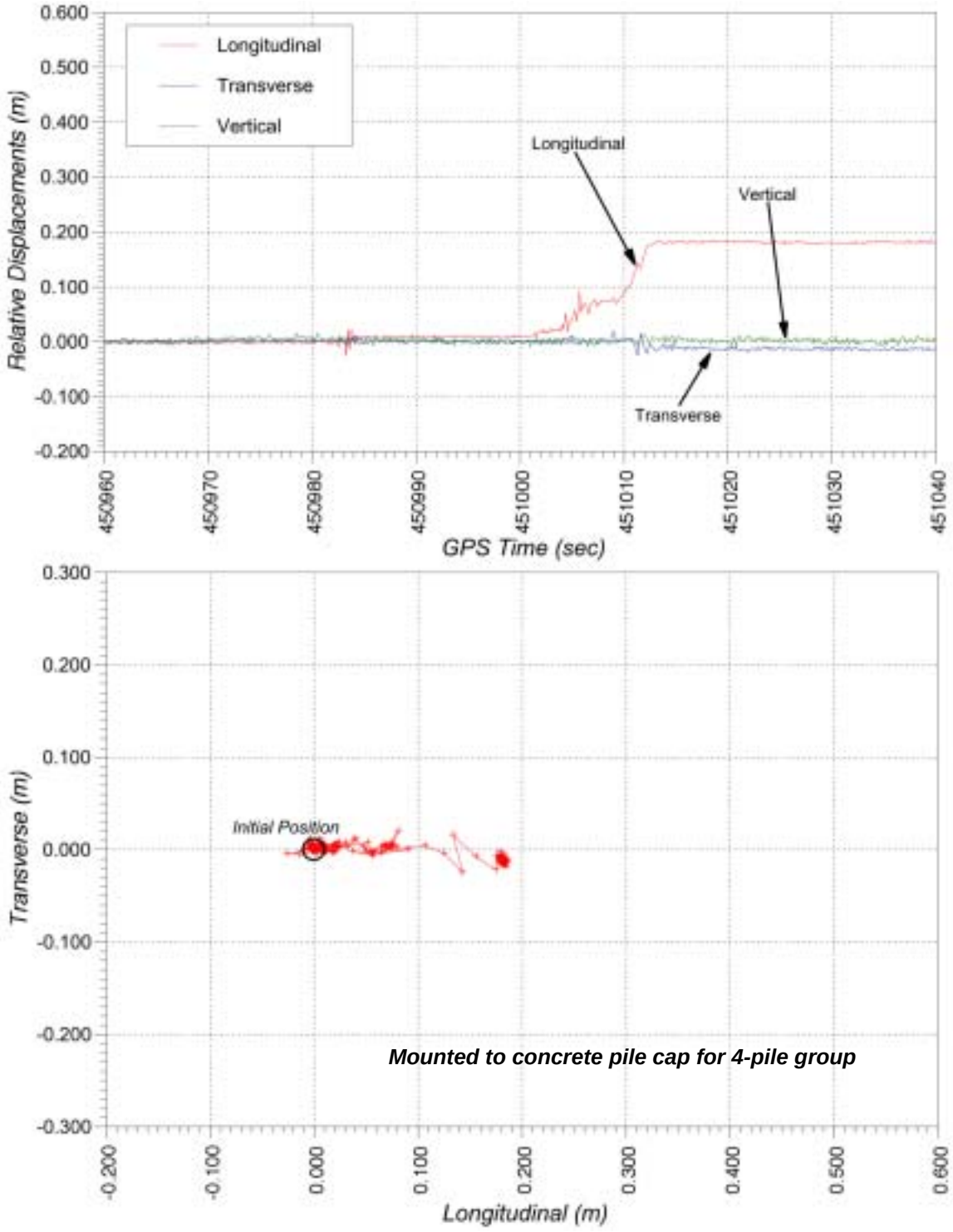

Figure 72 – Time-history record and plot for Unit 2A, December Test

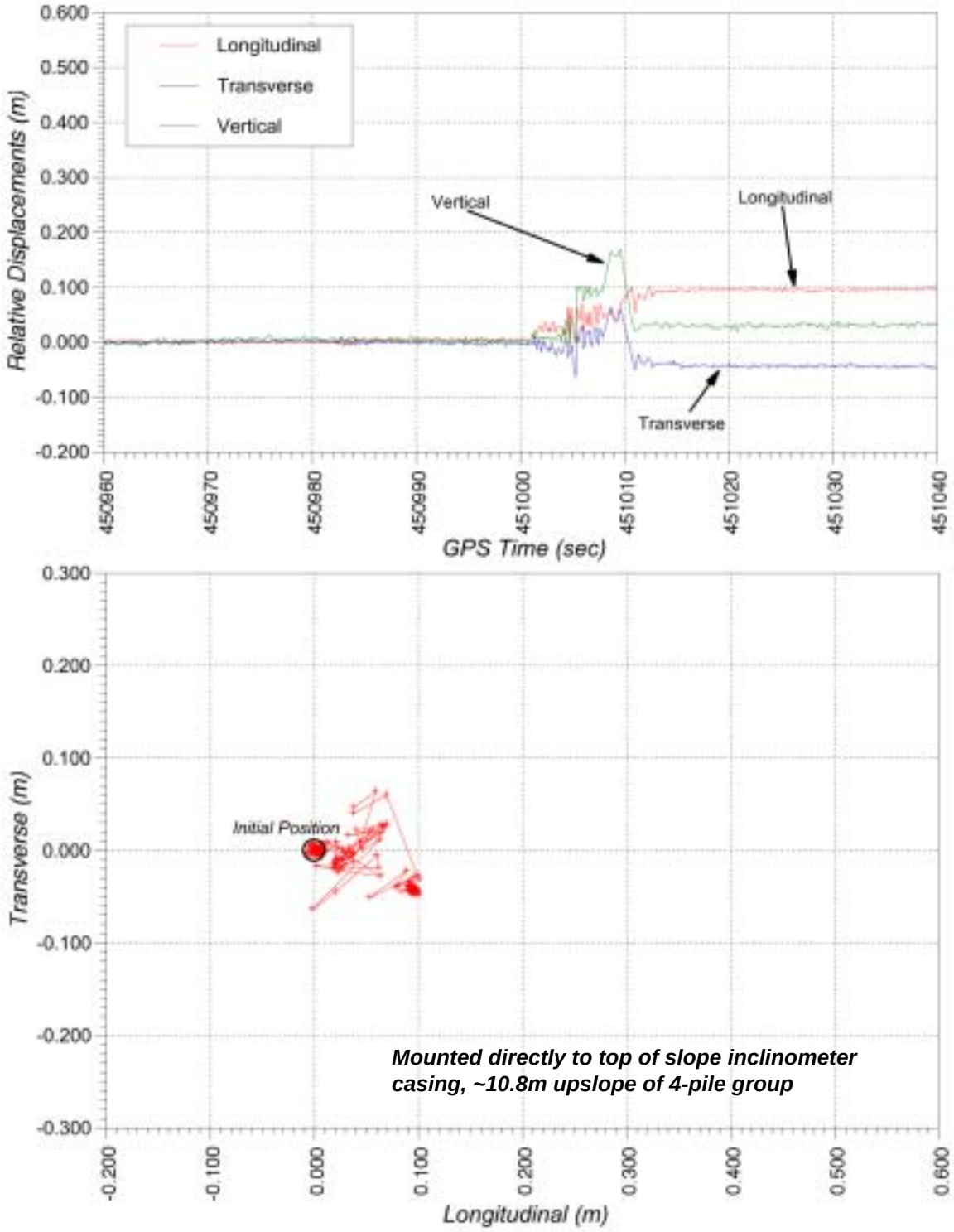

Figure 73 – Time-history record and plot for Unit 2B, December Test

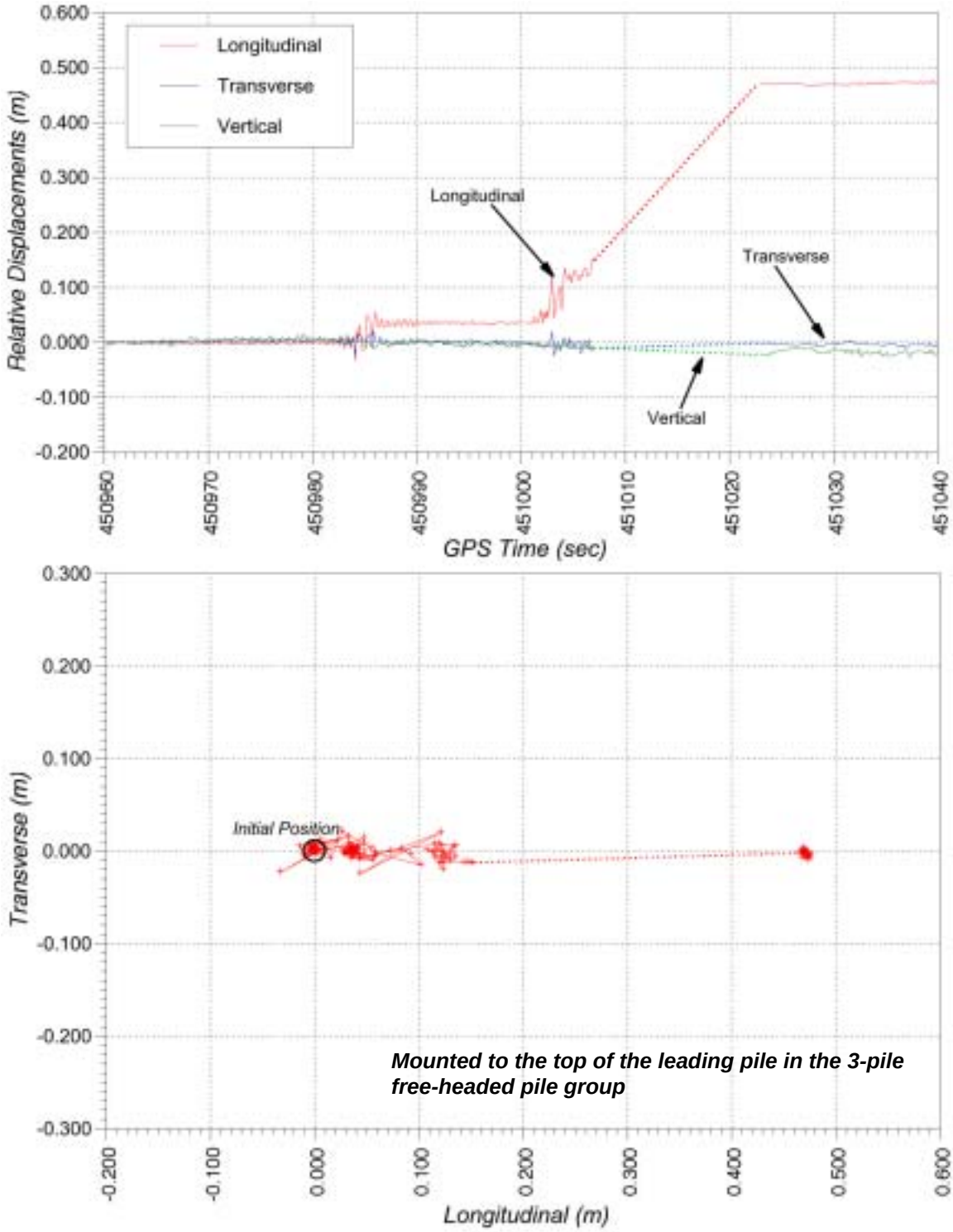

Figure 74 – Time-history record and plot for Unit 2C, December Test

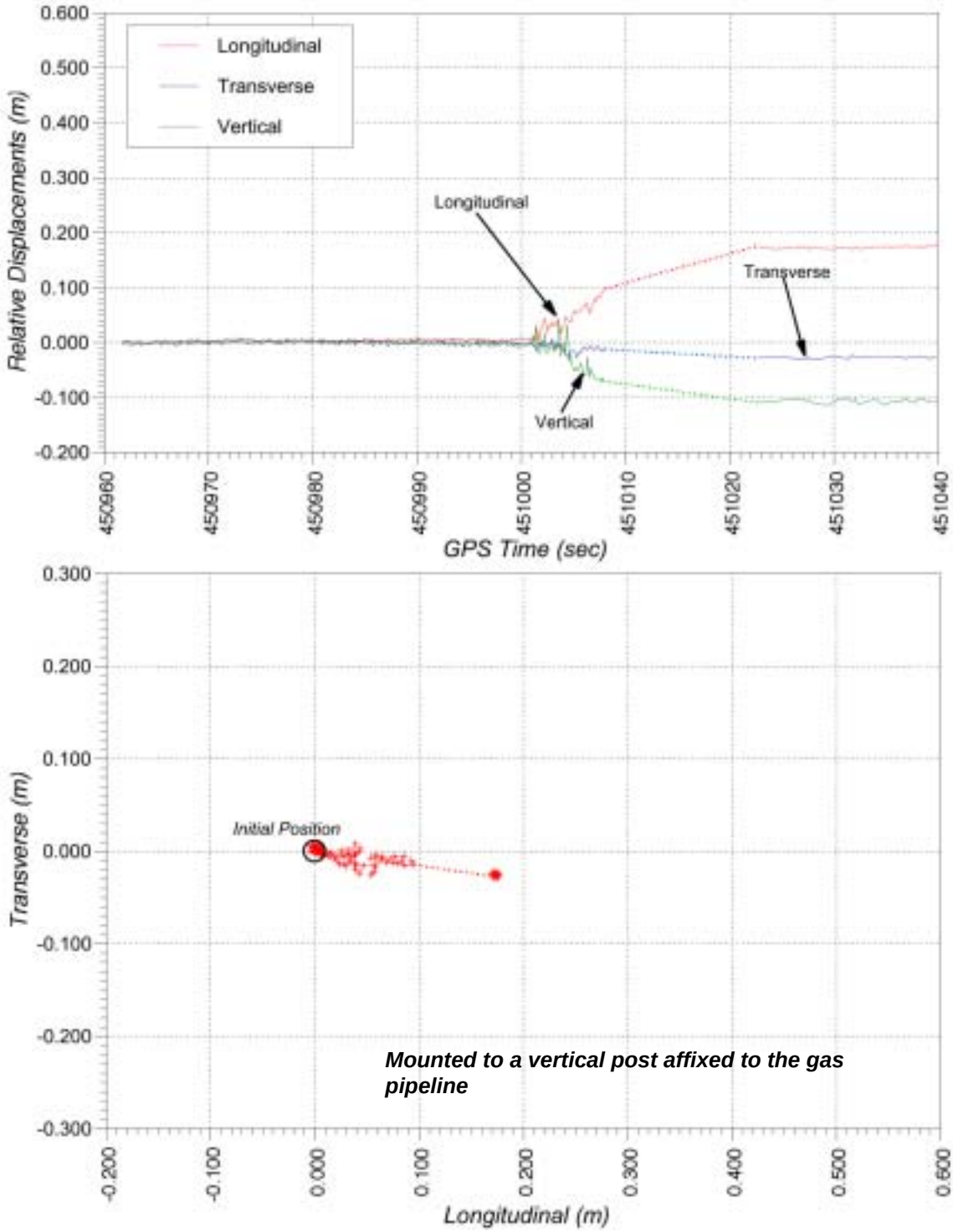

Figure 75 – Time-history record and plot for Unit 2D, December Test

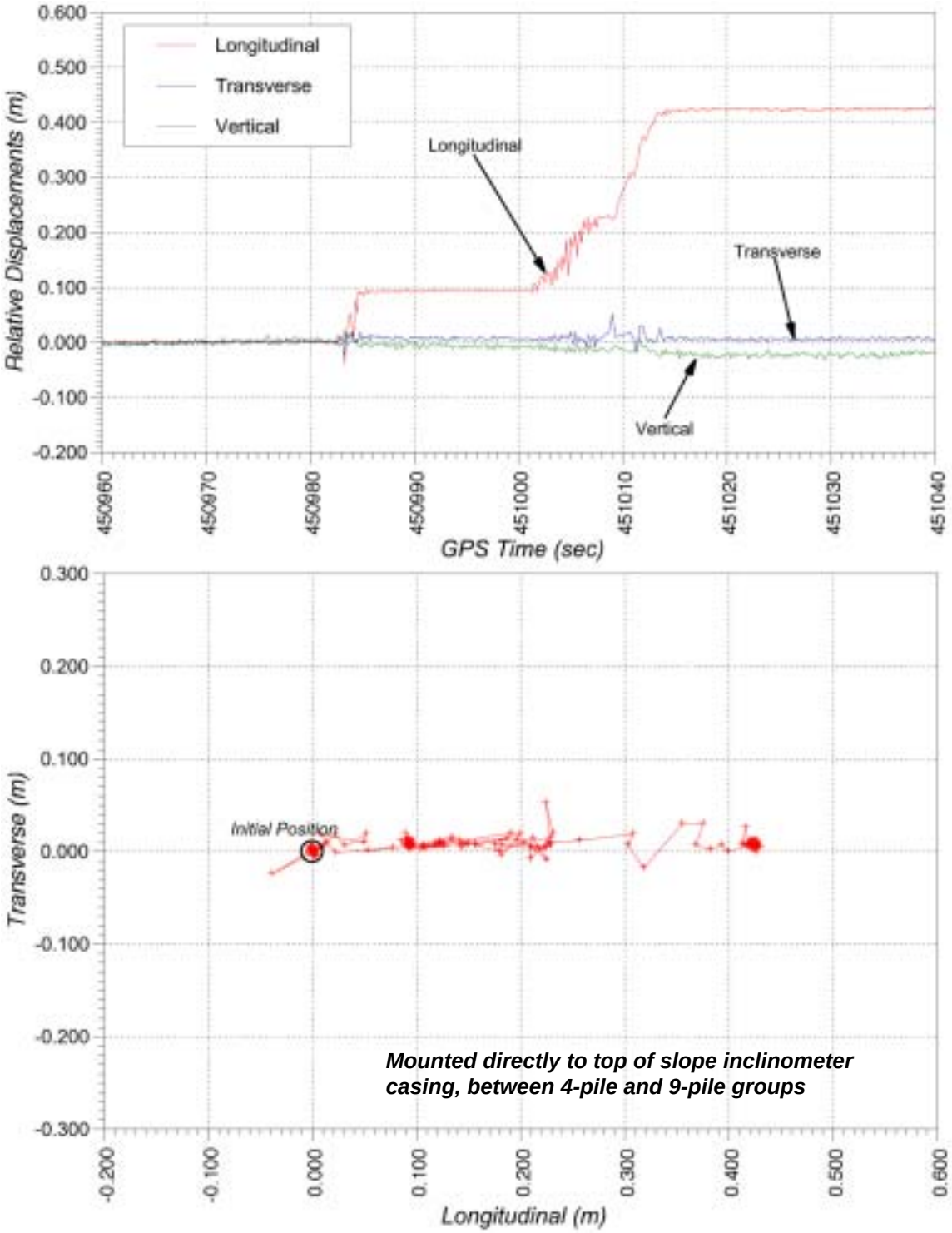

Figure 76 – Time-history record and plot for Unit 2E, December Test

6.2 General Discussion of Pre and Post-Blast Survey Results

Static measurements prior to and following the blasting provided important constraints on the short and long term displacement of the blast induced lateral spread. Dynamic measurements during the blast provided essential time history data to quantify the initiation, onset, and distribution of spread in time.

Positioning data for the tests were presented earlier in Tables 8 through 11 for measurements prior to, minutes after, and approximately 20 hours after the blasting. Significant displacements in the horizontal plane were measured and are summarized in vector displacement plots in Figures 78 and 79 for the November and December tests, respectively. These plots show the pre-blast antenna positions and the 20 hour post-blast positions (dashed line) of the GPS antennas. Horizontal displacement vectors are superposed on the plots and are shown with magnitudes multiplied by a factor of 3 for clarity. Final positions of the pile groups are also shown (dashed-line) based upon GPS measurements and the assumption that the groups moved downslope without any rotation or distortion in the horizontal plane. Although a formal survey was conducted by other researchers prior to and following the tests, that data was not available at the time of writing of this report.

The largest horizontal displacements measured during both tests were those for Unit 2C, mounted on top of the 3-pile group. Recall from Figure 42 that the GPS antenna was located approximately 1.8m above the ground surface. Following both tests, significant rotations were observed for all of the piles in the 3-pile group. Preliminary measurements from the November test showed that the pile

to which Unit 2C was attached had rotated approximately 5° as shown in Figure 77. This rotation accounted for roughly 15cm of the 54.7cm total horizontal displacement in the November test records. Similar pile rotations were observed in the December test. Tilt meter data collected by researchers from the University of California San Diego (UCSD) for both tests should be used and considered in future analyses when evaluating true ground deformations.

Figure 77 – Measuring rotation of pile, Unit 2C, November test

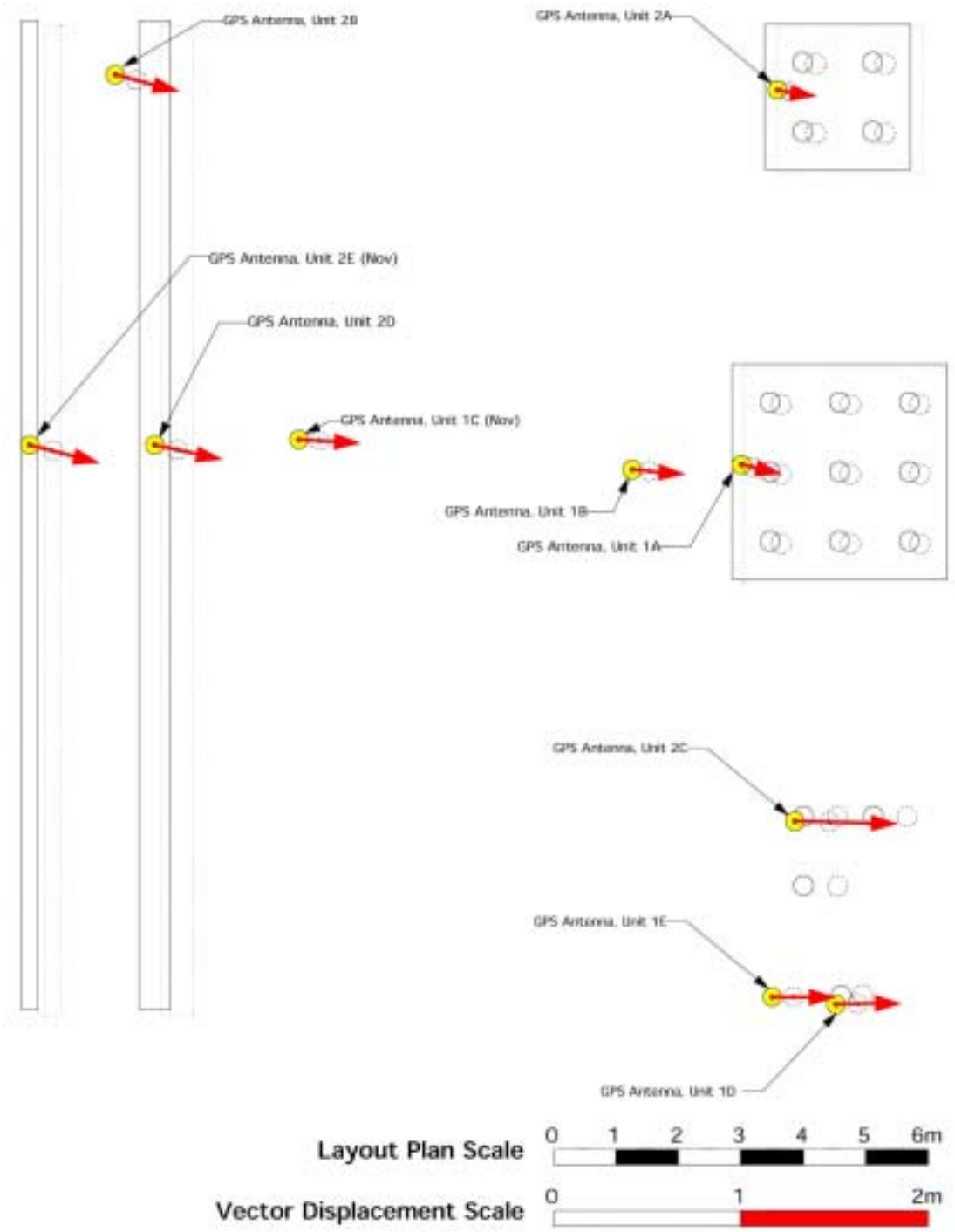

Figure 78 – Vector displacements in horizontal plane, November test

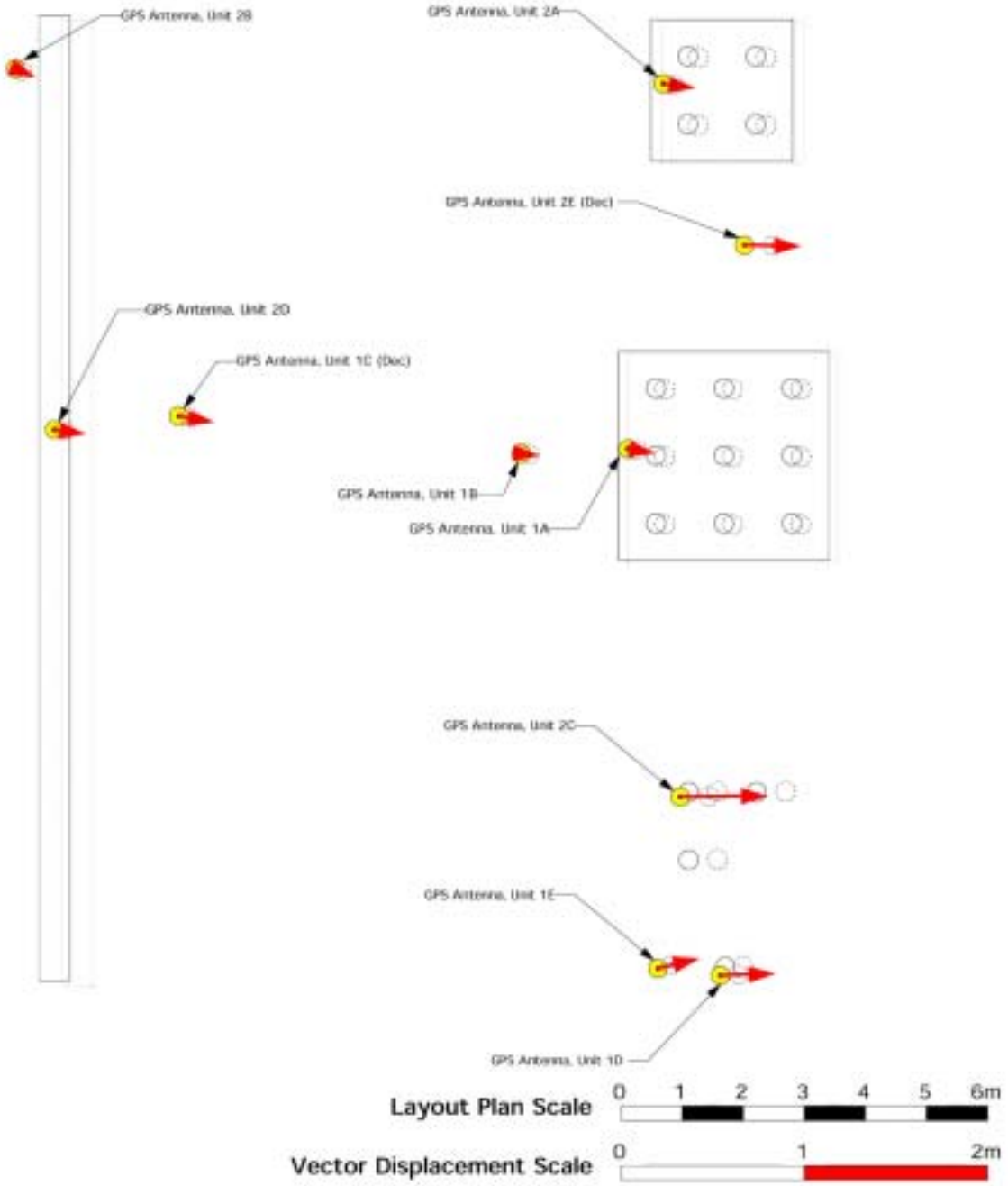

Figure 79 – Vector displacements in horizontal plane, December test

Significant deformations were observed in the vicinity of the pipelines during the November test. The two instrumented utility pipelines, Units 2D and 2E, as well as the free-field installation between the pipelines, Unit 2B, displaced approximately 35 to 38cm in the same direction with similar vertical settlements on the order of 9 to 13cm. These similar measurements could be interpreted in a number of ways. In one case, the pipelines may have constrained the movement of the upper soil layer during the lateral spread. Conversely, the pipelines may have deformed and displaced in unison with the surrounding soil during lateral spread. An examination of the strain results on the pipes from UCSD should help clarify the situation.

Data on and near the 9-pile group provided measurements that substantiated the expected lateral spread behavior. Units 1B and 1C provided upstream near and free-field ground surface measurements for the 9-pile group. The large concrete pile cap and pile group was expected to restrict the flow of soil in that area. During the November test ground surface measurements decreased as they got closer to the pile cap with horizontal measurements of 33cm, 28cm, and 18cm, for Units 1C, 1B, and 1A, respectively. Similar behavior was observed during the December test with horizontal measurements of 20cm, 15cm, and 15cm, for Units 1C, 1B, and 1A, respectively. An additional measurement was taken during the December test next to the pile cap with Unit 2E. As much as 46cm of horizontal displacement was measured. This was significantly more displacement than that measured by the near and free-field units. However, it should be noted that as much as 10cm of the total 46cm can be attributed to a local slope failure near the waterway resulting from the preliminary blasting.

In general, larger displacements were recorded for the November test than in the December tests. A combination of factors are likely to have contributed to this observation including the frozen surface crust and the densification of the site from previous blasting.

The data presented in Tables 8 through 11 were examined to determine if any significant creep or settlement occurred between minutes and hours following the blasting. For both tests, it appears as though the horizontal ground displacements associated with the lateral spread took place over the limited period during, and within tens of seconds following blasting. In general, the changes in the measured horizontal positions over a 20 hour period were within the potential error margins for RTK-GPS.

Although horizontal creep was not observed over the 20 hours following blasting, the data revealed evidence of 9 to 13cm vertical settlement throughout the test site over an extended period of time as pore water pressures dissipated. Figure 80 shows the change in vertical position of the GPS antennas over time on a semi-log plot for both tests. An initial data set collected following the blasting is shown at approximately 100 to 200sec. A final data set collected following the blasting is shown at approximately 80,000sec. As much as 29cm of vertical heaving during the blasting was observed as was presented in Figures 61 through 76. However, this detail is not shown in the plots in Figure 80 to provide clarity to long-term trends.

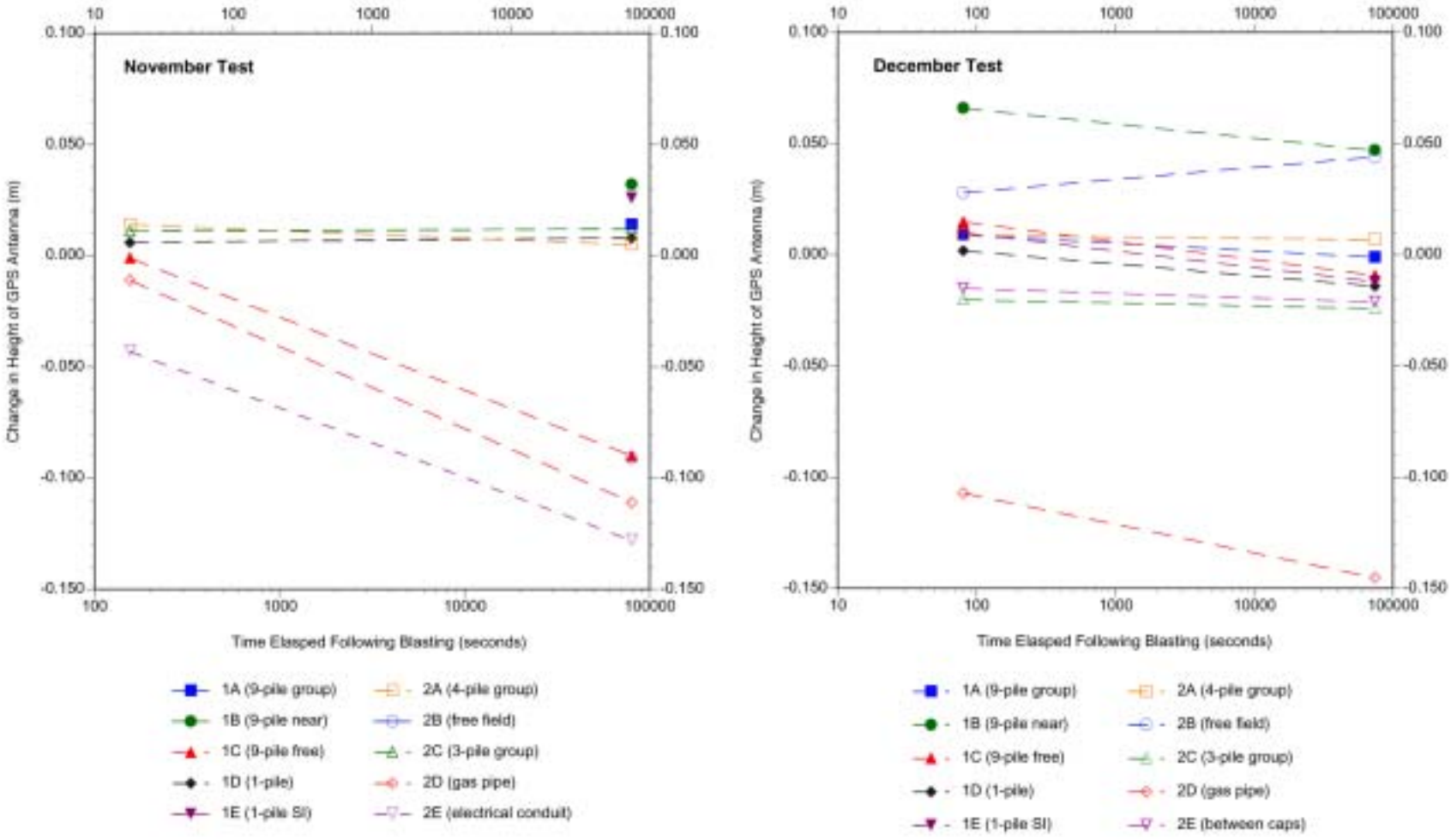

Figure 80 – Ground Surface Settlements, November Test (left), December Test (right)

During the November test significant settlements ranging from 9 to 13cm were measured for both free field installations (Units 1C and 2B) as well as for the two underground utilities (Units 2D and 2E). By contrast, measurements from the pile groups (Units 1A, 1D, 2A, and 2C) showed small upward heaving of less than 1cm during and following the blasting that did not subside over time. Although the vertical heaving estimates were near the vertical measurement resolution and could be attributed to measurement error, stability in the data trends seem to indicate otherwise. It is likely that short-term forces on the pipe piles from the blast induced soil heave displaced the piles upwards leaving a permanent vertical set. The GPS antennas installed directly onto slope inclinometer casings (Units 1B and 1E) showed evidence of permanent upward displacements between 2 to 3cm. Immediately following blasting, water was observed coming up through many of the inclinometer casings under high pressure. Figures 81 and 82 show photos of these observations after much of the water pressure was released. The release of pore water pressures through these casings in addition to potential buoyancy forces probably contributed to the upward movement of the casings. One of the inclinometer casings near the 4-pile group was observed to have risen in excess of 30cm as shown in Figure 83. Sand boils around the inclinometer casing can be seen in this photo.

Figure 81 – GPS Unit 1B shortly after blasting

Figure 82 – GPS Units 1D and 1E shortly after blasting

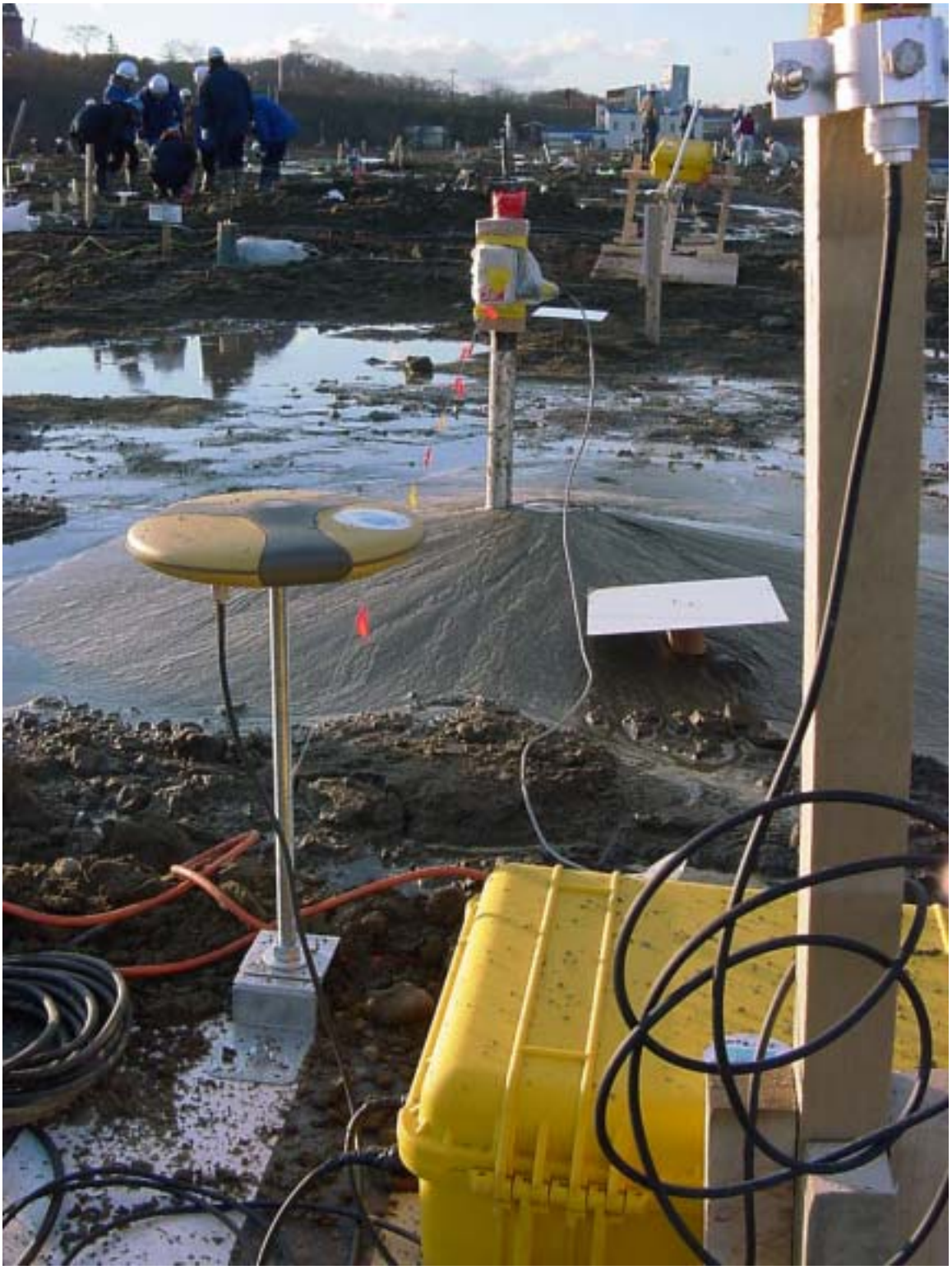

Figure 83 – GPS Unit 2A and adjacent inclinometer casing shortly after blasting

As was observed in the November test, the December test results showed significant settlement of the gas pipeline of approximately 14cm. However, unlike the November test significant settlements were not observed for the free field installations (Units 1C and 2B). In fact, Unit 2B showed an increase in vertical position of 4 to 5cm. As described elsewhere in this report, the GPS antennas for Units 1C and 2B were installed on rafts that were tied to adjacent slope inclinometer casings for the November test. This allowed the casing to rotate and move up and down without impacting the measurement of the location of the casing at ground surface. However, for the December test the GPS antennas were mounted directly to the inclinometer casings. Using this installation technique, the GPS could only capture the position of the top of the casing and not the true ground surface deformations. Snow buildup around the antenna mounts also made it difficult to assess relative changes between the casing and ground surface. Upward migration of pore water pressures through these casings in addition to potential buoyancy forces were likely to have caused many of the casings to rise such as measured with Units 1B and 2B.

6.3 General Discussion of Time-History Records

Detailed time-history records were presented in Figures 61 through 76 showing longitudinal, transverse, and vertical displacements over the period during blasting. These time-history records clearly illustrate the dynamic motion of the ground surface and installed test specimens during blasting. Consider the time-history record for Unit 1C during the November test as shown in Figure 84 below.

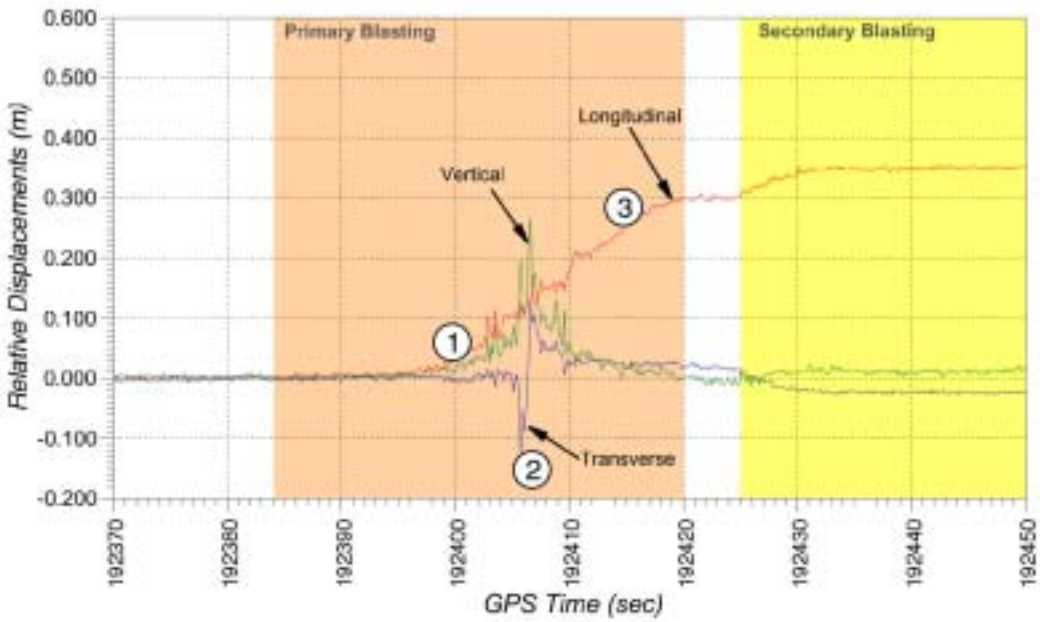

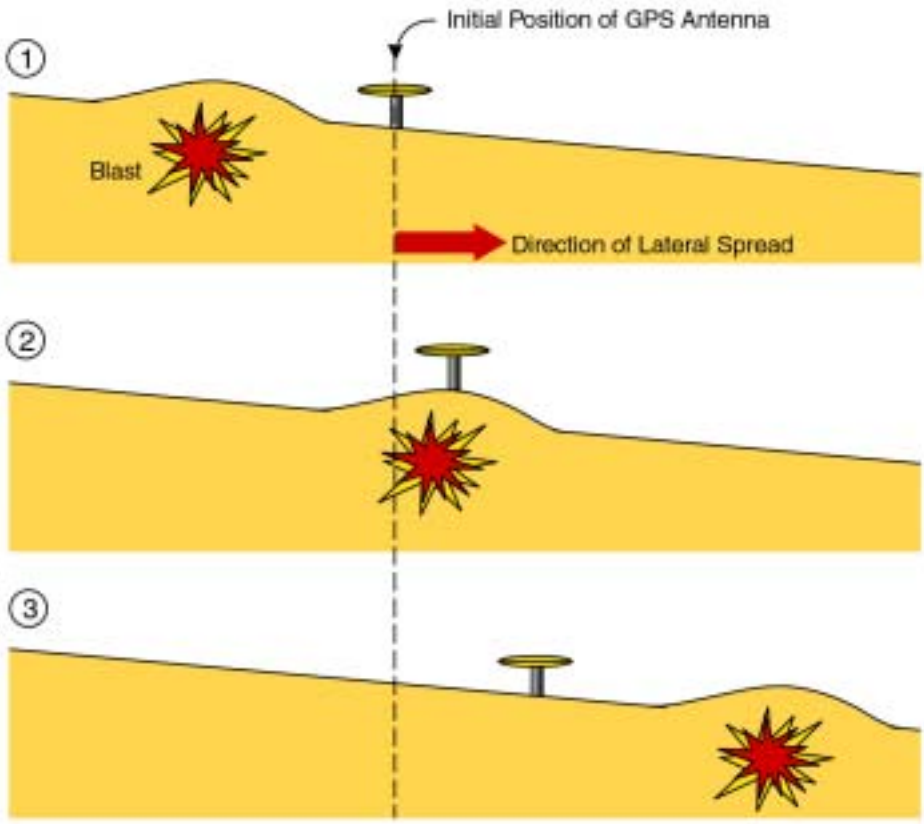

Figure 84 – Explanation of time-history record for Unit 1C, November test

As blasting proceeded from the back of the site to the front, compressive blasting forces raised pore water pressures throughout the site inducing liquefaction. The liquefaction, in turn, induced lateral spread, initiating longitudinal and vertical displacements as shown at time (1) in Figure 84. As blasting neared the location of the GPS antenna, greater deformations were recorded. Blasting near and below the location of the GPS antenna produced large vertical displacements and a quick transverse impulse as shown at time (2) in Figure 84. Recall from Figure 55 in Section 2.5 that the blasting proceeded sequentially in a series transverse rows. These transverse blasts were likely to have caused the large transverse motions in this particular record. With the blasting past the location of the GPS antenna, deformations were predominately longitudinal from lateral spread. Secondary blasting around the perimeter of the test site induced additional displacements.

Also notable, most of the GPS antennas were mounted on top of 5/8" threaded steel rod, cantilevered as much as 38cm, which was likely to have contributed to additional transient motions both transversely and longitudinally. The amount of additional motion from this type of installation was evaluated using a simple single degree of freedom model. Considering the stiffness from a 38cm long, 16mm diameter rod, and a GPS antenna with a mass of 1kg, the natural period of this system was calculated at approximately 0.25 seconds. Since the monitoring system was set up to acquire data at 10Hz, the 4Hz motions were most likely aliased and would appear as noise in the data. Time-history records did not provide a clear indication of additional horizontal motions. In fact, magnitudes

of noise in the vertical component were of similar magnitude as those in the horizontal components.

As described earlier in the report, a short series of blasts to loosen the toe were executed prior to the primary blasting sequence for the December test. Most of the time-history records reflect the occurrence of this initial blasting. For example, in the record for Unit 2E the initial blast occurs at approximately 450983 sec as indicated as time (1) in Figure 85. This initial blast caused significant longitudinal motions. The primary blasting began at approximately 451001 sec as noted by time (2), with completion of blasting at approximately 451013 sec as noted by time (3) in Figure 85.

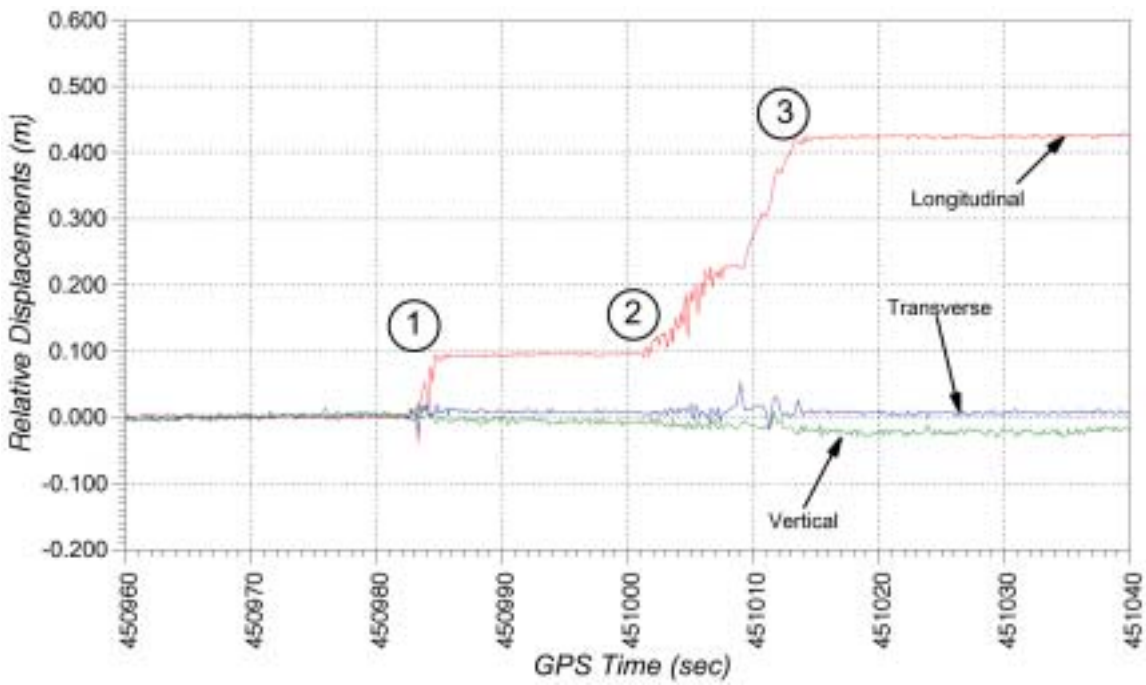

Figure 85 – Explanation of time-history record for Unit 2E, December test

6.4 Observations of Liquefaction from the November Test

During the November test, sensors attached to near the mid-span of the gas pipeline and electrical conduit provided a comprehensive data set on the initiation of liquefaction and ground surface deformations during blasting. Two GPS antennas, Units 2D and 2E, were installed at this location. Between the GPS antennas a research team from the UCSD had installed pore pressure transducers at multiple depths (Juirnarongrit 2002). Two of the three transducers in this area provided pore pressure data, one installed at elevation –1.00m (designated as PPT-AB-4M) and the other at elevation –3.00m (designated as PPT-AB-6M). The groundwater elevation at the time of the test was approximately +2.00m. Figure 86 shows the 60 second time-history at this location as blasting passed through this area.

Multiple data sets are displayed in Figure 86. Data for GPS Units 2D and 2E are plotted using the scale on the right side of the plot, corresponding to the longitudinal component of displacement in the direction of the lateral spread. Data for pore pressure sensors PPT-AB-4M and PPT-AB-6M are plotted using the scale on the left side, expressed in terms of pore pressure ratio.

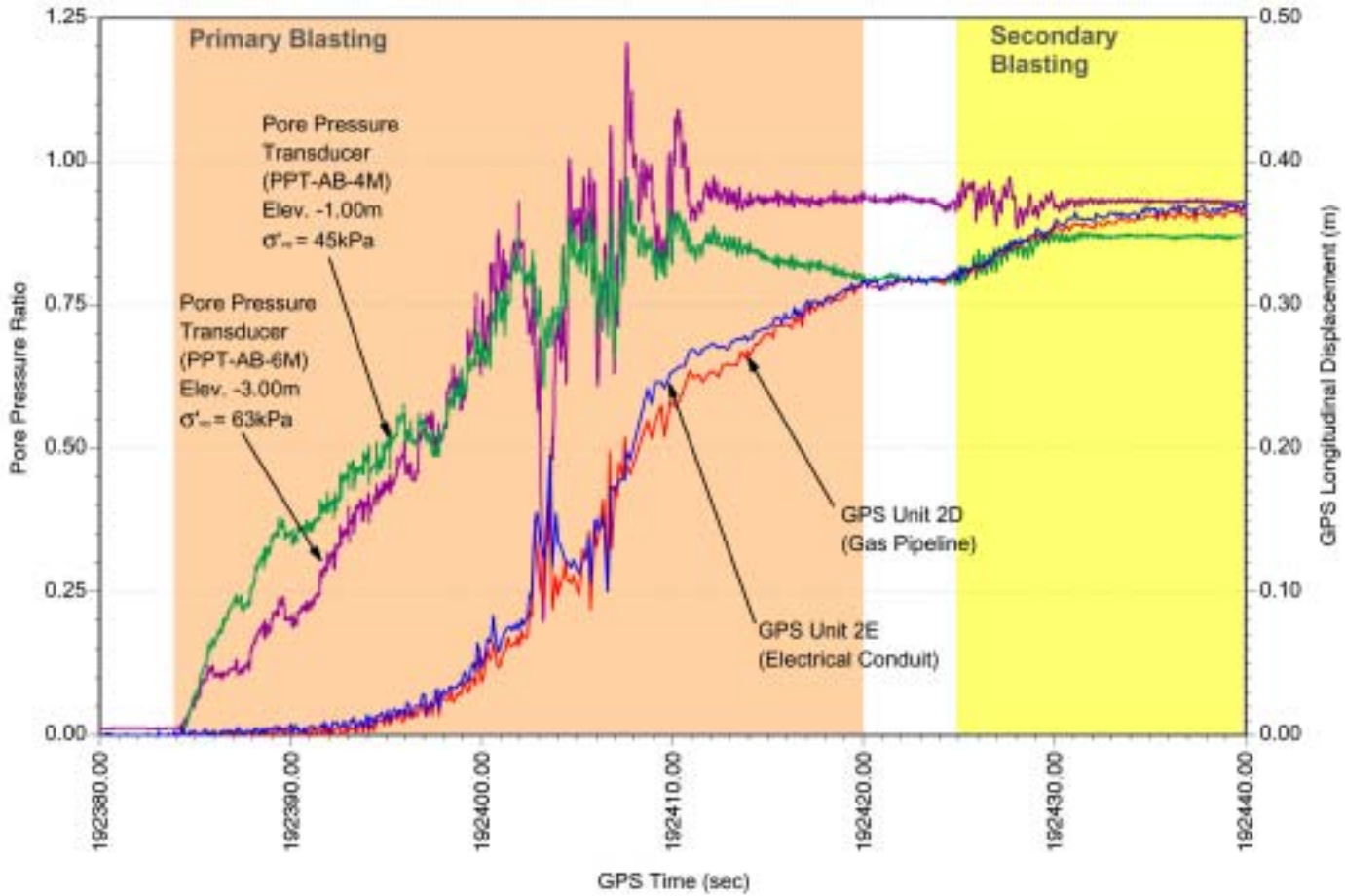

Figure 86 – Time-history of longitudinal displacement for GPS Units 2D and 2E, and filtered excess pore pressure for transducers PPT-AB-4M and PPT-AB-6M, November test

Recall that the pore pressure ratio, $\Delta u/\sigma_o'$, is the ratio of excess pore water pressure over the initial vertical effective overburden stress. Liquefaction has been defined by many as the stress state in which the excess pore water pressure, Δu, equals the initial consolidation effective stress, σ_o', in the soil (Kramer 1996). This can also be expressed as the condition where the pore pressure ratio, $\Delta u/\sigma_o'$, is equal to 1.

The GPS data shown in Figure 86 is displayed in an unfiltered 10Hz format. The raw pore pressure data was collected at 100Hz. However, to provide clarity in the plot, the raw pore pressure data was filtered using a 70 point (0.7 sec) centered moving average technique. The purpose of the filtering wasn't necessarily to reduce electrical noise, as is typically done with transducer data in electrically sensitive environments. Compression waves from the sequential blasting leading up to and following the location of the pore pressure transducers created large spikes and drops in the data at a relatively high frequency. These spikes and drops appear similar to electrical noise, however are clearly discernable as p-waves or compression waves. Figure 87 shows an expanded time history of one of the pore pressure transducers during blasting.

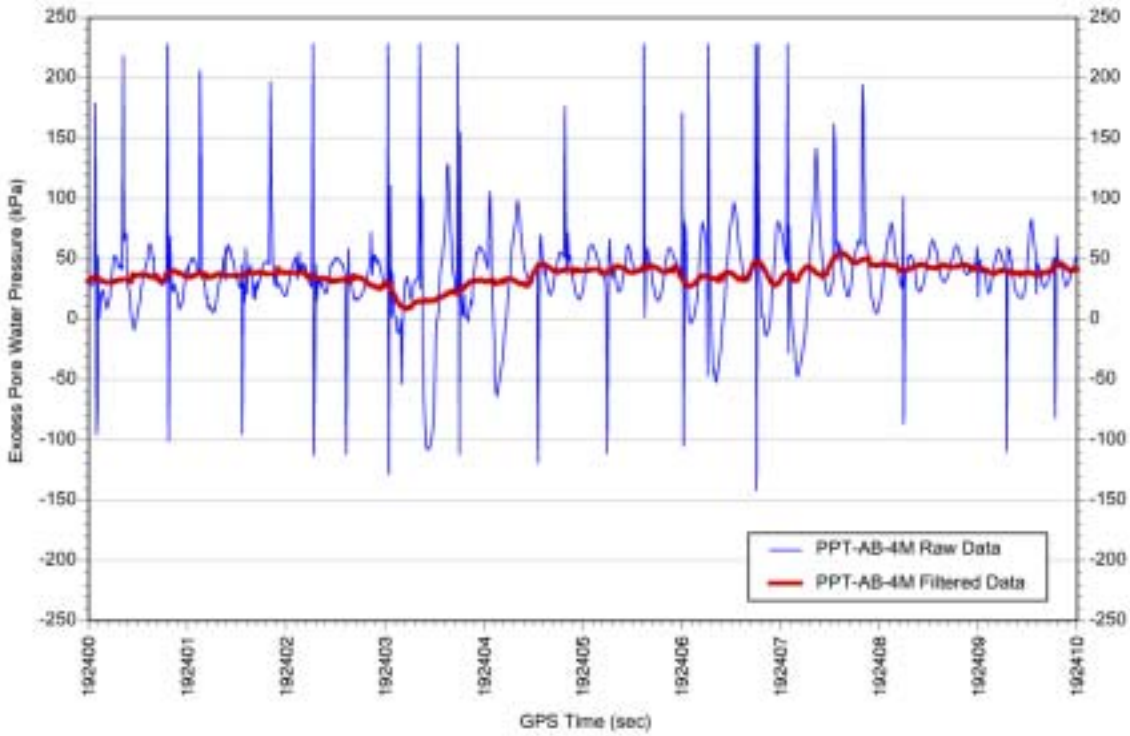

Figure 87 – Raw data time-history of excess pore pressure for transducer PPT-AB-4M

It is notable in Figure 87 that the data spikes occur at rate of about 2 per second. This rate is consistent with the timing of the primary blasting where 96 charges were detonated over a period of approximately 45 seconds. Information on the precise timing and sequencing of blasting was not available at the time of writing of this report.

Examining the plot in Figure 86, longitudinal ground surface deformations are first detectable at approximately 192384 seconds, GPS time, with the pore pressure transducers beginning to sharply increase at that time. Since the blasting commenced at 192384.30 seconds, it is clear from the data that significant

increases in pore pressures and small surface displacements occurred simultaneously at the onset of blasting with a pore pressure ratio of only 0.1.

The first blast in the primary sequence of blasting was detonated approximately 40 meters away from the location of the pore pressure transducers as was shown in Figure 55. As blasting progressed through the site, pore pressures increased relatively linearly in time from 192384.30 seconds to approximately 192403.00 seconds, the estimated time of the blast in the hole closest to the pore pressure transducers. Pore pressure measurements were observed to oscillate between 192403.00 seconds and 192413.00 seconds resulting from the nearby blasting with transient pulses of pore pressure ratio reaching as high as 1.20. However, these ratios leveled off after 192413.00 seconds with residual mean ratios ranging between 0.80 and 0.90.

Small but steady longitudinal displacements were measured from the onset of blasting at 192384.3 seconds up to approximately 192398.0 seconds, after which the rate of motion increased significantly with pore pressure ratios in excess of 0.5 and larger dynamic forces due to closer blasting. The rate of longitudinal displacements decreased after 192410.00 seconds. Pore pressure measurements from PPT-AB-4M indicated some dissipation at this time as well. Secondary blasting around the perimeter of the test site, beginning at approximately 192425 seconds, created additional deformations and a modest increase in pore pressure ratio for PPT-AB-4M back to its previous levels.

Based upon the measurements it appears that the ground movements were likely generated by a combination of blasting and high excess pore pressures. The smaller displacements at the onset of blasting (192384.30 to 192398.00 seconds) were likely due to a combination of compressive downslope forces created by spreading soil upslope and weakened soil near the GPS unit resulting from increased pore pressures. Although pore water pressure ratios were relatively low during this time period, ranging from 0 to 0.60, this may have been sufficient to induce some weakening of the soil. As blasting passed through this location, pore pressures reached peak ratios, the soil was nearing a liquefied state, and lateral spread was observed with an increased rate of displacement (192398.00 to 192410.00 seconds). As blasting proceeded in front of the location of the GPS units, compressive blast forces acting in the opposing direction may have contributed to the decrease in the rate of longitudinal displacement (beyond 192410.00 seconds). Since the GPS units were attached directly to the utility pipelines, the decrease in the rate of longitudinal displacement may have also been due to resistance from the flexure in the pipelines. Free-field measurements between the pipelines from Unit 2B showed displacements of similar magnitude and direction as those of the pipelines. However, since the Unit 2B was installed in the area of engineered backfill around the pipelines, it may not be a reliable indicator of true free field ground motions. Subsequent analysis of stresses in the pipelines may resolve this question.

6.5 Validity of Measurements

At a couple of locations, measurements with GPS were checked against secondary extensometer measurements. The UCSD research team installed one

extensometer between GPS Units 1A and 1B which spanned the distance between the 9-pile group cap and the near-field slope inclinometer casing (Juirnarongrit 2002). Another extensometer was installed between GPS Units 1D and 1E which spanned the distance between the single free-head pile and the near-field slope inclinometer casing adjacent to it. A summary of the relative displacements is shown in Table 12 based upon data collected during the November test. These measurements represent the change in total distance, vector sum of horizontal and vertical, between the two sets of GPS antennas as determined independently from GPS and extensometer measurements.

Location	GPS Measurement	Extensometer Measurement
GPS Units 1A and 1B	0.105m	0.096m
GPS Units 1D and 1E	.009m	.006m

Table 12 – Validation of GPS Measurements

In general, the extensometer data confirmed the GPS measurements. At both locations the GPS measurements were within 1cm of the extensometer measurements, which is the accuracy typically associated with RTK-GPS methods. Although extensive independent surveys of GPS locations prior to and following blasting were conducted by the Japanese research teams, the data was not available at the time of writing of this report.

7.0 Conclusions

Limitations in conventional displacement sensors have made large scale deformation monitoring applications challenging, such as those employed in the study of landslides and bridges. Highly accurate measurements using surveying techniques are often generated infrequently and at a significant cost. Surface extensometers, tilt meters, and similar technologies usually can only provide a qualitative assessment of deformation. Research efforts presented here show that GPS sensors are a viable alternative with the distinct advantage of providing accurate vectoral displacements relative to a stable satellite-based reference framework.

Interpretation of data using the Real Time Kinematic method appears to be the most relevant implementation of GPS for deformation monitoring, as it provides positioning solutions with centimeter accuracy at frequencies up to 20Hz. Other forms of GPS require either long collection and processing times to achieve the necessary accuracy, or deliver meter-level solutions when used in a real-time mode.

Validation test results clearly demonstrated the accuracy of RTK-GPS under static and dynamic conditions. Under dynamic motions of 1 to 3Hz, GPS measurements were in excellent agreement with independent measurements from a displacement transducer. Both single and dual-frequency receivers appear to provide similar accuracies under bench test conditions.

RTK-GPS technologies are well suited to automation as was proven in the deployment of a prototype networked RTK system at a Caltrans facility. Using autonomous power systems, wireless spread spectrum data transceivers, and internet technologies, such a system can be deployed for extended time periods in relatively remote locations. A cost effective system is achieved through the use of simplified field hardware and a centralized data processing and dissemination architecture.

The use of the system in two full-scale lateral spread tests in Japan demonstrated the flexibility and stability of the integrated system at its current stage in development. The combination of severe weather and blasting during the December test represented an extreme monitoring environment. However, system performance was impressive with relatively small losses in data during the critical measurements. The GPS measurements provided an otherwise unattainable data set for this type and scale of test. Subsequent analysis of the data sets by other members of the research team can be used to model the test events to gain new insight into the performance of pile foundation systems and pipelines during lateral spread.

Monitoring of planned deployments on two landslides and two bridges in California in the upcoming year will provide longer term performance and reliability data to support deployment of this type of system on a more routine basis.

8.0 Acknowledgements

I would like to acknowledge Professor Ross Boulanger, Professor Bruce Kutter, and Professor Scott Ashford for their work in reviewing the contents of this report. In addition, the assistance of Professor Scott Ashford in leading the overall U.S. effort in designing the lateral spread experiment and coordinating with the Japanese colleagues is gratefully acknowledged. I would also like to recognize the outstanding coordination provided by Dr. Sugano of PARI and Professor Hamada from Waseda University in effectively managing the Japan test site and the many contractors and research teams.

Cliff Roblee and Tom Shantz from Caltrans' Division of Research & Innovation are acknowledged for their help in setting up the GPS equipment for the Japan tests. The assistance of Cliff Roblee in providing comments on the early draft of this report is truly appreciated.

9.0 References

Celebi, M., Prescott, W., Stein, R., Hudnut, K., Behr, J., Wilson, S. (1999). GPS Monitoring of Dynamic Behavior of Long-Period Structures; *Earthquake Spectra (Journal of EERI)*, Volume 15, Number 1, pp.55-66

Dana, P.H., (1994). *"Global Positioning System Overview," The Geographer's Craft Project, Department of Geography, The University of Colorado at Boulder*, <http://www.colorado.Edu/geography/gcraft/notes/gps/gps_f.html> (April 11, 2003).

FreeWave Technologies, Inc. (2000). *FreeWave Spread Spectrum Wireless Data Transceiver User Manual*, Boulder, CO.

Hofmann-Wellenhof, B., Lichtenegger, H., and Collins, J. (1997). *GPS Theory and Practice*, Springer-Verlag, Wien, New York.

Holtz, R.D. and Kovacs, W.D. (1981). *An Introduction to Geotechnical Engineering*, Prentice-Hall, Inc., Englewood Cliffs, New Jersey.

Hudnut, K. W. and Behr, J. A. (1998). Continuous GPS Monitoring of Structural Deformation at Pacoima Dam, California; *Seismological Research Letters*, Volume 69, Number 4, July-August 1998.

Juirnarongrit, T., and Ashford, S.A. (2002). *(Personal Communication between January 1 to March 13, 2002)*, Department of Structural Engineering, University of California San Diego.

Juirnarongrit, T., and Ashford, S.A. (2002*). Performance of Lifelines Subjected to Lateral Spreading: Japan Blast Test Results*, Report No. TR-2002/04, Department of Structural Engineering, University of California San Diego, June 2002.

Kramer, S.L. (1996). *Geotechnical Earthquake Engineering*, Prentice Hall, Inc., Upper Saddle River, New Jersey.

Langley, R.B. (1998). *"RTK GPS,"* GPS World Magazine, September 1998.

Turner, L. (2002). *"Application of a Real-Time Kinematic Global Positioning System to Measure Liquefaction-Induced Ground Surface Deformations*," Thesis submitted for Master of Science , University of California Davis.

Turner, L. (2002). *"What's Shaking? Earthquake Trials Test Networked RTK*," GPS World Magazine, Vol. 13, No. 4, April 2002.

Turner, L., (2000). *Stage 1 Report, Continuous GPS: Pilot Applications*; Caltrans Internal Report to the Project Advisory Panel.

Turner, L., (2001). *Stage 2 Project Status Report, Continuous GPS: Pilot Applications*; Caltrans Internal Report to the Project Advisory Panel.

Turner, K. A., and Schuster, R. L., (1996). *Landslides, Investigation and Mitigation, Special Report 247*, Transportation Research Board, National Research Council, Washington D.C.

U.S. Department of Transportation, U.S. Department of Defense (1999). *1999 Federal Radionavigation Plan*, Final Report, DOT-VNTSC-RSPA-98-1, DOD-4650.5, Washington, DC.

Waypoint Consulting, Inc.. (2000). *RTKNav, Rt Engine Rt DLL Windows 95/98/NT Real-time GPS Processing Software*, (Software Manual), Calgary, Alberta, Canada.

Appendix A - Cost Estimate for 4-Unit Single Frequency System

Table A.1 provides cost information for an autonomous GPS-based remote monitoring system specified to provide positioning data from four points at a remote site up to 20 miles away, while producing reliable centimeter-level solutions in real-time at up to 10 positions per second. This system assumes clear line of sight between the field units and the location of the RTK-GPS Processing PC. An autonomous solar power system was chosen for this example.

Item Description	Qty.	Unit Cost	Extension
GPS Receiver (CMC Starbox/Allstar 10Hz)	5	$835	$4,175
GPS Antenna w/cable (AeroAntenna AT575-75T)	5	$420	$2,100
Data Transceiver (Freewave DGR-115R)	8	$1,010	$8,080
Transceiver Antenna w/cable (Antennex 3dB Omni)	8	$100	$800
GPS Processing Software (Waypoint RTEngine)	1	$5,000	$5,000
Laptop PC (Toshiba P3, 500Mhz, Windows 2000)	1	$1,500	$1,500
Field Enclosure (TwoSeas NEMA4) with 100Ah Battery, charge regulator	4	$700	$2,800
Solar Panel (Solarex SX, 65W, 3.77A)	4	$300	$1,200
Misc. Hardware	1	$200	$200
TOTAL			$25,855

Table A.1 – Cost of 4-Unit System

Appendix B – Software Diagrams

Software for the *RTK-GPS Data Processing PC* as well as the *Server* was developed using National Instrument's *Labview 6.0*. The code diagrams for the software are provided in Figures B.1 through B.10.

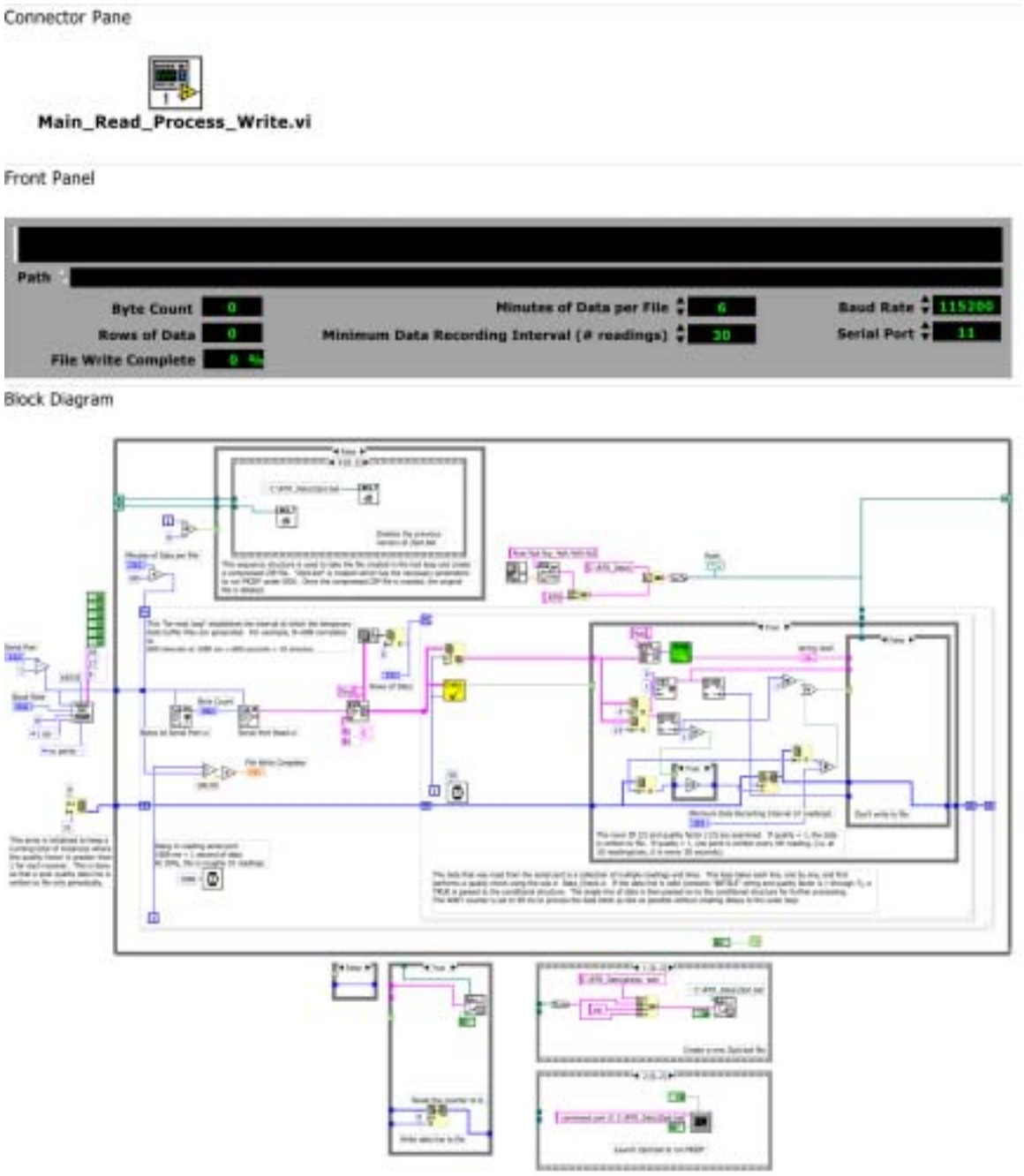

Figure B.1 – RTK-GPS Processing PC Code

Position in Hierarchy

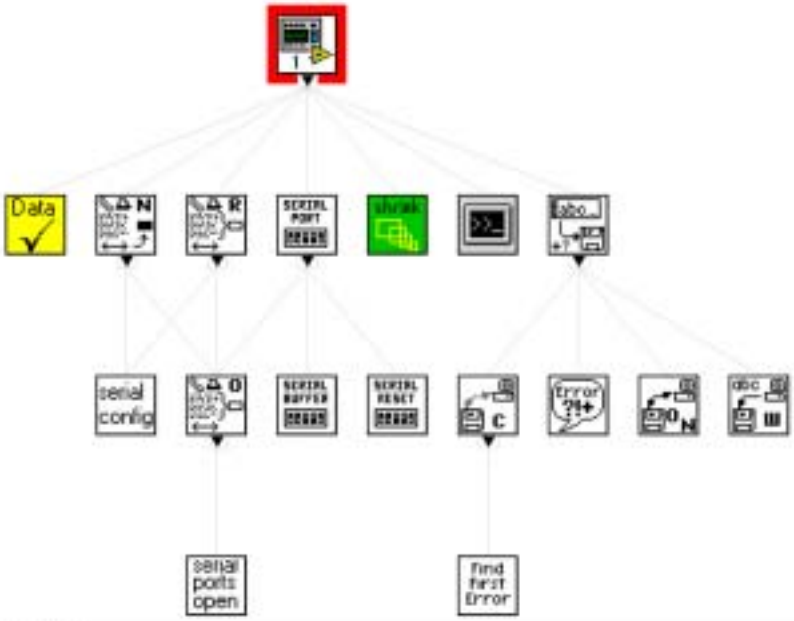

List of SubVIs

Serial Port Init.vi
C:\Program Files\National Instruments\LabVIEW 6\vi.lib\Instr\Serial.llb\Serial Port Init.vi

Serial Port Read.vi
C:\Program Files\National Instruments\LabVIEW 6\vi.lib\Instr\Serial.llb\Serial Port Read.vi

Bytes At Serial Port.vi
C:\Program Files\National Instruments\LabVIEW 6\vi.lib\Instr\Serial.llb\Bytes At Serial Port.vi

Write Characters To File.vi
C:\Program Files\National Instruments\LabVIEW 6\vi.lib\Utility\file.llb\Write Characters To File.vi

Data_Check.vi
C:\Documents and Settings\Administrator\My Documents\Continuous GPS\Loren's VIs\Field PC Code\Data_Check.vi

String_Reduce.vi
C:\Documents and Settings\Administrator\My Documents\Continuous GPS\Loren's VIs\Field PC Code\String_Reduce.vi

Figure B.2 – RTK-GPS Processing PC Code

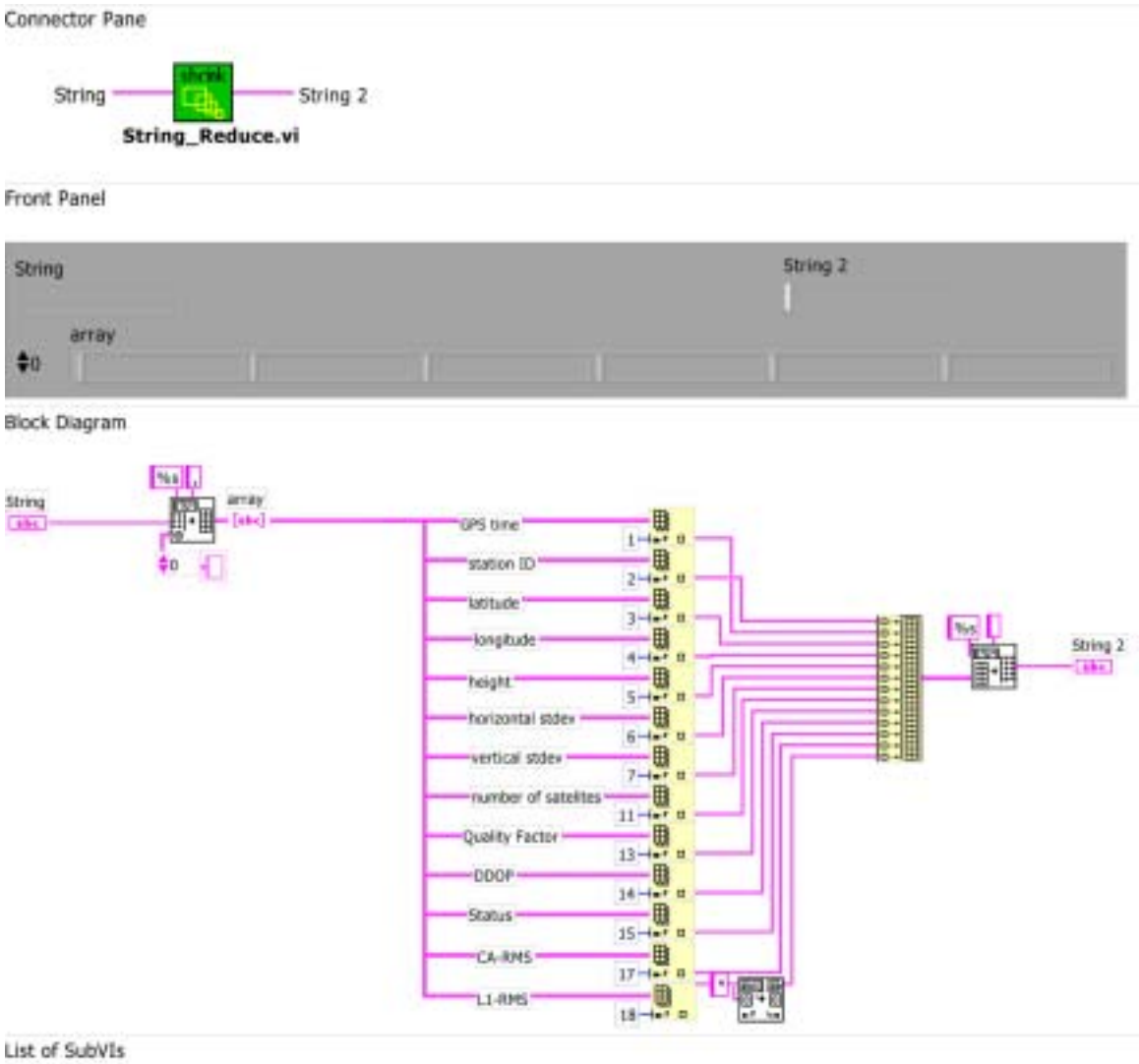

Figure B.3 – RTK-GPS Processing PC Code

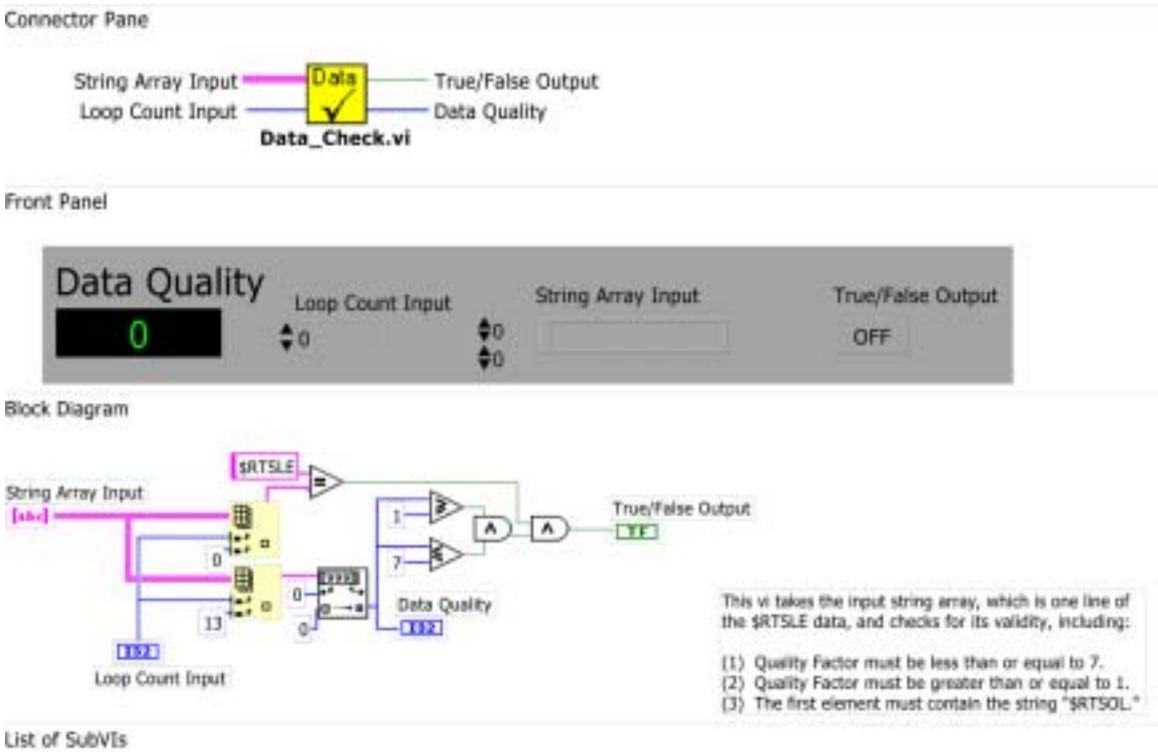

Figure B.4 – RTK-GPS Processing PC Code

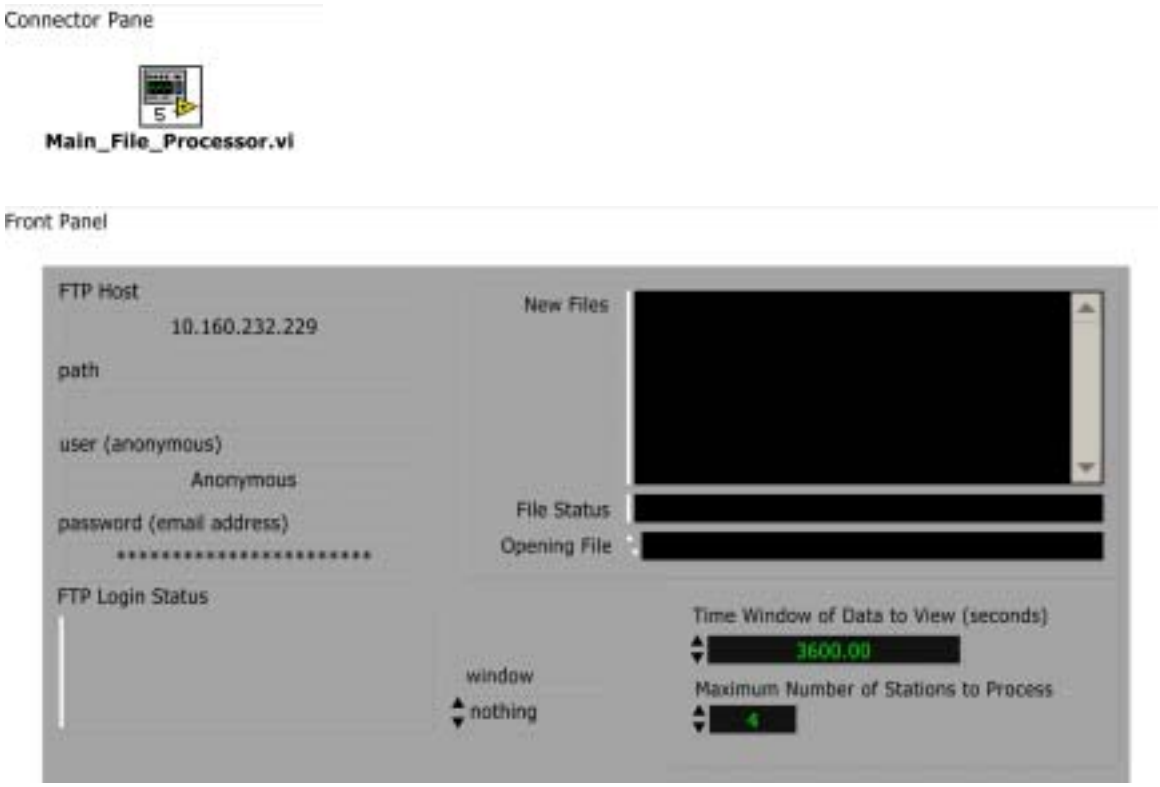

Figure B.5 – Server PC Code

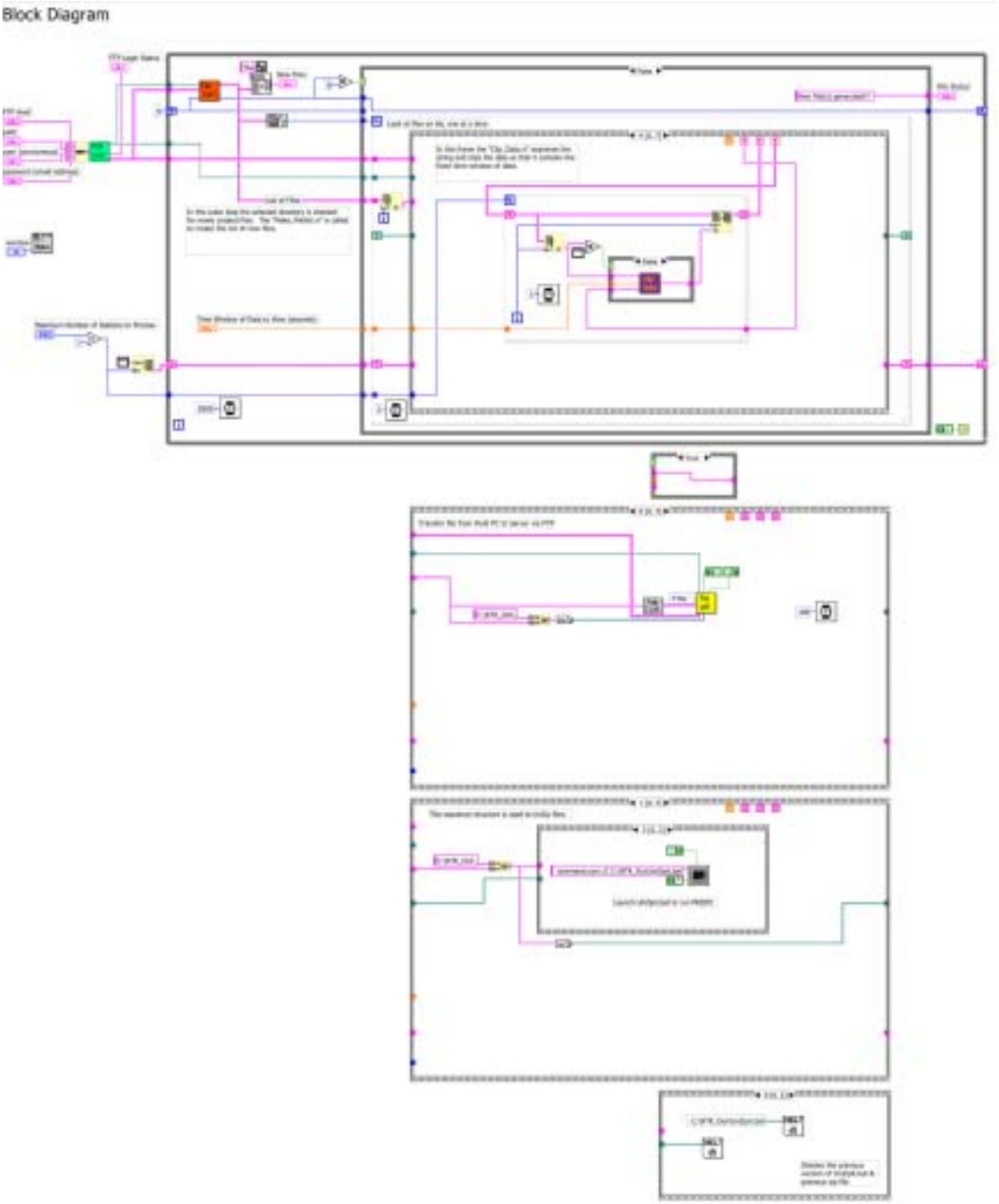

Figure B.6 – Server PC Code

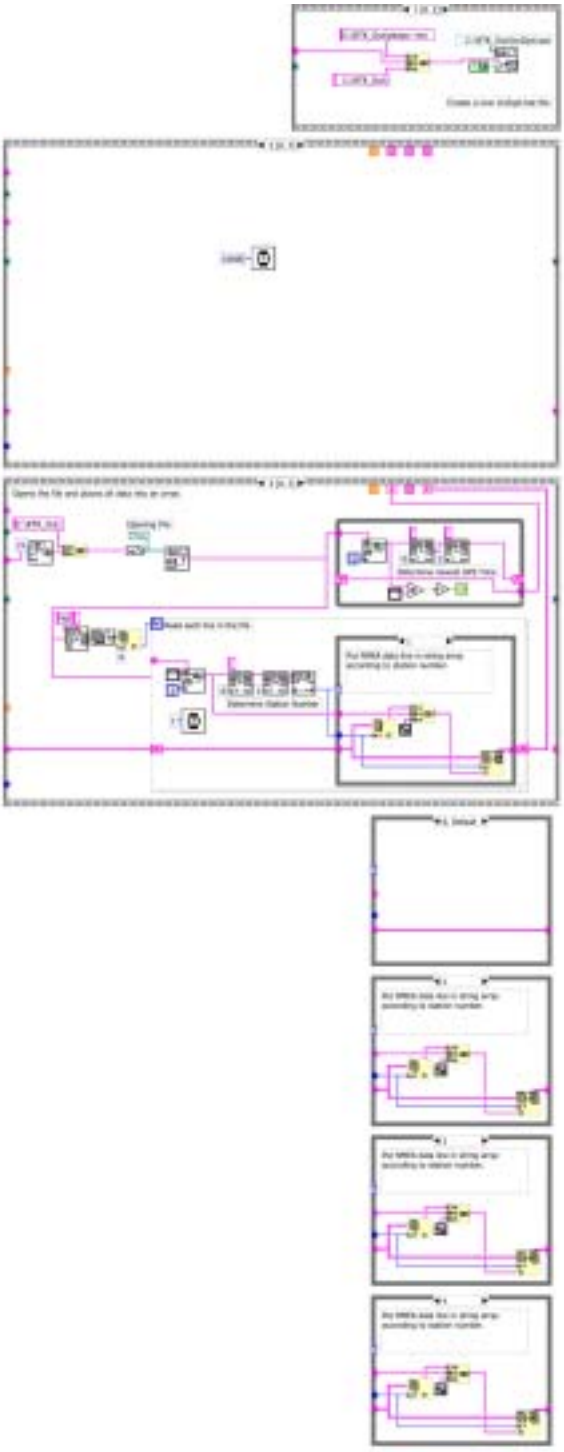

Figure B.7 – Server PC Code

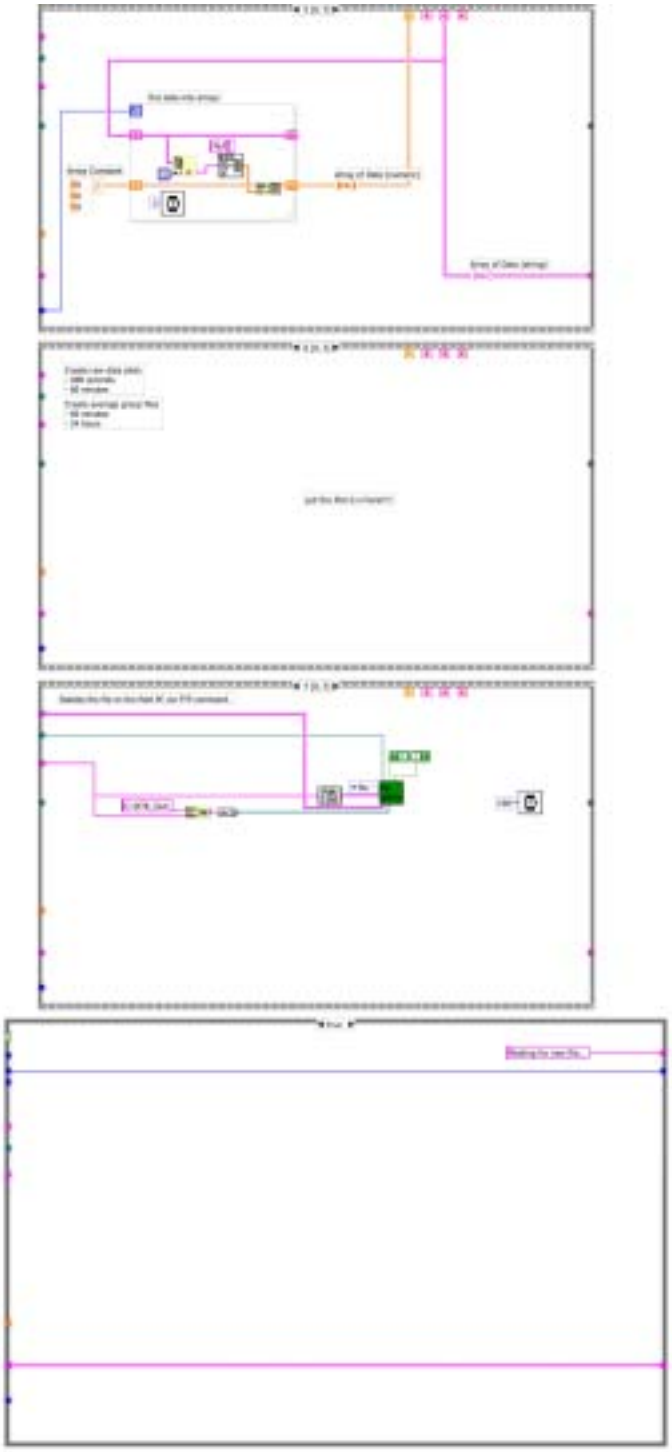

Figure B.8 – Server PC Code

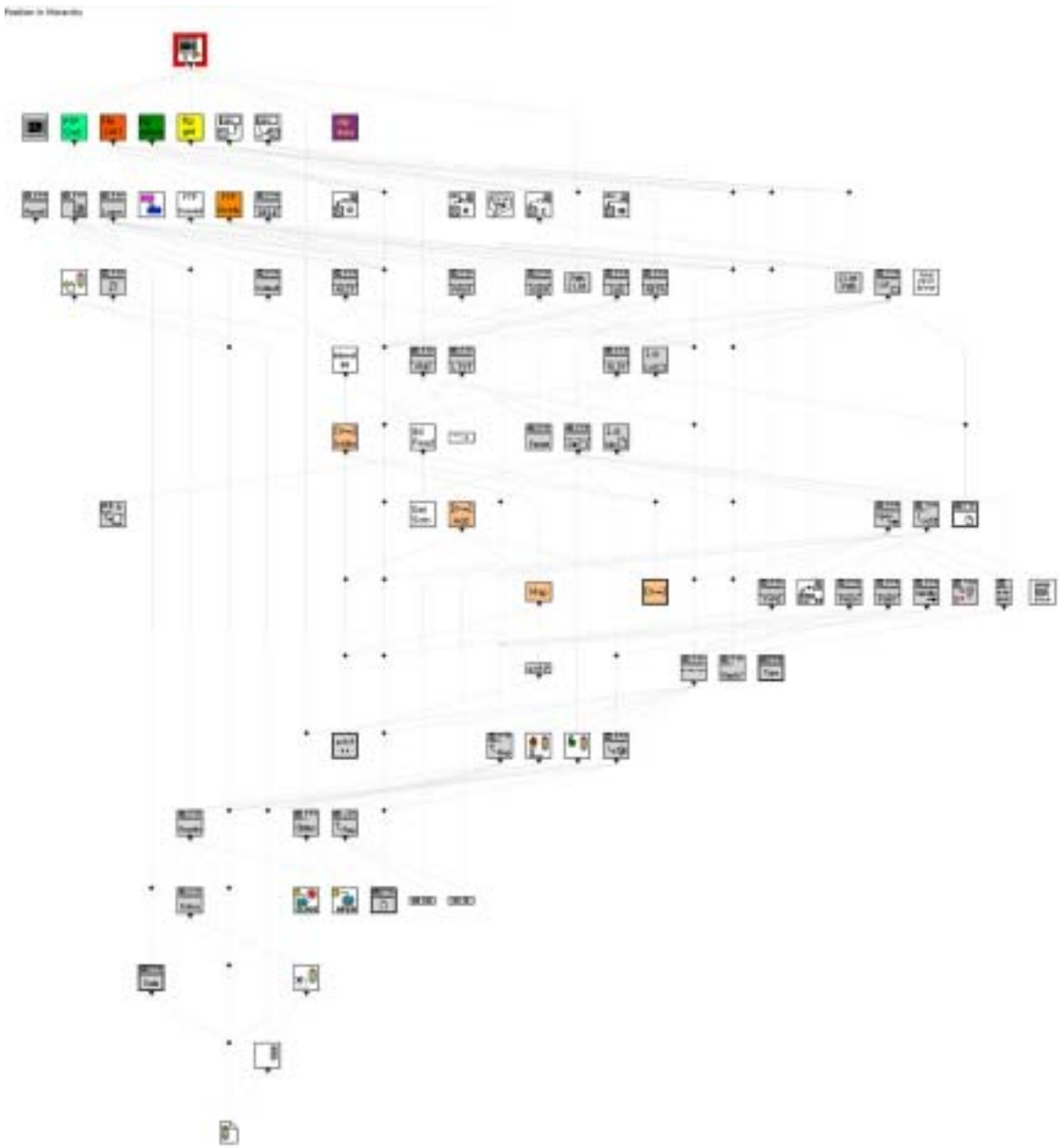

Figure B.9 – Server PC Code

List of SubVIs

Write Characters To File.vi
C:\Program Files\National Instruments\LabVIEW 6\vi.lib\Utility\file.llb\Write Characters To File.vi

Clip_Data.vi
C:\Documents and Settings\Administrator\My Documents\Continuous GPS\Loren's VIs\Server PC Code\Clip_Data.vi

Make_Filelist.vi
C:\Documents and Settings\Administrator\My Documents\Continuous GPS\Loren's VIs\Server PC Code\Make_Filelist.vi

Path to List.vi
C:\Program Files\National Instruments\LabVIEW\EXAMPLES\internet\ftp_brsr.llb\Path to List.vi

FTP_Connect.vi
C:\Documents and Settings\Administrator\My Documents\Continuous GPS\Loren's VIs\Server PC Code\FTP_Connect.vi

Read Characters From File.vi
C:\Program Files\National Instruments\LabVIEW 6\vi.lib\Utility\file.llb\Read Characters From File.vi

FTP Status
C:\Program Files\National Instruments\LabVIEW 6\vi.lib\addons\internet\ftp\ftp2.llb\FTP Status

FTP_Download_file.vi
C:\Documents and Settings\Administrator\My Documents\Continuous GPS\Loren's VIs\Server PC Code\FTP_Download_file.vi

FTP_Delete_file.vi
C:\Documents and Settings\Administrator\My Documents\Continuous GPS\Loren's VIs\Server PC Code\FTP_Delete_file.vi

System Exec.vi
C:\Program Files\National Instruments\LabVIEW 6\vi.lib\Platform\system.llb\System Exec.vi

Figure B.10 – Server PC Code

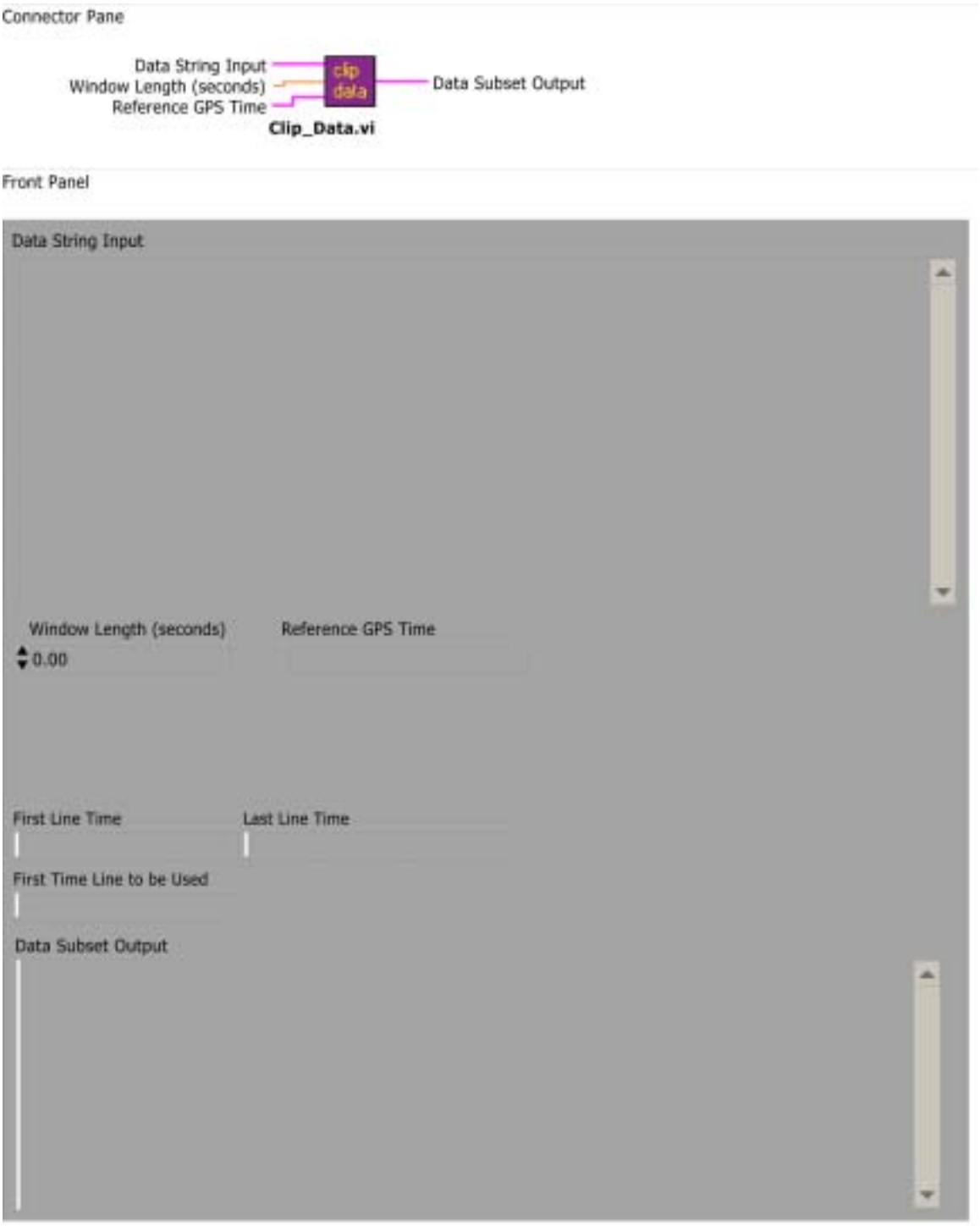

Figure B.11 – Server PC Code

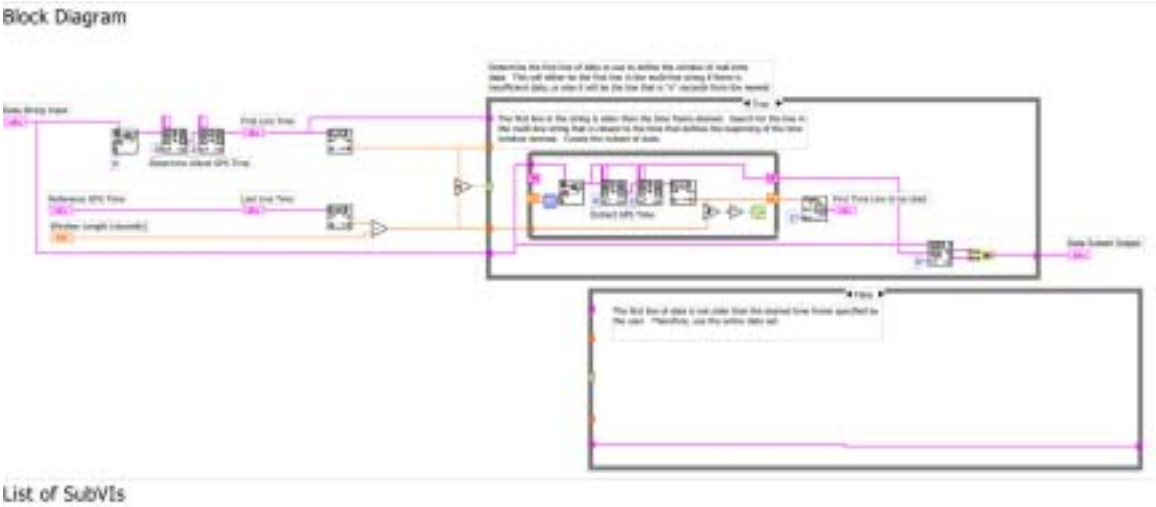

Figure B.12 – Server PC Code

Appendix C - Prototype Landslide Field Unit

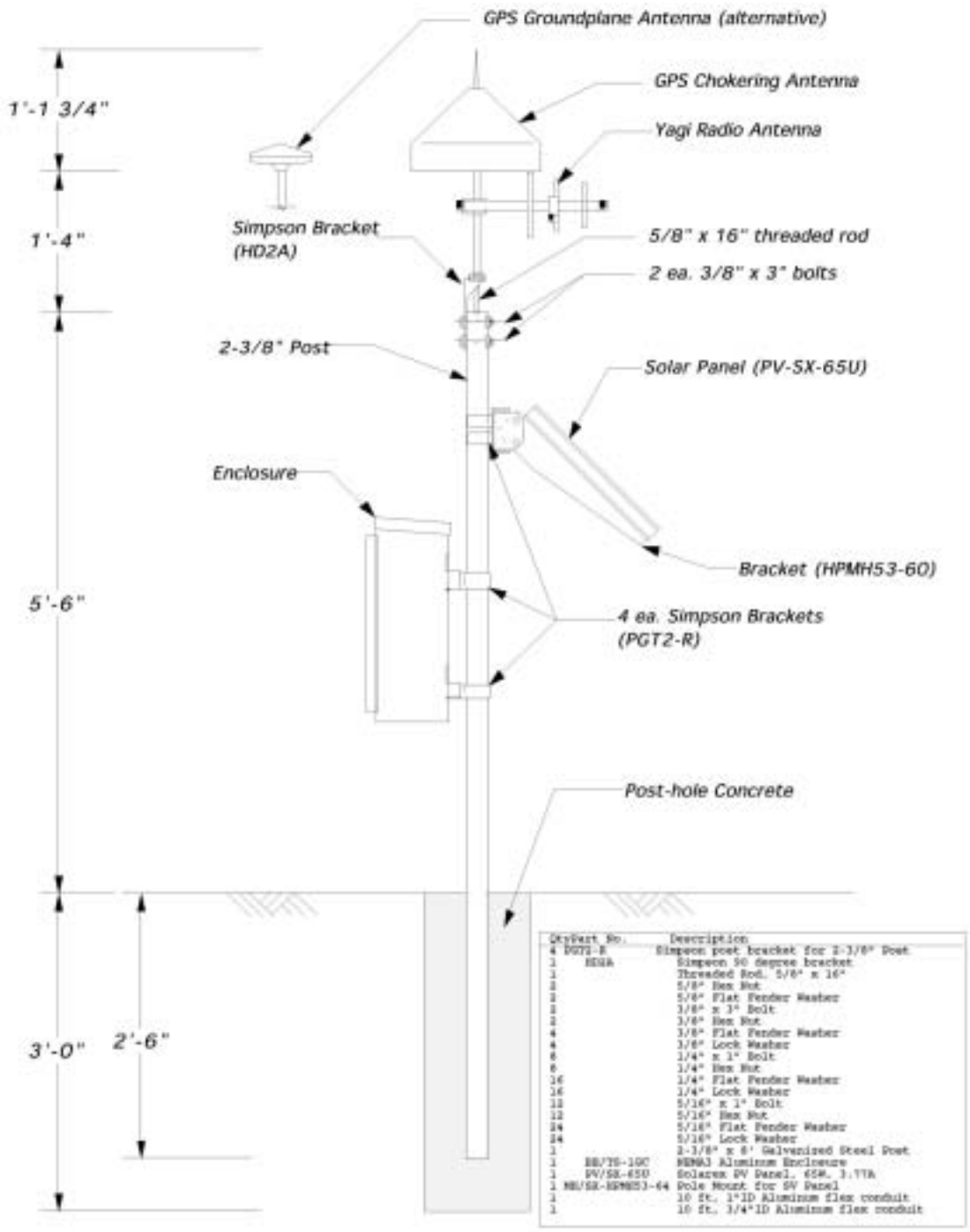

Figure C.1 – Prototype Landslide Monitoring Field Unit

Appendix D – Japan Test System Equipment List

A comprehensive list of components with serial numbers and cost information is provided in Table D.1 for the system deployed for the November and December 2001 tests in Japan.

Shipping Container	Contents	Serial Number	Value
1A	Topcon GPS Legacy-E GD GPS L1/L2 Receiver with LegAnt L1/L2 Antenna	UHD00492/LA2764	$7,259.00
	FreeWave DGR-115R Spread Spectrum Transceiver	906-5978	$1,010.00
	12V 7AH Sealed LA Battery, cables, power supply		$300.00
1B	Topcon GPS Legacy-E GD GPS L1/L2 Receiver with LegAnt L1/L2 Antenna	UHD00478/LA2755	$7,259.00
	FreeWave DGR-115R Spread Spectrum Transceiver	906-5984	$1,010.00
	12V 7AH Sealed LA Battery, cables, power supply		$300.00
1C	Topcon GPS Legacy-E GD GPS L1/L2 Receiver with LegAnt L1/L2 Antenna	UHD00469/LA2781	$7,259.00
	FreeWave DGR-115R Spread Spectrum Transceiver	906-6008	$1,010.00
	12V 7AH Sealed LA Battery, cables, power supply		$300.00
1D	Topcon GPS Legacy-E GD GPS L1/L2 Receiver with LegAnt L1/L2 Antenna	UHD00504/LA2771	$7,259.00
	FreeWave DGR-115R Spread Spectrum Transceiver	906-5980	$1,010.00
	12V 7AH Sealed LA Battery, cables, power supply		$300.00
1E	Topcon GPS Legacy-E GD GPS L1/L2 Receiver with LegAnt L1/L2 Antenna	UHD00479/LA2778	$7,259.00
	FreeWave DGR-115R Spread Spectrum Transceiver	906-5982	$1,010.00
	12V 7AH Sealed LA Battery, cables, power supply		$300.00
2A	Topcon GPS Legacy-E GD GPS L1/L2 Receiver with LegAnt L1/L2 Antenna	UHD00467/LA2758	$7,259.00
	FreeWave DGR-115R Spread Spectrum Transceiver	906-6007	$1,010.00
	12V 7AH Sealed LA Battery, cables, power supply		$300.00
2B	Topcon GPS Legacy-E GD GPS L1/L2 Receiver with LegAnt L1/L2 Antenna	UHD00486/LA2768	$7,259.00
	FreeWave DGR-115R Spread Spectrum Transceiver	906-5963	$1,010.00
	12V 7AH Sealed LA Battery, cables, power supply		$300.00
2C	Topcon GPS Legacy-E GD GPS L1/L2 Receiver with LegAnt L1/L2 Antenna	UHD00480/LA2754	$7,259.00
	FreeWave DGR-115R Spread Spectrum Transceiver	906-6004	$1,010.00
	12V 7AH Sealed LA Battery, cables, power supply		$300.00
2D	Topcon GPS Legacy-E GD GPS L1/L2 Receiver with LegAnt L1/L2 Antenna	UHD00488/LA2775	$7,259.00
	FreeWave DGR-115R Spread Spectrum Transceiver	906-6002	$1,010.00
	12V 7AH Sealed LA Battery, cables, power supply		$300.00
2E	Topcon GPS Legacy-E GD GPS L1/L2 Receiver with LegAnt L1/L2 Antenna	UHD00496/LA2780	$7,259.00
	FreeWave DGR-115R Spread Spectrum Transceiver	902-4718	$1,010.00
	12V 7AH Sealed LA Battery, cables, power supply		$300.00
NTR-01	Topcon GPS Legacy-E GD GPS L1/L2 Receiver with LegAnt L1/L2 Antenna	UHD00499/LA2763	$7,259.00
	FreeWave DGR-115R Spread Spectrum Transceiver	906-5977	$1,010.00
	FreeWave DGR-115R Spread Spectrum Transceiver	906-5983	$1,010.00
	FreeWave DGR-115R Spread Spectrum Transceiver	906-6006	$1,010.00
	FreeWave DGR-115R Spread Spectrum Transceiver	906-5979	$1,010.00
	FreeWave DGR-115R Spread Spectrum Transceiver	906-5981	$1,010.00
	Toshiba Tecra 8100 Laptop	41302036U	$2,578.00
	Edgeport/8 USB to Serial Hub	04-15-000777	$500.00
	Cables		$400.00
NTR-02	Topcon GPS Legacy-E GD GPS L1/L2 Receiver with LegAnt L1/L2 Antenna	UHD00476/LA2769	$7,259.00
	FreeWave DGR-115R Spread Spectrum Transceiver	906-6005	$1,010.00
	FreeWave DGR-115R Spread Spectrum Transceiver	906-5976	$1,010.00
	FreeWave DGR-115R Spread Spectrum Transceiver	906-6003	$1,010.00
	FreeWave DGR-115R Spread Spectrum Transceiver	906-6001	$1,010.00
	FreeWave DGR-115R Spread Spectrum Transceiver	902-4182	$1,010.00
	Edgeport/8 USB to Serial Hub	04-15-000880	$500.00
	Toshiba Tecra 8100 Laptop	31279892U	$2,578.00
	Cables		$400.00
NTR-03	Antennex antennas (20 total)		$1,500.00
	Cables, tools, fasteners		$500.00
	TOTAL		**$119,264.00**

Table D.1 – Japan Test Equipment List

Appendix E - FreeWave Transceiver Configuration

The FreeWave DGR-115R data transceivers are configurable for point-to-point or point-to-multipoint operations. For the GPS application a point-to-point configuration is utilized with a single pair of transceivers transmitting data for a single GPS rover unit. Although this configuration facilitates effective data throughput, it is necessary to co-locate multiple master transceivers in close proximity to the *RTK-GPS Data Processing PC*. Based upon experiences over the course of this project, the close proximity of the transceivers and antennas introduced significant interference between the master transceivers, as they tend to transmit and receive at different intervals.

This problem was solved by synchronizing the master transceivers using the *Multi Master Synch* technique, a built in feature of these transceivers. This synchronization technique effectively coordinates the transmission and receiving times of all master transceivers such that no single transceiver is transmitting while others are receiving. This technique was first effectively used during the December test in Japan and significantly improved the reliability of the communications link as compared to the November tests, where more data loss occurred.

Specific transceiver settings used during the December test are presented in Table E.1 below.

Box	Unit		Color	Slave	Call Book (Master)	COM	Slave Radio Transmission Parameters				
							Frequency Key	RF Data Rate	Xmit Rate	RF Xmit Power	Multi Master Sync
1	A	G2	Orange	906-5978	906-5977	COM5	0	2	1	2	0
1	B	G3	Orange	906-5984	906-5983	COM6	1	2	1	2	0
1	C	G4	Orange	906-6008	906-6006	COM7	2	2	1	2	0
1	D	G5	Orange	906-5980	906-5979	COM8	3	2	1	2	0
1	E	G6	Orange	906-5982	906-5981	COM9	4	2	1	2	0
2	A	G8	Yellow	906-6007	906-6005	COM5	5	2	1	2	0
2	B	G9	Yellow	906-5963	906-5976	COM6	6	2	1	2	0
2	C	G10	Yellow	906-6004	906-6003	COM7	7	2	1	2	0
2	D	G11	Yellow	906-6002	906-6001	COM8	8	2	1	2	0
2	E	G12	Yellow	902-4718	902-4182	COM9	9	2	1	2	0

		Grand Master	Sub Master	Call Book	Master Radio Transmission Parameters				
					Frequency Key	RF Data Rate	Xmit Rate	RF Xmit Power	Multi Master Sync
	Base 1	906-5977		906-5978 906-5983 906-6006 906-5979 906-5981 906-6005 906-5976 906-6003 906-6001 902-4182	0	2	0	2	0
			906-5983	906-5984 906-5977	1	2	1	2	1
			906-6006	906-6008 906-5977	2	2	1	2	1
			906-5979	906-5980 906-5977	3	2	1	2	1
			906-5981	906-5982 906-5977	4	2	1	2	1
	Base 2		906-6005	906-6007 906-5977	5	2	1	2	1
			906-5976	906-5963 906-5977	6	2	1	2	1
			906-6003	906-6004 906-5977	7	2	1	2	1
			906-6001	906-6002 906-5977	8	2	1	2	1
			902-4182	902-4718 906-5977	9	2	1	2	1

Table E.1 – Multi Master Synch Transceiver Settings